Free Valve

The Effect of Different Valve Strategies on In-Cylinder Flow, Emissions and Performance in a Heavy Duty Diesel Engine

STEFAN OTTOSSON
TED HOLMBERG

KTH Industrial Engineering and Management

Master of Science Thesis
Stockholm, Sweden 2011

Free Valve

The Effect of Different Valve Strategies on In-Cylinder Flow, Emissions and Performance in a Heavy Duty Diesel Engine

Stefan Ottosson
Ted Holmberg

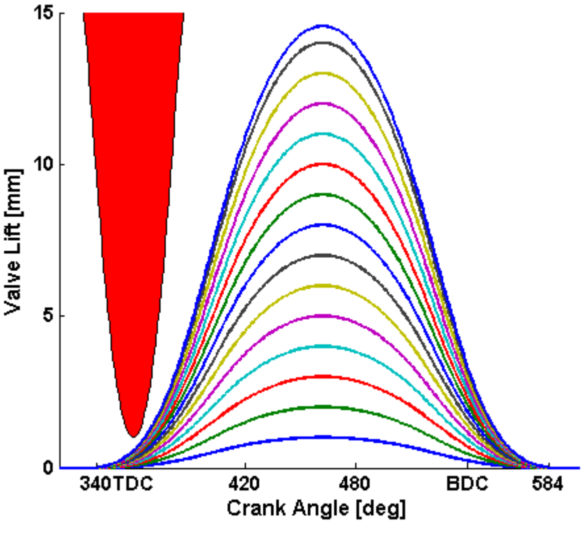

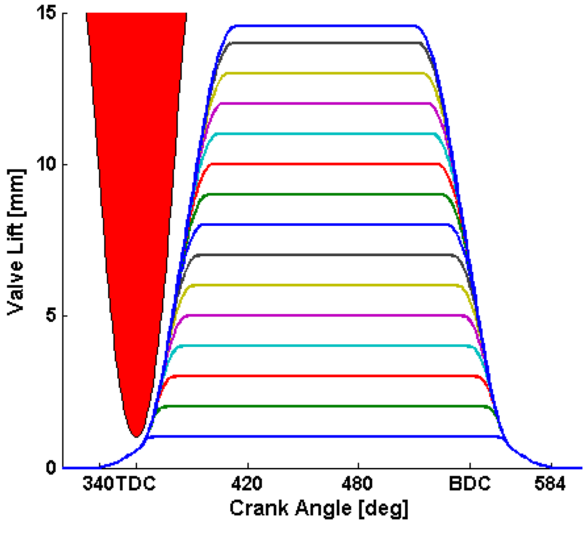

Master of Science Thesis MMK 2011:06 MFM123
KTH Industrial Engineering and Management
Machine Design
SE-100 44 STOCKHOLM

KTH Industriell teknik och management

Examensarbete MMK 2011:06 MFM123

Fria Ventiler

Olika ventilstrategiers effekt på cylinderströmning, emissioner och prestanda i en heavy duty dieselmotor

Stefan Ottosson
Ted Holmberg

Godkänt	Examinator	Handledare
110217	Prof. Hans-Erik Ångström	Prof. Hans-Erik Ångström
	Uppdragsgivare Scania CV AB	Kontaktperson Henrik Dembinski

Sammanfattning

Denna rapport beskriver ett examensarbete utfört på Scania CV AB, Södertälje, i samarbete med Kungliga Tekniska Högskolan, Stockholm, inom ämnet förbränningsmotorteknik.

Dagens krav på allt mer miljövänliga fordon ställer allt högre krav på motortillverkarna. Att optimera en motor för flera olika driftsfall är långt ifrån trivialt, då det som är optimalt för en driftspunkt inte behöver vara det för en annan. Att utnyttja ett system med variabel ventilstyrning ökar motorns flexibilitet och underlättar därmed denna optimering. Detta examensarbete syftar till att studera hur cylinderströmningen kan påverkas av olika ventilstrategier, och hur detta i sin tur påverkar emissioner och prestanda.

Flödesmätningar har utförts för att studera snurr och tumble. Dessa tester har visat att snurrgenereringen kan ökas med 75% om ventilen till den raka kanalen deaktiveras. Dessutom kan ytterligare en ökning erhållas, 93% högre än original, om den krokiga kanalen blockeras istället för att deaktivera ventilen, då det visat sig att ventiltallrik och ventilskaft till denna kanal har en positiv inverkan på snurrgenereringen. Tumblerörelsen ökar kraftigt då en ventil deaktiveras eller då en kanal blockeras. Till skillnad från snurren så ökar tumblegenereringen med lägre lyfthöjder med dessa strategier. Med en ventilprofil med maximal lyfthöjd på 5 mm erhålls en medeltumble 4,5 gånger större än originalfallet som har en maximal lyfthöjd 14,55 mm.

Motorcellskörningar visar att ökningen i snurr kan utnyttjas för att reducera sotemissioner då en högre efteroxidation kan erhållas. Tester för att simulera en transient visar att sotemissionerna kan reduceras från 0,40 mg/m^3 med original ventil strategi till 0.06 mg/m^3 med ventilen till den krokiga kanalen deaktiverad och till 0,08 mg/m^3 med den krokiga kanalen blockerad. Dock ger den högre snurren i regel högre NO_x emissioner samt om en allt för hög snurrnivå utnyttjas även högre CO emissioner. I kombination med EGR kan dock NO_x emissionerna sänkas. Med enbart ventilen till den raka kanalen aktiv med 13 mm maxlyft, kunde likvärdiga sot och CO emissioner erhållas vid 35% EGR som med standardfallet och 26% EGR, samtidigt som NO_x emissionerna sänktes med 60%.

Vid högre varvtal visar dock strategierna med en ventil deaktiverad eller en kanal blockerad på en lägre total verkningsgrad än originalfallet. Detta beror till största del på högre pumpförluster. Upp till 1400 rpm kan volymetriska verkningsgraden vara högre med en ventil deaktiverad, men totala verkningsgraden blir något lägre än för originalfallet redan vid ett motorvarvtal på 1056 rpm på grund av pumpförlusterna. Fria ventiler kan användas för att kraftigt påverka cylinderströmningen, men total verkningsgraden kan bli lidande redan vid medelhöga varvtal. Att blockera den krokiga kanalen med hjälp av ett spjäll kan vara en betydligt enklare lösning för att höja snurrgenereringen, men denna metod begränsar valmöjligheten av önskad cylinderströmning. Som fortsatt arbete bör djupare studier i hur tumble rörelsen påverkar förbränningen utföras.

KTH Industrial Engineering and Management	**Master of Science Thesis MMK 2011:06 MFM123** **Free Valves** The Effect of Different Valve Strategies on In-Cylinder Flow, Emissions and Performance in a Heavy Duty Diesel Engine Stefan Ottosson Ted Holmberg	
Approved 110217	Examiner Prof. Hans-Erik Ångström	Supervisor Prof. Hans-Erik Ångström
	Commissioner Scania CV AB	Contact Person Henrik Dembinski

Abstract

This report describes a master thesis performed at Scania CV AB, Södertälje, in cooperation with the Royal Institute of Technology, Stockholm, within the subject combustion engines.

In today's society, with more stringent emission legislations, the demands on engine manufactures are increased. To optimize an engine for several load points are far from trivial, since what's optimal on one load point doesn't have to be the best on another load point. To use a variable valve actuation system increases the flexibility of the engine and facilitates such optimizations. This master thesis aims to study how different valve strategies affect the in-cylinder flow, and how this in turn affects the emissions and performance.

Flow measurements have been performed to study swirl and tumble. These tests have shown that the swirl generation can be increased by deactivating the valve to the straight port by 75%. Additionally, a further increase, 95% higher than the standard case, can be achieved by instead blocking the curved port, since the valve head and stem to this channel has a positive effect on the swirl generation when the flow comes from the straight port. The tumble motion also increases when deactivating a valve or blocking a port. Unlike the swirl motion the tumble motion increases with lower valve lifts. With a valve profile with a maximum valve lift of 5 mm a 4.5 times higher mean tumble is achieved in comparison to the standard strategy with 14.55 mm maximum valve lift.

Engine cell tests have shown that the increase in swirl motion can be used to reduce the soot emissions since a higher after oxidation can be obtained. At a load point simulating a transient the soot emissions can be reduced from 0.40 mg/m^3 for the original case to 0.08 mg/m^3 with the valve to the curved port deactivated, and to 0.06 mg/m^3 with the curved port blocked. In general the higher swirl motion increases the NO_x emissions though, and a too high swirl motion increases the CO emissions. But in combination with EGR the NO_x emissions can be reduced. With only the valve to the straight port active, and a maximum valve lift of 13mm, similar soot and CO emissions could be obtained at 35% EGR level compared to the standard case at 26% EGR, meanwhile the NO_x emissions could be lowered with 60%.

At higher engine speeds the strategies with one valve deactivated or one port blocked shows lower total efficiency. This is mostly dependent on higher pumping losses. Up to 1400 rpm the volumetric efficiency can be is increased with one port blocked, regardless of this the total efficiency is decreased already at higher engine speeds than 1056 rpm because of the pumping losses. Free valves can be used to greatly affect the in-cylinder flow, but the efficiency of the engine may suffer already at medium engine speeds. To block the curved port with a throttle can be a considerably simpler solution to increase the swirl motion, but this method limits the options of desired in-cylinder flow. As further work a deeper study of the tumble motions affect on the emissions should be performed.

Acknowledgements

The authors of this master thesis wishes to do the following acknowledgements:

We had the privilege of doing our Master Thesis at the advanced combustion department, NMPF, at Scania CV AB in Södertälje, Sweden, during the autumn term of 2010. All the staff on the group have been very helpful and always took the time to talk to us whenever we needed to. Thanks for a great and enjoyable time! We would like to thank everybody that in some way have been involved with our work, and some special thanks to

Henrik Dembinski, our supervisor that always have been there for us with great guidance.

Björn Lindgren, Hans Lindström and James Davy at the flow bench laboratory a Scania, where we always were welcome to perform new tests and ask questions.

Anders Björnsjö, Stefan Olsson, Daniel Norling and Per Risberg at NMPF that always have been very supportive in times of need.

Kristian Andersson for great help and guidance during the cell tests performed at Scania, and for all the time he has spent in the test cell preparing it for our tests.

Hans-Erik Ångström, our examiner at KTH that also has worked as a supervisor to us during the master thesis.

And finally, but not least, to our families for great support and understanding.

Stefan Ottosson and Ted Holmberg, February 2011

Table of Contents

1 Introduction

In today's modern society, with ever more stringent demands placed on environmentally friendly vehicles, more development and optimization are required on heavy duty diesel engines to stay competitive. To optimize a diesel engine the goal is to improve the fuel consumption, reduce the NO_x emissions and lower the soot emissions. As these requirements are dependent on each other or even directly opposed, a suitable compromise is often difficult to find. A classic problem for diesel engines is the Soot-NO_x trade-off, which states that when lowering the soot emissions, the NO_x emissions will increase and vice versa. One of the major factors influencing the NO_x emissions is the in-cylinder air motion. To describe the air motion it is common to separate the air flow into two distinct categories, the swirl motion and the tumble motion. The Swirl motion describes the air flow around the cylinder axis and is most commonly studied with regards to diesel engines. The tumble motion describes the air flow perpendicular to the cylinder axis and is mostly studied with regards to spark ignited engines. An illustration of the two air motions can be seen in Figure 1.

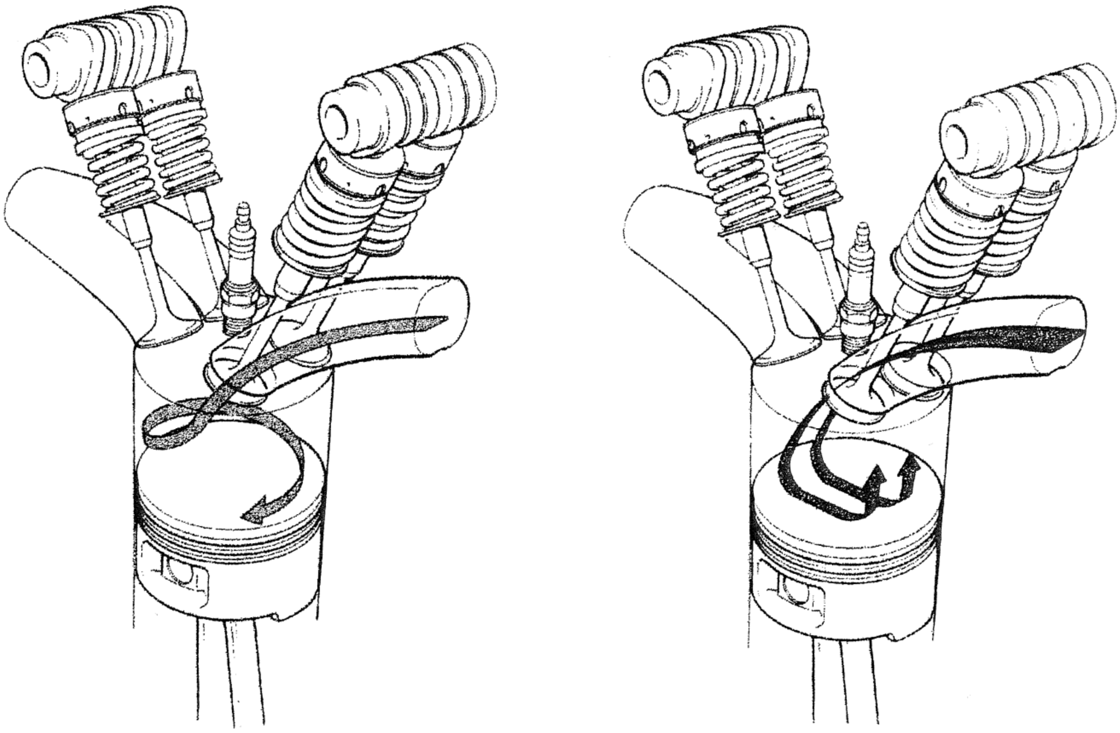

Figure 1. *Illustration of the swirl motion (left) and tumble motion (right).* [**1**]

It is generally accepted that a higher swirl motion lowers the soot emissions, while increasing the fuel consumption due to higher heat and pumping losses. Therefore the swirl level of a cylinder head is a carefully balanced compromise between these parameters. However during certain engine operating conditions, for example a transient load, a higher swirl level would be desired as the soot emissions limit the engine's power output. At other operation conditions it might be more important to decrease the NO_x emissions and lower the fuel consumption and as a result a lower swirl level would be desired. Therefore to be able to optimize the engine for different loads and engine speeds, it would be desirable to vary the swirl motion to suit the current engine conditions.

1.1 Background

Scania CV AB has been interested in the application of variable swirl on a heavy-duty diesel engine for several years and during the spring of 2010 the authors of this master thesis participated in a joint project between Scania and the Royal Institute of Technology, KTH, Stockholm, to test the possible benefits of valve generated swirl. The project [2] studied the effects of valve strategies with different swirl levels at a stationary load point which simulated a transient, i.e. a low inlet manifold pressure and a high load. At the studied load point it was found that a higher swirl than original was beneficial to reduce the soot emissions, which made possible to operate the engine at significantly lower lambda values and thereby increasing the power of the engine.

To investigate the effects of the valve strategies on higher engine speeds, some tests were performed at 1700 rpm for the same operating conditions as the lower engine speed. At this engine speed the valve strategies with the highest swirl level produced higher smoke emissions than the standard 2V valve strategy, which illustrates that one swirl level is rarely best for all operation conditions. Another downside was that these valve strategies produced significantly lower brake torque, as the volumetric efficiency decreased considerably compared to the original valve strategy.

From this limited study it was clear that more tests had to be done to investigate the potential benefits of valve generated swirl.

2 Literature Study

Variable Valve Actuation has been studied extensively on gasoline engines, as the pumping losses can be reduced greatly due to lower throttle losses and higher performance can be achieved by changing the valve overlap and timing. For diesel engines the potential benefits are not as clearly defined, as they already run unthrottled. Another factor which limits the use of VVA in diesel engines is the small valve clearances between the valves and the piston at top dead center, due to the high compression ratio. This restricts the movement of the valve profile close to the piston and therefore the traditional cam-phasing variable valve timing, VVT, has limited applicability on HD diesel engines.

Consequently the majority of the research with regards to diesel engines and VVA has been focused on applying the Miller or Atkinson cycle. One example of this is He et al [3] which investigates the effects of implementing Late Intake Valve Closing, LIVC, on a 0.56 liter single cylinder research diesel engine with a FFVA-system, Fully Flexible Valve Actuation. With LIVC the effective compression ratio is reduced since the intake valves are open during the beginning of the compression stroke. The lower compression ratio, which in turn lowers the compression temperature has a major influence on the emission formation during the combustion, in the paper the process is illustrated with a graph, see Figure 2.

The lower compression temperature leads to a longer ignition delay which results in a better air fuel mixing and a lower soot formation. The NO_x formation is also reduced as this is heavily dependent on the peak combustion temperature. The major disadvantage with LIVC is that it reduces the volumetric efficiency and therefore it is mostly suitable for operating points with fairly high Air Fuel Ratio, AFR, were the AFR remains high enough even with LIVC in order for the combustion quality to be maintained. This limits the power range of where it is suitable to run a Miller cycle unless much higher boost pressure is available. To be able to run a miller cycle in a certain power range and a standard cycle at full load a VVA system is required.

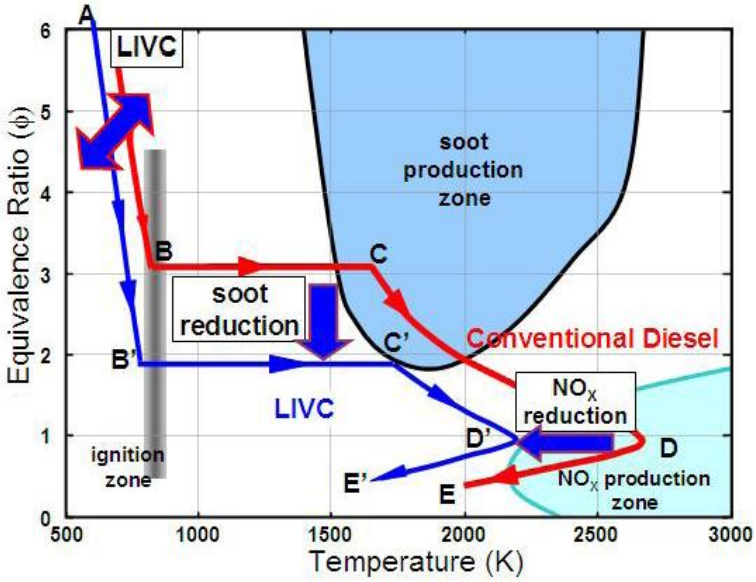

Figure 2. *Illustration of the potential benefits of LIVC on soot and NO_x emission.* [**3**]

The VVA system opens up the possibility to vary the valve profiles freely and Grimaldi et al. [4] investigated the effects of asymmetric valve lifts on swirl and tumble generation on a high performance four valve SI cylinder head from a Ducati motorcycle. The analysis is performed using a steady state flow bench. As this type of engine is designed for maximum power the flow through the intake valves generates no swirl in its standard configuration, in other words when both intake valves have the same lift. However as the lift of one valve is reduced the swirl number starts to increase and reaches a maximum when one of the valves is closed, see Figure 3. Since the ports of the studied engine are symmetrically placed in relation to a center line of the cylinder, the swirl map is symmetric with both valves creating an equal amount of swirl.

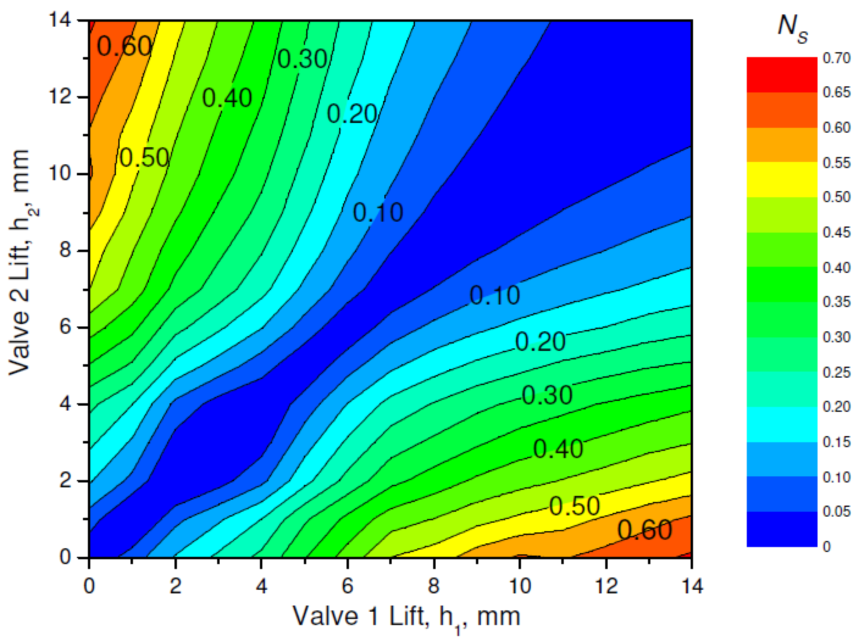

Figure 3. *Contour plot of the SN with asymmetric valve lifts on a high performance SI engine cylinder head.* [**4**]

As the majority of diesel engines in production today generate swirl using the shape of the intake ports, the trend for diesel engines will most likely not be as symmetrical. Despite the differences between diesel engines and the SI engine studied in this paper, these results indicates that it is possible to generate a significant amount of swirl with the use of asymmetric valve lifts.

The paper also investigates the effect on tumble generation with asymmetric valve lifts. It is shown that tumble motions are heavily dependent on valve lift, see Figure 4. From the figure it can be observed that the tumble number increases significantly if the valve lift is higher than around 7 mm and the maximum tumble number is reached at maximum valve lift on both valves. Where the maximum swirl is reached, i.e. with one valve closed, the tumble is at medium strength and at maximum tumble, i.e. with both valves fully open, the swirl has its minimum.

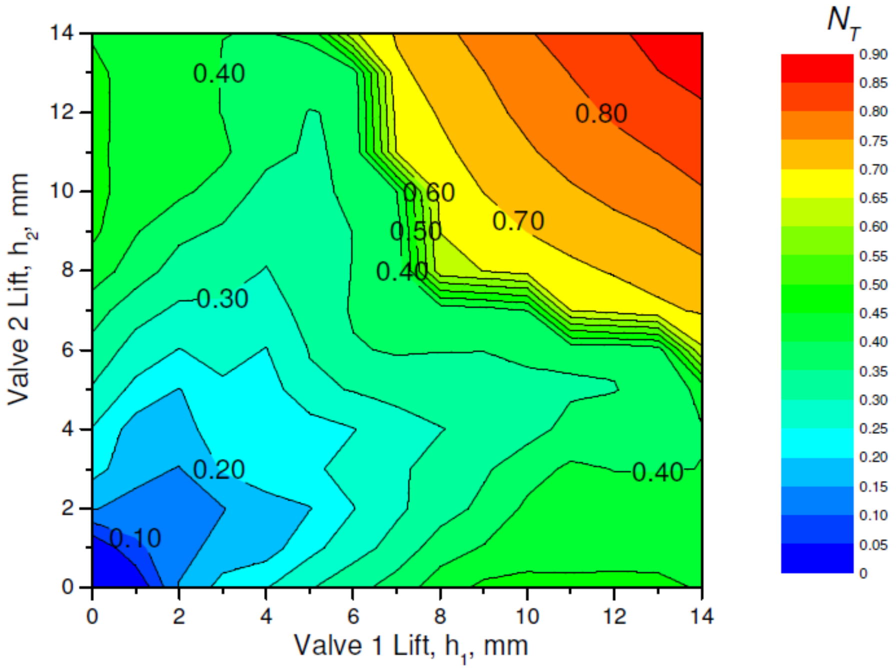

Figure 4. *Contour plot of the TN with asymmetric valve lifts on a high performance SI Engine cylinder head.* [**4**]

Port injected SI engines use tumble motion to enhance the turbulent flame front propagation and achieve a good combustion. As the tumble motion is not considered a significant parameter for a diesel engine in general, the trends might not be as clear on a diesel engine.

The traditional way of generating swirl in diesel engines is by the geometry of the intake ports. Blechstein et al. investigated [5] three different intake port geometries, see Figure 5, with the same swirl number using a DGV (Doppler Global Velocimetry) flow bench. The flow bench results were then compared to measurements of smoke emissions from a single cylinder diesel engine. Despite having the same swirl number, the different port geometries produced substantial differences in smoke emissions. The authors draw the conclusion that describing the flow characteristics by only using the swirl number and flow coefficient is a too simplified representation. Instead a few observations are made regarding the positive effects of the flow field characteristics on diesel combustion. A high swirl number over the course of the valve lift in conjunction with a homogeneous, centrally positioned vortex seems to produce the lowest smoke emissions.

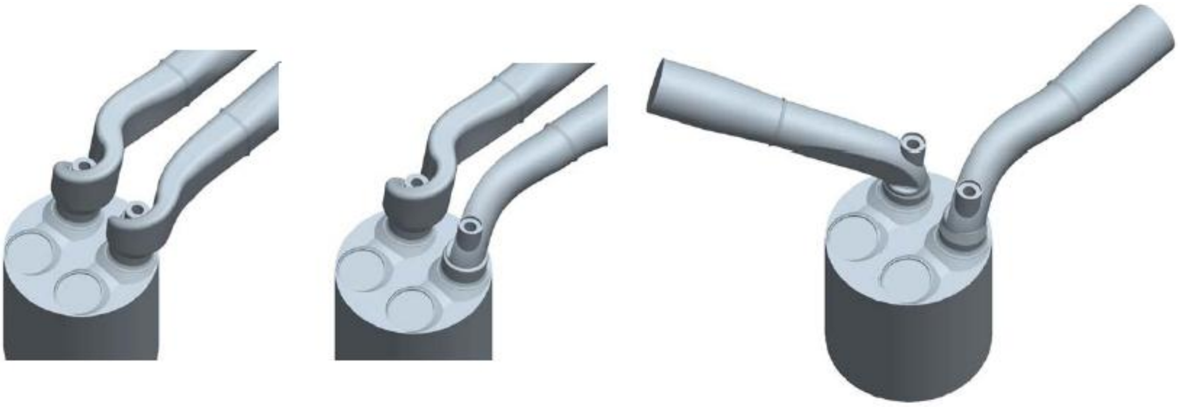

Figure 5. *The different port geometries investigated by Blechstein et al.* [**5**]

While there were no papers directly studying the effects of valve generated swirl for diesel engines, there were some older papers investigating variable swirl. Shimada et al [6] investigated different inlet systems with variable swirl to see its effects on emissions and performance on a 6 cylinder, 11.2 liter diesel engine. To vary the swirl two different ways of implementing a throttle valve in the intake port were investigated using a flow bench. The solution with the best overall flow coefficient, a helical port with high swirl combined with a sub port to decrease the swirl when opened, was considered to be the best and tested on the engine. Four different swirl ratios were investigated and from the engine tests an optimum swirl map was obtained with regards to engine speed and load. For the port configuration and the swirl map see Figure 6.

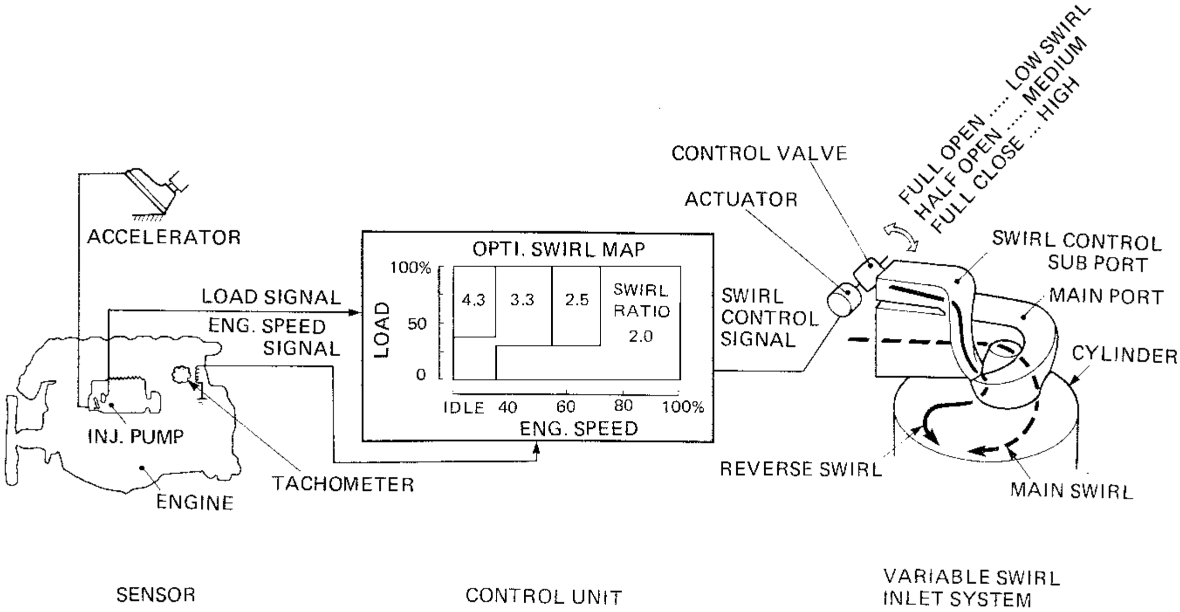

Figure 6. *A schematic sketch over the variable swirl inlet system with an optimized swirl map.* [**6**]

From the engine tests the conclusion was drawn that a lower swirl ratio decreased the NO_x emissions, the peak pressure and the pressure gradient. The Brake Specific Fuel Consumption, BSFC, and smoke emissions decreased at high speed with decreased swirl ratio but were decreased with an increased swirl ratio at low engine speed. From these findings the optimum swirl map was obtained. Compared to a conventional port the variable swirl port improved BSFC and lowered smoke emissions without sacrificing NO_x emissions as a whole.

3 Problem

This master thesis aims to investigate the potential of varying the in-cylinder air motions with different valve strategies on a heavy duty diesel engine, and their effect on combustion and emissions. Since it would be preferable to vary the in-cylinder motions at different engine conditions, the advantages and disadvantages with different valve strategies at a selection of load points is of interest. Also the effect of Exhaust Gas Recirculation, EGR, is to be studied with different in-cylinder motions.

An easier way of varying the in-cylinder motion is to block one of the inlet ports, while both inlet valves still are active. Therefore it is interesting to study how the flow from the open port is affected by the valve disc and stem from the blocked port. It is also of interest to study the effects on the gas exchange from the different methods.

There are several calculation methods for characterization of the in-cylinder flow. Because of this it would be interesting to investigate how well different methods illustrates the phenomena's caused in an engine.

The master thesis will investigate the previously described problems with the following limitations:

- Load points to be run during in the engine test cell is mostly taken from the WHSC-cycle
- No pilot injection will be used
- Only inlet valve strategies will be investigated
- The timing of the inlet valve profiles will be kept constant, i.e. the inlet valve opening and closing will be the same for all strategies
- Only the Thien method and the model used in GT-Power for calculating mean swirl and tumble will be compared

The questions that will be answered in this paper are the following:

- How is the in-cylinder air motion influenced by different valve strategies?
- How do the calculated swirl values differ between the Thien method and the GT-power method and which provides the better correlation with engine test data?
- What is the influence of the valve stem and valve head when comparing port deactivation with valve deactivation?
- What is the effect of different valve strategies on combustion and emissions?

4 Method and equipment

Measurements of swirl and tumble numbers were performed in a flow bench at Scania. A in-cylinder air flow study with the individual intake valves investigated separately, the differences between valve and port deactivation and also the influence of the intake manifold were performed. To analyze the flow bench results two different methods of calculating mean swirl and tumble were used, the more traditional Thien method and with the simulation software GT-Power [7].

From the results of the swirl and tumble calculations, different valve strategies were created with varying in-cylinder air motions. Single cylinder engine tests were performed with the selected valve profiles to analyze their effects on combustion and emissions at different load points.

With help of the engine tests the methods of calculating mean swirl and tumble were then compared regarding calculation results and correlation to soot emissions.

The steady state flow bench, the single cylinder engine setup, the created valve profiles and the test cases run during engine tests will be thoroughly described in the following chapters.

4.1 Steady State Flow Bench

A schematic sketch over the steady state flow bench can be seen in Figure 7. The cylinder head to be investigated (1) is placed on the cylinder liner (2) on the top of the flow bench box (4). A fan (8) is used to suck air through the intake ports and through the flow bench. When performing the tests the pressure drop over the inlet ports is kept constant at 25 mBar regardless of the valve lift by adjusting the flow through the bench and the pressure drop is monitored by a water gauge (5).

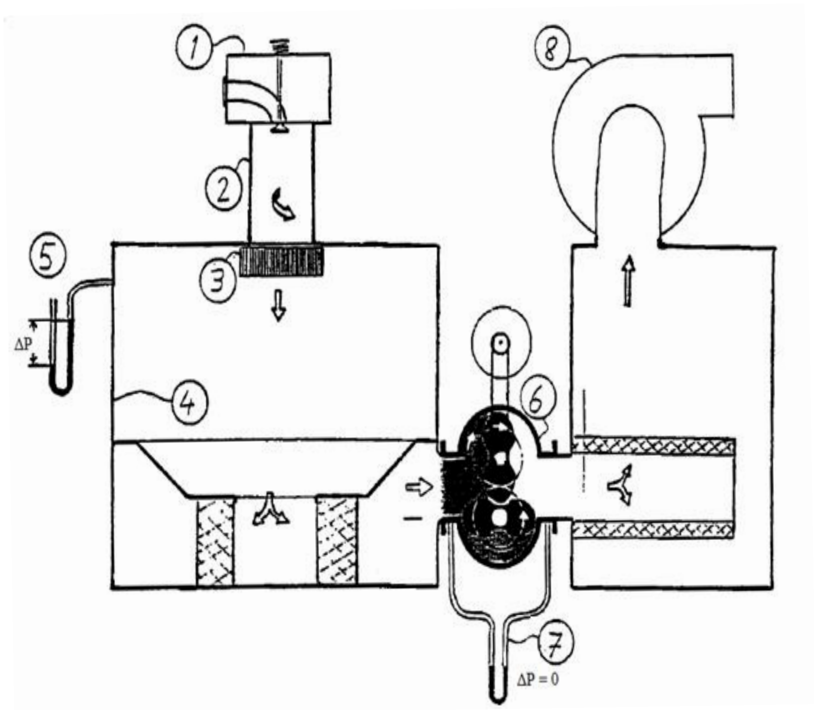

Figure 7. *A schematic sketch over the steady state flow bench with the different parts marked with numbers. Reference B. Lindgren*

The amount of air flow through the bench is measured by a roots blower, which functions as an air flow meter (6). The rotational speed of the blower is adjusted so that the pressure drop is zero across it, which is monitored by a water gauge (7). Thereby the air flow is directly proportional to the rotational speed.

The generated swirl is measured by a honey comb torque meter (3) in the bottom of the cylinder liner, which registers the angular momentum induced by the rotating air flow on the honey comb.

During the swirl measurements the lift of the valves are adjusted by a step motor that rotates a screw with 1 mm pitch that pushes on the valve bridge. In this way both the inlet valves can be lifted symmetrically, or if a half valve bridge is used one valve at a time. During this master thesis there was a need for lifting the valves asymmetrically. In order to do this a new test setup was created with two screws, each pushing on one valve, see Figure 8.

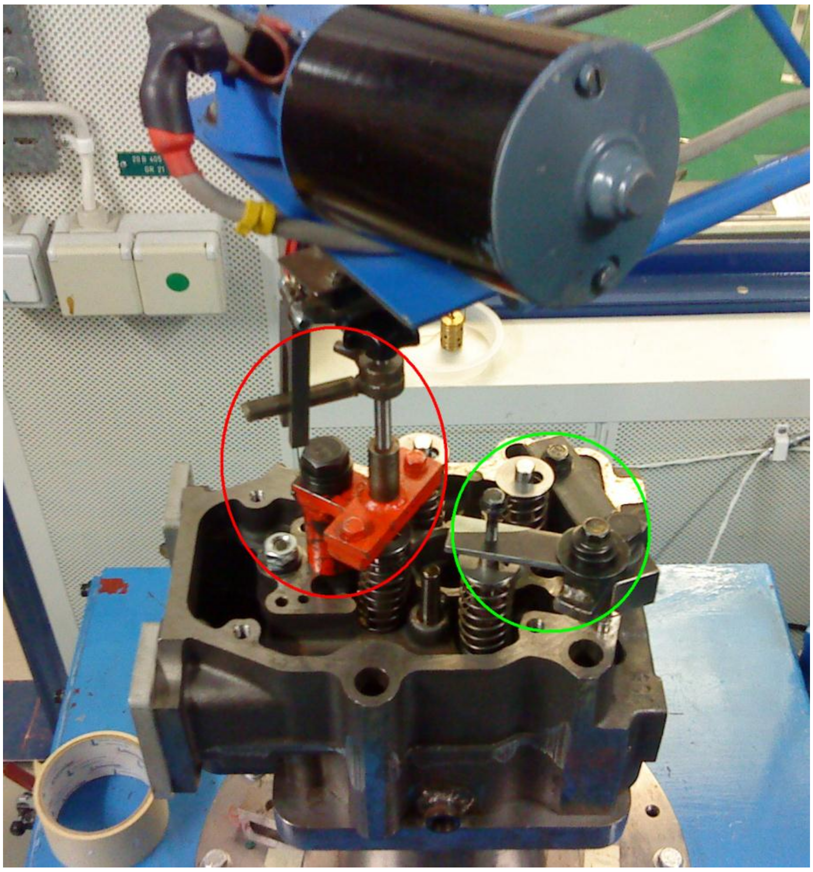

Figure 8. *The additional test setup to perform asymmetrical valve lifts. The additional screw fixture (green) and the already existing system (red) together with the step motor on top.*

In order to measure the generated tumble the cylinder liner is replaced by a pipe with a 90 degree bend, see Figure 9, with the same inner diameter as the cylinder liner. In this way the tumble motion generated by the cylinder head is transformed into a swirl like motion travelling down the pipe, which can be measured by the honey comb torque meter in the same way as the swirl.

Figure 9. *The pipe with a 90 degree bend to transfer the tumble motion from the cylinder head to a swirl like motion at the honey comb torque meter in the flow bench.*

The problem with this method to measure tumble is that the cylinder head must be turned to a specific angle to get the main tumble motion to get transferred down the pipe. During the tests performed in this master thesis a zero angle was defined as the position where the inlet side of the cylinder head was perpendicular to the floor according to Figure 10. Turning the cylinder head in the clockwise direction was then defined as a positive angle and in the counterclockwise direction as a negative angle.

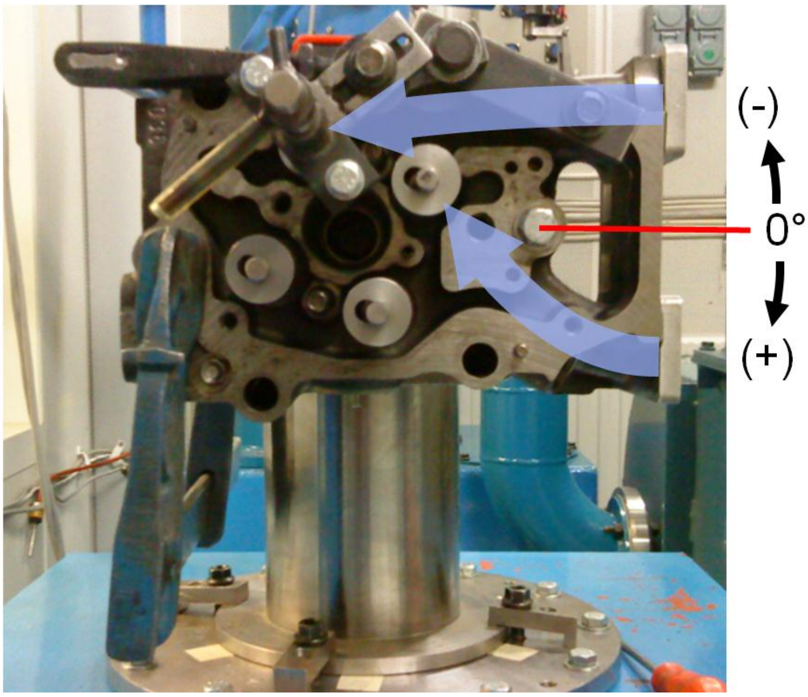

Figure 10. *The zero-position for the cylinder head angle used in this master thesis and the definition of a positive or negative angle.*

4.2 Engine setup

Originally the intent of this paper was to use the single cylinder engine at KTH to investigate the effects of the selected valve strategies on combustion and emissions. Unfortunately due to mechanical problems in the test cell the testing had to be continued at Scania in a similar single cylinder test cell. Both the engines at KTH and at Scania are hybrids constructed with the engine block of the previous engine platform D12 combined with a modified cylinder head from the current engine platform DL. The resulting engine has the smaller bore of 127 mm of the older platform, compared to 130 mm of the current platform, but with the larger intake valves from the current generation. The cylinder head was initially a low swirl version with a swirl number of 1.4, according to Thien, which was modified with valve seats from a cylinder head with a swirl number of 2.1, giving a final swirl number of 1.59. The common specification for the single cylinder engines is displayed in Table 1.

Table 1. *The common engine specification for the two test cells.*

Displacement	1.95 dm^3
Bore x Stroke	127 mm x 154 mm
Compression ratio	17.3
Injector Flow	207 pph
Injector Nozzle Holes	8

Inevitably there is some disparity between the two tested setups and in the following paragraphs the most significant differences will be discussed.

As maximum freedom in studying different intake valve profiles are desired, the standard valve actuation consisting of camshaft, pushrods and valve springs has been replaced with a hydraulic valve actuation system. The system is built by Lotus and is referred to as the Lotus Active Valve Train (AVT). It is a self-contained system designed solely for the purpose of experimental testing, as it is too bulky and requires too much power for use in a vehicle. Because the hydraulic pump is powered externally, the brake power of the engine will be higher than for an engine equipped with conventional valve actuation. The engine at KTH uses hydraulic actuators for all four valves, while for the engine at Scania, the original valve actuation has been retained for the exhaust valves in an attempt to increase the reliability of the system. The reason for this change is due to the fact that the exhaust valves are much more highly stressed than the intake valves, which drastically shortens the lifetime of the seals in the hydraulic actuators. Since this master thesis is limited to only investigate the intake valves, this change adds no further restrictions on the study.

As these test cells are used for engine predevelopment it is desirably to be able to run on a multitude of fuels, therefore the intake manifolds are custom made to enable port injection of alternative fuels. The two intake manifolds are shown in Figure 11. Both of the intake manifolds share a similar build consisting of a separate plenum and significantly longer intake runners compared to a normal production engine. The difference in runner length is not considered an important deciding factor between the manifolds, but the fact that the air flows in from opposite ends of the plenums might influence the in-cylinder motion.

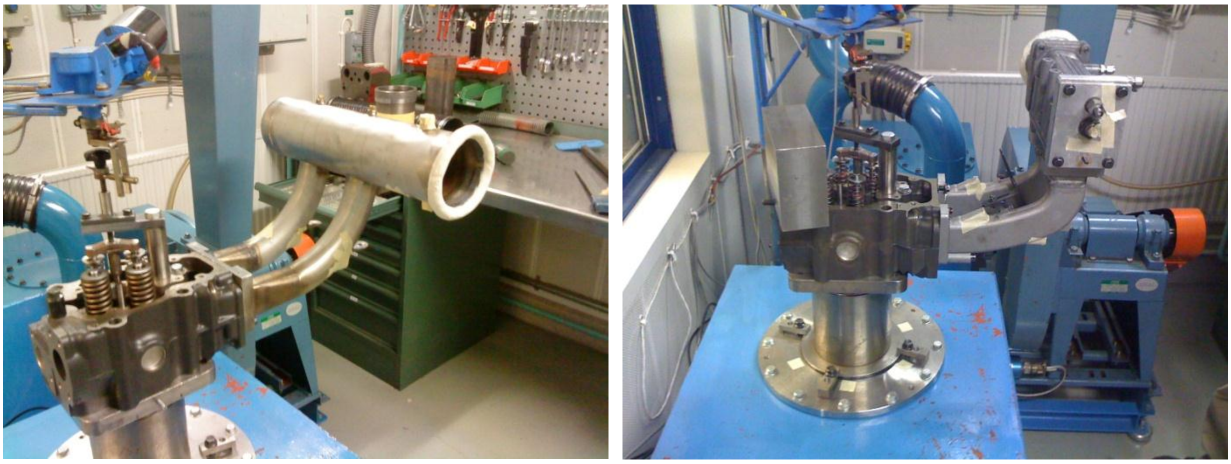

Figure 11. *The intake manifold used at KTH(left) and the intake manifold used at Scania(right).*

The fuel injection is based on the Scania XPI Common-Rail system modified for single cylinder operation. Although both engines use the same injector and the same high pressure pump there are significant differences between the two setups. One is in how the pumps are powered, at KTH there is an electric motor powering the pump enabling it to be controlled independently from the engine. The pump at Scania is powered by the crankshaft and will therefore affect the brake power of the engine. At KTH the fuel injection is controlled by a custom software made for test cell use called Cell4. At Scania the ATI Vision 3.5 is used.

The measurements with EGR were done exclusively in the test cell at Scania. To supply the engine with EGR a externally powered roots blower pumps a fraction of the engine's own exhaust gases through a EGR-cooler and it is then feed into the intake piping upstream of the intake manifold. As the roots blower requires a minimum pressure differential to be able to perform as a pump, the back pressure in the exhaust manifold must be at least 0.1 bar higher than the intake manifold pressure. To achieve this pressure differential the back pressure is regulated with a valve in the exhaust system. The EGR-cooler is cooled by the engine's coolant, which is kept at a constant 90 degrees Celsius, to reduce the risk of water condensation in the system. Therefore to be able to keep the intake air temperature constant, the temperature of the fresh air is lowered and used to cool the intake air mixture.

The charge air is supplied in both cases by large externally powered compressors, which can generate up to 3.5 bar absolute pressure. Therefore the engines aren't equipped with turbochargers and the back pressure in the exhaust manifold is adjusted by valves to provide realistic running conditions.

4.2.3 Data Logging

The control system for the single cylinder test cell at Scania uses software created in-house running on a PDP. This system records the slow measurement data from the test cell with a sampling frequency of 10 Hz during 90 seconds and then calculates the mean value for each logged signal.

Cylinder pressure is logged during 100 cycles with a resolution of 0.1 CAD using a flush mounted piezoelectric pressure transducer from Kistler, model 7061B. The signal is recorded with a AVL Indiset Advanced Plus system. Analysis of the cylinder pressure data is done with the software AVL Concerto [8]. The program automatically pegs the cylinder pressure curves by assuming adiabatic compression between the crank angle degrees -110 and -90 before TDC and from this calculates an offset which adjusts the cylinder pressure curves. The heat-release rate is also calculated with functions included in this program.

4.2.4 Emission Measurements

To measure smoke emissions in the test cell at Scania a AVL 483 Micro Soot Sensor (MSS) was used. It measures the soot emissions continuously and as the response time is very fast, signal rise time ≤ 1 seconds, it can perform transient measurements of soot concentration. Compared to the conventional indirect methods of measuring soot, i.e. the opacity or the blackening of a filter paper, the MSS has the advantage of measuring the soot concentration directly in the unit mg/m³ and can therefore measure extremely low soot emissions with good accuracy. The accuracy is specified to ± 3% with the settings used in this project and the measurement range is 0.005 – 50 mg/m³ with the resolution 1 µg/m³.

The soot measurements at KTH are done using an AVL 415 Smoke meter. It is a conventional filter-type smoke meter and samples therefore the exhaust gasses during a fixed duration, in this project the sample time was set to 30 seconds.

The other emissions, NO_x, CO and HC, were measured using a Horiba MEXA-7100EGR at Scania and a Horiba ESXA-1500 at KTH.

4.3 Valve Profiles

In order to be able to investigate the effects on the in-cylinder flow from different valve strategies several valve profiles have been created. Since this master thesis was limited to only investigate differences caused by the inlet valves, a standard Scania D12 exhaust valve profile was used for both the exhaust valves for all tests.

To create different intake valve profiles the Lotus software Engine Valve Profile Generator, EVPG, [9] was used. This is a MatLab [10] based program and the interface can be seen in Figure 12. From this program different valve profiles can be stored with a specific index in a matrix. This matrix can then be used during engine tests and the different valve profiles can be used by calling on the specific index.

With this program different valve profiles can be created from scratch using different calculating methods to create polynomial profiles, double lift profiles and trapezoidal profiles. It is also possible to create a new valve profile by means of modifying a user defined valve profile. In this project new valve profiles is created by lowering the maximum valve lift for a standard Scania D12 inlet valve and then scaling the valve lift for the entire profile.

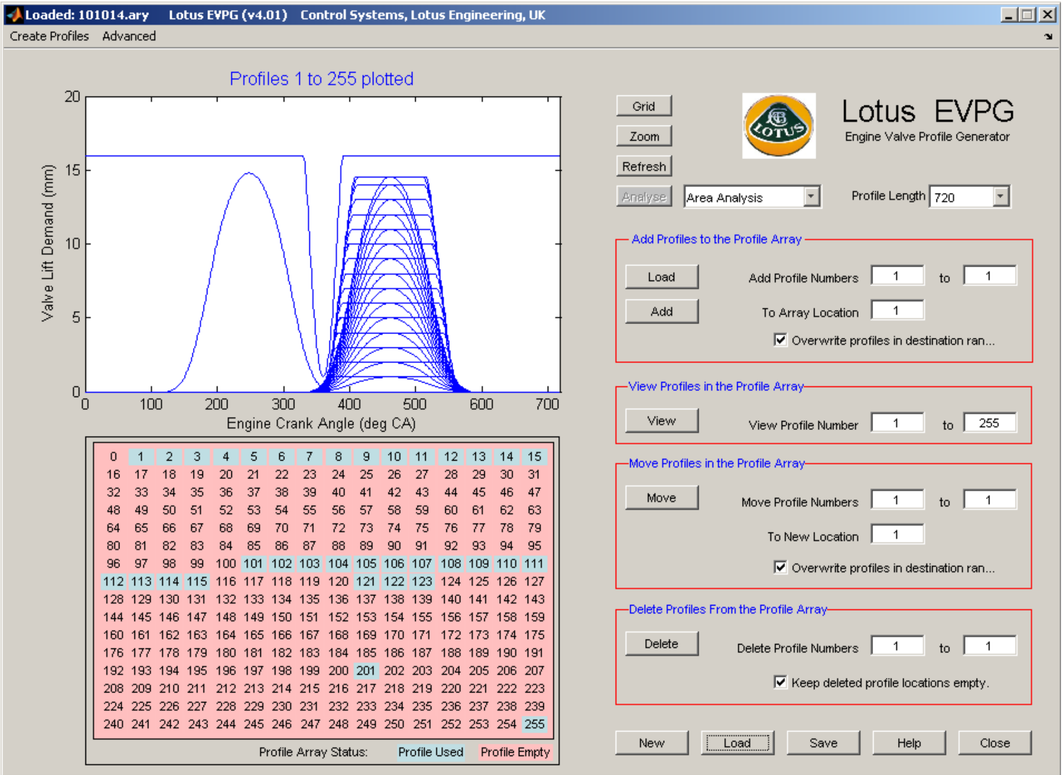

Figure 12. *Lotus EVPG interface with the matrix to store different valve profiles with a specific index in the left corner.*

For the standard valve profile the maximum valve lift is 15 mm, but there is also a 0.45 mm valve lash with the cam-driven system. This valve lash is measured at cold engine conditions and when the engine is running the valve lash decreases. Without it the valves will not close properly due to thermal expansion. Since it is difficult to estimate the valve lash during different engine conditions, the standard profile have been adjusted with the valve lash from cold engine condition. Therefore the maximum valve lift used in this master thesis is 14.55 mm.

Since the master thesis was limited to only investigate different valve lifts, the inlet valve opening, IVO, have been kept at 340 CAD and the inlet valve closing, IVC, have been at 584 CAD for all the profiles. Profiles with a lift curve of standard appearance with maximum valve lifts from 1 mm to 14.55 mm have been created with 1 mm step. These profiles together with the piston limitations can be seen in Figure 13, where also trapezoidal profiles with the same maximum lifts can be seen. To create the trapezoidal profiles a MatLab script has been written, since the predefined function in the EVPG-software had limited adjustability.

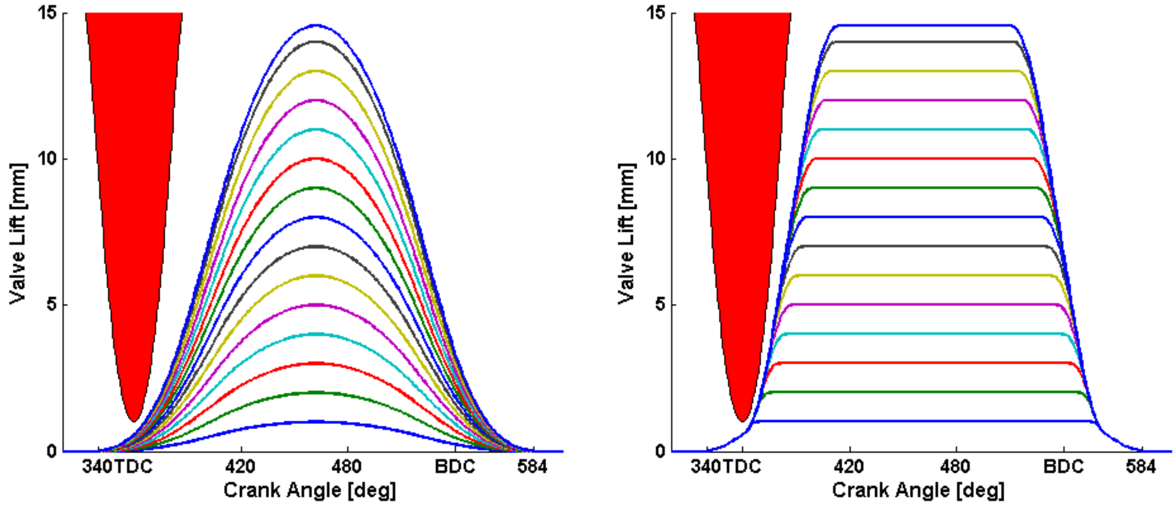

Figure 13. *The created valve profiles with standard appearance to the left, trapezoidal to the right and the piston limitation in red.*

The aim with the trapezoidal profiles in respect to the standard profiles is that a certain level of valve lift can be used during a longer duration and thereby the pumping losses can be reduced. Another advantage is that the duration of the maximum valve lift is much longer for trapezoidal valve profiles and thereby increasing the swirl generation, which is at its highest level at the maximum valve lift.

4.4 Load Points

The different load points that have been used during this master thesis are presented in Table 2. The engine speed and lambda sweep were performed at KTH, while the cell at Scania were used for the other load points.

Table 2. *The load points tested in this master thesis.*

Case	Engine Speed	SOI	Inj. Dur.	lambda	P_{CR}	P_{in}	$P_{exhaust}$	T_{in}	EGR
-	rpm	CA°	ms	-	bar	bar	bar	°C	%
Transient	1056	-5.0	2.17	~1.25	1077	0.59 – 0.87	0.55	25	0
SCR	1316	-7.0	1.38	~2.04	1186	0.81 – 1.44	0.83	25	0
EGR25	1316	-7.7	1.15	~1.57	1224	1.18 – 1.55	1.28 – 1.65	42	25
EGR30	1316	-7.7	1.15	~1.44	1224	1.23 – 1.31	1.33 – 1.41	42	30
EGR32.5	1316	-7.7	1.15	~1.37	1224	1.22 – 1.34	1.32 – 1.44	42	32.5
Engine Speed Sweep	1700 – 800	-10 to -3	1.4	~1.25	1500	0.12 – 0.34	0	25	0
Lambda Sweep	1000	-2	0.72 – 1.86	3 – 1	2000	0.5	0	25	0

Engine Speed and Lambda Sweep

In the project [2] preceding this master thesis the smoke emissions increased rapidly at higher engine speeds for the valve strategies which generated high swirl. Although this might have been a characteristic of the specific cylinder head used in the project, which was modified to generate a very high swirl number of 3.74 with the standard valve profiles. Therefore it was of interest to perform another engine speed sweep with the cylinder head used in this paper, which has a much lower swirl number of 1.59 and see whether the trends are similar. The same load point as in the project was used to conduct the test. The SOI was adjusted for each valve strategy and engine speed so that the maximum cylinder pressure was kept around 13 CAD. As the goal was to simulate a transient with a stationary load point, the engine was to run almost naturally aspirated. The inlet manifold pressure for the standard valve strategy was initially set at 0.12 bar and thereafter adjusted slightly so that a lambda value of 1.25 was achieved for each tested valve strategy, regardless of pumping losses and engine speed.

As it was known from the earlier project [2], some valve strategies had the potential to reduce the smoke emissions dramatically. To illustrate these differences a test was created in which the lambda values was swept from 3 to 1. This was achieved by increasing the injection duration and keeping the inlet manifold pressure fixed at 0.5 bar. SOI was kept constant and a common rail pressure of 2000 bar was used.

WHSC mode 9

To evaluate the influence of different valve strategies under realistic running conditions it was decided early on in the project that the majority of the load points were to be chosen from the WHSC emission test cycle, see Table 3.

Table 3. *The WHSC emission test cycle with the selected load point.* [11]

Mode	Speed	Load	Weighting Factor	Mode Length†
-	%	%	-	s
0	Motoring	-	0.24	-
1	0	0	0.17/2	210
2	55	100	0.02	50
3	55	25	0.10	250
4	55	70	0.03	75
5	35	100	0.02	50
6	25	25	0.08	200
7	45	70	0.03	75
8	45	25	0.06	150
9	55	50	0.05	125
10	75	100	0.02	50
11	35	50	0.08	200
12	35	25	0.10	250
13	0	0	0.17/2	210
Sum			1	1895
† Including 20 s ramp				

As the intention originally was to perform all the engine tests at KTH, special consideration had to be taken for the hydraulic actuators mounted on the exhaust valves. Thus the highest power levels and engine speeds were eliminated as possible test cases. The lowest power levels were likewise eliminated as the soot emissions at these load points were already very low and as a result it would be difficult to measure the difference in emissions between the valve strategies. Based on these requirements WHSC load points with a medium engine speed and a medium load were desired. As earlier engine tests had primarily been conducted at an engine speed of 1000 rpm, it was decided that it would be more rewarding to test a higher engine speed. This narrowed the possibilities further and the final choice fell on WHSC mode 9.

To determine the actual running conditions of the single cylinder engine, data was provided for a Scania DL6 480 hp Euro 5 engine equipped with EGR and a Scania DL6 440 hp Euro 5 engine equipped with Selective Catalytic Reduction, SCR, running the WHSC test cycle. The correct injection durations were found by matching the IMEP of the full-size engines with the single cylinder engine using the standard valve profiles and the inlet manifold pressure for the production engines, 0.83 bar for the SCR and 1.3 bar for the EGR load point. When changing the valve profiles the inlet manifold pressure were adjusted in order to keep the same lambda for all the strategies.

WHSC Transient

As the production engines are optimized to be able to meet the strict emission standards in the WHSC cycle it is unlikely that the load points specified in Table 3 will create large amounts of smoke. To be able to observe the effects of small differences in valve strategies, a higher initial smoke level was desired. For this purpose a load point was created in which the torque requirement goes from 50% to 100% at the same engine speed. As the majority of testing is done at 1316 rpm, it was decided to use a lower engine speed of 1056 rpm for this load point. In other words this simulates going from mode 11 to mode 5 in the WHSC cycle.

To create the worst case scenario for the smoke emissions the start of the transient is simulated, in other words the inlet manifold pressure is kept at the level of mode 11, 0.64 bar for the standard profiles, while the lambda value is lowered to 1.25 with an increased injection duration. When changing the valve profiles the inlet manifold pressure were adjusted in order to keep the same lambda for all the strategies.

EGR Sweep

The use of EGR to control NO_x emissions generally results in higher soot emissions. The soot that is generated during combustion can be oxidized in the later stages of the expansion stroke with the help of the swirl motion. To investigate the effects of different valve strategies on emissions with higher EGR levels, the mode 9 EGR case was run with two additional EGR levels of 30% and 32.5%.

As a starting point the standard valve profiles was used to determine a new reference lambda value at the new EGR level. During the tests the inlet manifold pressure was adjusted for the different valve strategies to achieve the reference lambda value. This was done to be able to compare valve strategies with large differences in volumetric efficiency in a reasonable manner. For the next EGR level the inlet manifold pressure was reset to the default level of mode 9 and a new reference lambda value was determined.

5 Calculations and Simulations

From the steady state flow bench tests different flow parameters can be calculated in order to describe the characteristics of the flow in the cylinder. The parameters investigated in this master thesis are swirl, tumble and μσ. However there are several definitions on how to calculate the different parameters. In this project two methods for calculating the flow parameters have been studied, the traditional Thien method and with the 1D engine simulation software GT-Power.

5.1 Thien flow parameters

Thien [12], [13], [14], has developed a method to characterize the in-cylinder flow to be able to optimize the air flow in a four-stroke diesel engine. His work has been the base for the study of the flow parameters, and in chapters 5.1 a review of the used equations and formulas in this master thesis can be seen.

5.1.1 Thien Swirl

The dimensionless swirl number, N, is describing the rotational speed of the air in the cylinder, most commonly at BDC, normalized against a fictitious engine speed. Before the use of a honey comb torque meter in the flow bench a paddlewheel measuring the rotational speed was used, and then the Swirl Number was defined according to

$$N = \frac{n_D}{n} \tag{1}$$

$n_D =$ the paddlewheel rotational speed, measured during test
$n =$ a fictitious engine speed.

The fictitious engine speed is given by the assumption that the air flow velocity in the cylinder of the flow bench, w_2, is equal to a fictitious mean piston velocity, c_m, were

$$w_2 = \frac{q}{\frac{\pi D^2}{4}\rho_2} \tag{2}$$

$q =$ mass flow of air through the flow bench, measured during test
$D =$ cylinder bore
$\rho_2 =$ density of the air in the cylinder

and

$$c_m = \frac{s \cdot n}{30} \tag{3}$$

$s =$ engine stroke.

Equation (2) and (3), together with the assumption that $w_2 = c_m$, gives the expression

$$n = \frac{30q}{s\frac{\pi D^2}{4}\rho_2}. \tag{4}$$

With the use of a honey comb torque meter in a flow bench an equation for a fictitious paddlewheel rotational speed, n_d, is used according to

$$n_D = \frac{60\omega}{2\pi} \tag{5}$$

where

$\omega =$ the angular velocity of a fictitious paddlewheel, is given by

$$\omega = \frac{8M}{qD^2} \tag{6}$$

$M =$ the torque at the honey comb, measured during test.

Equation (5) and (6) together with equation (1) and (4) gives the expression

$$N = 2s \cdot \frac{M \cdot \rho_2}{q^2} \tag{7}$$

for the Swirl Number, were only ρ_2 is unknown. This can be calculated by the isentropic relation between the gas inside and outside of the flow bench, giving the expression

$$\rho_2 = \rho_1 \left(\frac{p_1 - \Delta p}{p_1}\right)^{\frac{1}{\kappa}} \tag{8}$$

$p_1 =$ air pressure outside the flow bench, the barometric pressure, measured during test
$\Delta p =$ pressure drop over the ports, set during test
$\kappa =$ coefficient for isentropic compression

and ρ_1, density of the air outside the flow bench box, is given by

$$\rho_1 = \frac{p_1}{R \cdot T_1} \tag{9}$$

$R =$ universal gas constant
$T_1 =$ temperature outside the flow bench box, measured during test.

5.1.2 Thien Mean Swirl

To be able to describe the air movement in the cylinder during an intake stroke, the cylinder charge is assumed to be a solid cylinder with the volume equal to the cylinder displacement, V_s, with the angular momentum equal to the sum of the torque of the impulses of incoming air. The angular impulse generated in the time increment dt is then described by the rotational speed of a cylindrical air head, $n_D(\alpha)$, with a volume equal to the incremental air quantity dV.

The mean swirl number according to Thien, $\left(\frac{n_D}{n}\right)_{mean}$, is then defined as

$$\left(\frac{n_D}{n}\right)_{mean} = \frac{1}{V_s} \int_{TDC\ (V=0)}^{BDC\ (V=V_s)} \frac{n_D(\alpha)}{n} dV \tag{10}$$

$\alpha =$ crank angle.

The swirl number during the flow bench test indicates a fictitious paddlewheel's rotational speed in relationship to a fictitious mean piston speed, c_m. Because of this, the instantaneous swirl number during a simulated intake stroke, $n_D(\alpha)/n$, is dependent of the instantaneous swirl number from the test, $N(\alpha)$, and the instantaneous piston speed $\mathrm{c}(\alpha)$ according to

$$\frac{n_D(\alpha)}{n} = N(\alpha)\frac{c(\alpha)}{c_m}. \tag{11}$$

If $z(\alpha)$ is defined as the relationship between the instantaneous cylinder volume, $V(\alpha)$, and the piston displacement volume according to

$$z(\alpha) = \frac{V(\alpha)}{V_s} \tag{12}$$

then the instantaneous piston speed can be defined as

$$c(\alpha) = s\frac{dz(\alpha)}{dt} = s\frac{d\alpha}{dt}\cdot\frac{dz(\alpha)}{d\alpha} = \frac{s\cdot n}{30}\cdot\pi\cdot\frac{dz(\alpha)}{d\alpha}. \tag{13}$$

Equation (3) together with (13) gives the equation

$$\frac{c(\alpha)}{c_m} = \pi\frac{dz(\alpha)}{d\alpha} \tag{14}$$

and thereby equation (11) can be written as

$$\frac{n_D(\alpha)}{n} = N(\alpha)\cdot\pi\cdot\frac{dz(\alpha)}{d\alpha}. \tag{15}$$

The derivative of equation (12) gives

$$dV = V_s\frac{dz(\alpha)}{d\alpha}d\alpha \tag{16}$$

and equation (15) together with (16) inserted to equation (10) leads to the expression

$$\left(\frac{n_D}{n}\right)_{mean} = \pi\int_{TDC}^{BDC} N(\alpha)\left(\frac{dz(\alpha)}{d\alpha}\right)^2 d\alpha\,. \tag{17}$$

From a given valve profile this equation can be calculated from a steady state flow bench test if an expression for $\frac{dz(\alpha)}{d\alpha}$ is derived. From a geometrical study of the piston movement related to the crank angle, see Figure 14, an expression for the piston velocity, $\frac{dy(\alpha)}{d\alpha}$, can be derived according to

$$\frac{dy(\alpha)}{d\alpha} = R\sin(\alpha) + \frac{L \cdot h^2 \cdot \sin(\alpha)\cos(\alpha)}{\sqrt{1 - h^2 \cdot \sin^2(\alpha)}} \tag{18}$$

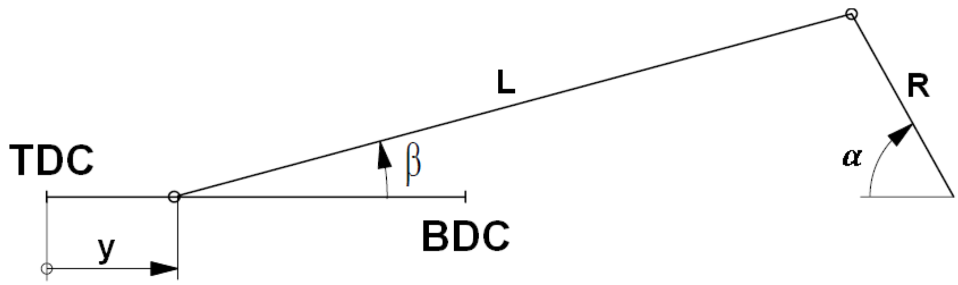

Figure 14. *A geometrical illustration of the piston movement.*

were

$R =$ crank radius
$L =$ connecting rod length
$\beta =$ connecting rod angle (help parameter to get the expression)

and

$$h = \frac{R}{L}. \tag{19}$$

From equation (18) and (19) together with the relationship

$$z = \frac{y}{s} = \frac{y}{2R} \tag{20}$$

an expression for $\frac{dz(\alpha)}{d\alpha}$ is obtained according to

$$\frac{dz(\alpha)}{d\alpha} = \frac{dy(\alpha)}{d\alpha} \cdot \frac{1}{2R} = \frac{1}{2}\sin(\alpha) + \frac{h}{2} \cdot \frac{\sin(\alpha)\cos(\alpha)}{\sqrt{1 - h^2 \cdot \sin^2(\alpha)}}. \tag{21}$$

Since the amount of air entering the cylinder is described with the volume change with Thien mean swirl, a disadvantage with this method occurs. The volume change is only positive from TDC to BDC during the intake stroke, and thereby the intake of air in the cylinder only can be described from TDC to BDC. To some extent air can flow into the cylinder even with a negative volume change due to pulsations in the inlet system and this is neglected with this method. With some valve strategies, for example miller with Late Inlet Valve Closing, LIVC, also a great amount of backflow with air from the cylinder back to the inlet ports occurs. Such phenomena's effects on the mean swirl cannot be described with this method either.

In Figure 15, the part of the valve lift contributing to the mean swirl according to Thien can be seen for a standard Scania D12 inlet valve profile. There it can be seen that, for this profile, the part that is neglected at the valve opening is really small, but that there is a bit bigger part neglected at the valve closing.

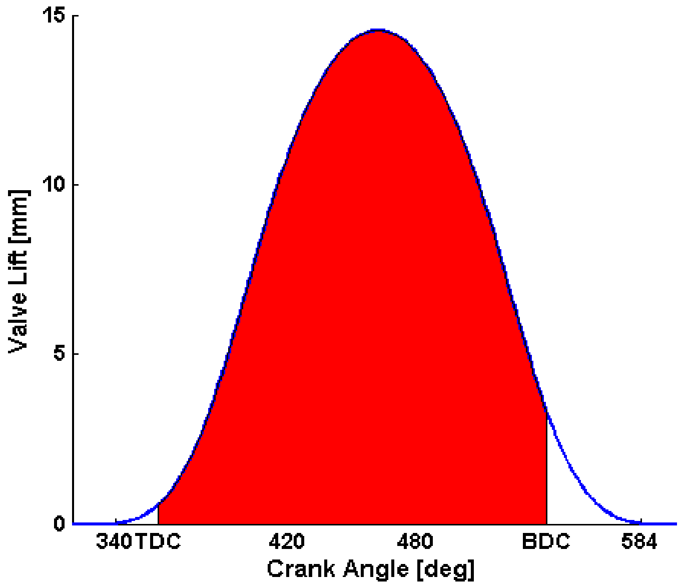

Figure 15. *The part of the valve lift that contributes to the mean swirl calculation for a standard Scania D12 inlet profile.*

As a whole the neglected parts from the valve lift can still be considered as reasonable small for the standard profile.

5.1.3 Thien Tumble and Thien Mean Tumble

To evaluate the tumble motion generated from the inlet ports the same equations were used as for the swirl motion, both for the steady state tumble number for different valve lifts and for the mean tumble.

One big difference for the tumble measurement in contrast to the swirl measurement is that it has one more degree of freedom, which is the angle of the cylinder head. This is because the angle of the maximum tumble is affected by the strength of the swirl motion The traditional way of measuring the tumble motion is to start with measuring tumble at the maximum valve lift at different angles to find the angle that gives the highest tumble. After this the angle is fixed and the tumble motion is measured for the different valve lifts.

In this project another strategy was used. The tumble motion for a specific angle was measured for every valve lift from maximum to zero with 1 mm steps, and this was done with 15 degree steps for the cylinder head angles. The reason for this was to study if maximum tumble was obtained at different angles for different valve lifts. A comparison of the methods is illustrated in Figure 16.

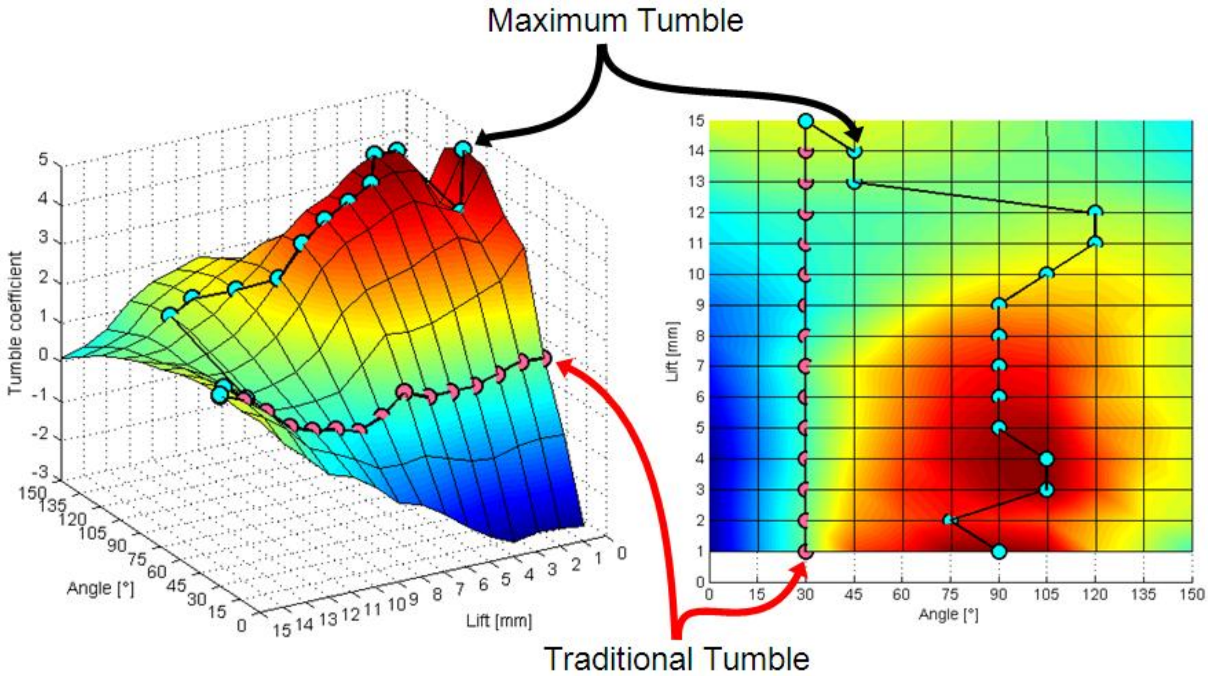

Figure 16. *Graphs comparing the two measuring methods for tumble motion measured with only the valve to the straight port active. The same case is plotted in both graphs, they are only illustrated in two different ways.*

Here it can be seen that the different methods widely differs in the results. If the traditional method is used the information of the large peak in tumble at lower lifts is lost. For this particular case, the traditional method gives a mean tumble of 1.36 according to Thien, while the method with maximum tumble gives a mean tumble of 2.68 with the standard valve profile. Valve profiles with lower maximum valve lifts gives even greater difference in the mean tumble values between the two methods.

Because of the differences between the methods the maximum tumble has been used when calculating the mean tumble in this master thesis. This is perhaps not the optimal method as the tumble motion at one valve lift might be disrupted by the tumble motion at another valve lift if the angle between them changes too drastically. As the maximum tumble angle changes very little in the region of high tumble, this effect is assumed to be negligible.

5.1.4 Thien μσ

$\mu\sigma$ is a parameter describing how effective the intake ports are when it comes to transporting air into the cylinder, or on the other hand how effective the outlet ports transports exhaust away from the cylinder. This is done by comparing the actual air flow through the ports, q_{eff}, by an ideal air flow, q_{teor}, calculated with a reference area, A_0, according to

$$\mu\sigma = \frac{q_{eff}}{q_{teor}} = \frac{q_{eff}}{w_2 A_0 \rho} \tag{22}$$

were

$\rho = \rho_m =$ mean air density through the ports = $\frac{\rho_1+\rho_2}{2}$, given by equation (8) and (9)

and

$w_2 =$ theoretical flow velocity through the ports. This is given by the assumption of a lossless and incompressible flow used together with the Bernoulli equation leading to the expression

$$w_2 = \sqrt{\frac{2\Delta p}{\rho_m}}. \tag{23}$$

Depending on the geometric layout of the inlet and outlet ports the reference area, A_0, is calculated in a different way if it is the inlet or outlet ports that are studied. For the inlet ports, that are separated all the way from the plenum to the cylinder, the ideal flow is limited by the inner valve seat diameter, d, giving the equation

$$A_{0,Inlet} = n\frac{\pi d^2}{4} \tag{24}$$

$n =$ number of valves used.

On the other hand, the two outlet ports are joined together before the outlet from the cylinder head, causing the outlet diameter of the joined ports, d_{out}, to be the limitation of the ideal flow, with the expression

$$A_{0,Outlet} = \frac{\pi d_{out}^2}{4}. \tag{25}$$

For the outlet ports the calculation of $\mu\sigma$ can be done using two different methods, the total-static pressure method or the total-total pressure method causing different calculations for ρ_1 and ρ_2. Since this master thesis mostly have been focused on the inlet ports no deeper analysis of the methods will be given here, but the methods is described in one of Thien's reports [12]. Also the equations leading to the expression for the mean $\mu\sigma$ according to

$$\mu\sigma_{mean} = \frac{1}{\pi\sqrt{\int_{TDC}^{BDC}\left(\frac{dz(\alpha)}{d\alpha}\right)^3\left(\frac{1}{\mu\sigma(\alpha)}\right)^2 d\alpha}} \tag{26}$$

can be found there.

5.2 GT-Power Simulation

GT-Power is a powerful simulation tool for engine development used by engineers worldwide. From the beginning of this project a GT-Power model was given for the single cylinder setup in Cell 4 at KTH, see Figure 17. The aim with this master thesis was to investigate how GT-Power is describing the in-cylinder flow of an engine, so the focus has mostly been on this part of GT-Power. The program has been used to simulate different inlet valve strategies and study the given swirl and tumble values.

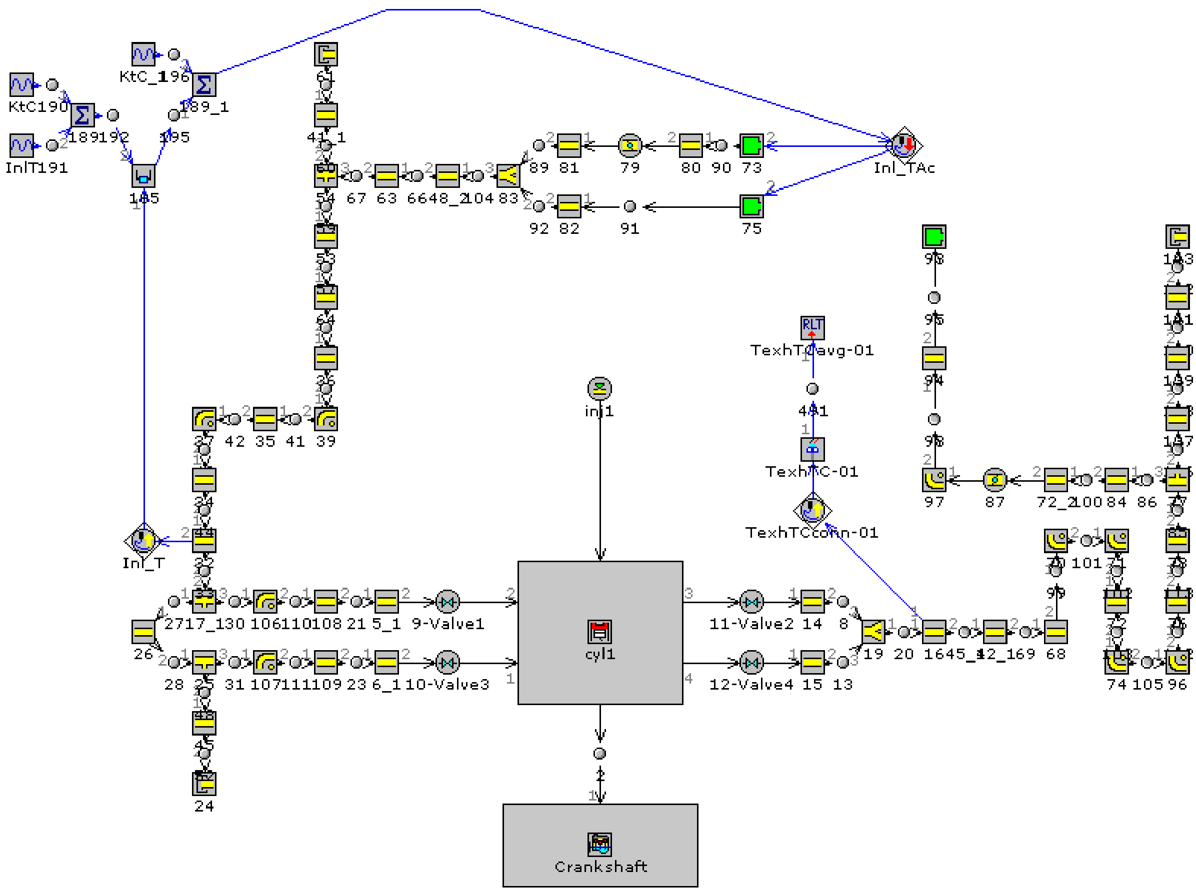

Figure 17. *The GT-Power model for the single cylinder engine at KTH, with the system for the inlet on the left side, the outlet on the right side and the engine in the middle.*

5.3 GT-Power flow parameters

From data obtained at the steady state flow bench different flow parameters can be calculated to be input to a GT-Power model. These parameters are *Forward CD*, *Reverse CD*, *Swirl Coefficient* and *Tumble Coefficient*. In the chapter below these parameters are described and how they should be calculated are defined. The parameters are also described in the Engine Manual for GT-Power [15].

5.3.1 GT-Power Swirl and Tumble Calculations

The swirl and tumble Coefficient in GT-Power is parameters describing how much swirl and tumble torque that will be applied to the in-cylinder gases, depending on the amount of mass flow in to the cylinder. The equations

$$C_s = \frac{2T_s}{\dot{m} \cdot U_{is} \cdot D} \tag{27}$$

$$C_t = \frac{2T_t}{\dot{m} \cdot U_{is} \cdot D} \tag{28}$$

are used to calculate the parameters for different valve lifts were

C_s = swirl coefficient
C_t = tumble coefficient
T_s = swirl torque, from the steady state flow bench
T_t = tumble torque, from the steady state flow bench
$\dot{m}$ = mass flow rate, from the steady state flow bench
D = cylinder bore

and U_{is} is the isentropic air velocity given by

$$U_{is} = \sqrt{RT_o}\left\{\frac{2\gamma}{\gamma - 1}\left[1 - P_R^{\frac{\gamma-1}{\gamma}}\right]\right\}^{1/2} \tag{29}$$

R = universal gas constant
T_o = upstream stagnation temperature, measured during test (temperature outside the flow bench box)
γ = specific heat ratio (1.4 for air at 300K)
P_R = absolute pressure ratio, according to

$$P_R = \frac{p_1 - \Delta p}{p_1}. \tag{30}$$

The parameters p_1 and Δp are also given from the steady state flow bench test, see equation (8).

In GT-Power a quite complex model for calculating Swirl and Tumble at different crank angles is implemented. This model is thoroughly described in a paper written by Morel, T and Keribar, R [16].

To calculate the swirl and tumble the air motion inside the cylinder is assumed to be performing a rigid body rotation. From the swirl and tumble coefficients together with the calculated mass flow through the ports, given by the pulsating flow and the discharge coefficient, a torque is calculated that is added to the angular momentum of the rigid body in the swirl and tumble direction. In addition to this a friction model is used to describe how the rigid body is decelerated by the friction between the air and the cylinder wall.

The positive thing with this model in respects to the Thien model is that the swirl and tumble motion can be calculated during the whole intake stroke since the mass flow is used instead of the volume change to describe the flow into the cylinder. This doesn't have any great effect on the calculations if a standard valve profile is used, as can be seen in Figure 15, but can affect greatly if valve profile with for example LIVC is used in a Miller strategy.

Another thing is that the mass flow is calculated from the given geometry of the pipes, and if the model of the engine-layout is good, then the mass flow really well can be describing the real actual flow into the cylinder. This means that also effects of pressure pulses causing pulsating flow is taken into account by the model. The model is also active during the whole engine cycle so the change in swirl and tumble can be seen during the compression stroke and combustion. The swirl and tumble number used in this report to compare the different models is the one given at BDC.

5.3.2 GT-Power CD

The description of how to calculate discharge parameters for GT-Power, *CD*, is best found in the Flow Theory Manual for GT-Power [17]. The formulas provided in the manual gives the same final equation for calculating *CD* for GT-Power as Thien $\mu\sigma$, see equation (22) to (25).

As input parameters for the flow efficiency GT-Power needs both forward and reverse discharge coefficients. The forward discharge coefficient is used when the flow is in the regular direction, which is for example from the inlet through the valve and into the cylinder from the inlet side, and this is the one regularly measured during flow bench tests. That is also the most important one because the flow is mostly in the forward direction, and a very small amount of backflow occurs. For this reason only the forward *CD* was measured during the flow bench tests, and then the assumption was made that the reverse *CD* should be equal to the forward *CD* when implementing it into GT-Power. In reality there can be some differences between these two parameters, but since the reverse *CD* only effects the backflow and this is a small part of the flow this assumption should have a little effect on the simulation.

5.3.3 GT-Power Turbulent Intensity

GT-Power also has a parameter describing how turbulent the flow in the cylinder is. The turbulent intensity is mostly dependent on the speed of the air flow that is passing the valves into the cylinder, where a higher speed causes a higher Reynolds number and therefore a higher turbulence. Also the turbulent intensity is calculated with a quite complex model and this is described in the paper by Morel, T and Keribar, R [16].

The parameter that is obtained from the GT-Power simulations is the normalized turbulent intensity, defined at 100 CAD before TDC fire, TDCF. This parameter is defined in the help section in GT-Power for the *EngCylinder* template according to

$$nti = \frac{u'}{V_p} \tag{31}$$

$nti =$ normalized turbulent intensity
$u' =$ turbulent intensity
$V_p =$ mean velocity of the piston.

5.4 Implementing the Flow Coefficients in GT-Power

From steady state flow bench tests and calculations of the flow parameters the coefficients for GT-Power had to be implemented in the model. The inlet ports in the cylinder head and the valves are described in the model by a template called *ValveCamConn*. Under *Flow Arrays* in this template the different flow coefficients calculated is implemented. The different coefficients are, in this project, added for every valve lift from 0 mm to 15 mm with 1 mm step. The interval can be chosen freely because of the use of a reference array. The reference parameter is simply the value of the valve lift divided by the valve seat diameter. One important thing when implementing the parameters is that the reference array must start with 0 and end with 1.

One major problem with this method for calculating the flow parameters is that there are one *ValveCamConn* for each valve and no way have been found to make the different valves communicate with each other. For a real engine the flow is dependent on the valve lift for both the inlet ports since the flow from the two ports are interacting with each other.

Therefore three different models were developed for different cases. For the first model flow coefficients from the flow bench with symmetrical valve lifts were used for both the valves, causing the model to be accurate when both the valves are lifted equally during the whole intake stroke. This model will be referred to as the *2V model*.

In the second model, flow coefficients from data with only one valve active at a time were used and implemented in the respective valve template. This model will be referred to as the *1V model* and is accurate for cases when only one inlet valve is used during the whole intake stroke. In the same way data from measurements with one port blocked at a time was implemented in the third model, and will be referred to as the *Blocked model*, that will be accurate when only one port is open but with symmetrical valve lift during the whole intake stroke.

6 Results

In chapter 6 the results from the flow bench, the comparison of the Thien and GT-Power method and from the engine tests are presented.

6.1 Flow Bench Results

In the following chapters the results from the steady state flow bench tests are presented and discussed. Tests have mostly been performed with the cylinder head described in the engine setup chapter, with a mean swirl of 1.59 with the original valve profiles. If nothing else is mentioned it is this cylinder head the results are from.

In order to bring an understanding of the labeling of the different tests a short description will be given here. Tests have been performed with both the inlet valves lifted equally, i.e. symmetrical valve lifts. This case will be labeled 2V (Original). Another strategy is to deactivate one of the inlet valves, and these cases will be labeled 1V Curved Port when only the valve to the curved port is active, and 1V Straight Port when the valve to the straight port is active. In addition to this it is interesting to see how the flow from one port is affected by the valve head and stem from the other valve. In order to do so tests have been performed with symmetrical valve lifts and one of the intake ports blocked. These cases will be labeled 2V Curved Port (Straight Port Blocked) and 2V Straight Port (Curved Port Blocked).

For the swirl measurements, studies also have been performed with asymmetrical valve lifts. This was done with a fix valve lift on the valve to the straight port while sweeping the lift on the valve to the curved port. After a complete lift sweep of the curved port, the lift was changed on the straight port and then the same procedure was repeated.

For all the tests presented in the following chapters the pressure drop over the ports have been set to 25 mBar. To investigate how the pressure drop over the ports influence the swirl measurements tests were performed with a higher pressure drop, 50 mBar. These tests showed on a very small variation of the test results depending on the pressure drop. The data from this measurement can be found in Appendix 1.

6.1.1 Swirl

The swirl number according to Thien for the different valve strategies as a function of valve lift can be seen in Figure 18. Here it is seen that the swirl increases with increasing valve lift regardless of the valve strategy, at least for valve lifts over 6 mm. One thing that should be pointed out is that the measurement of the swirl number at low valve lifts, especially at 1 mm lift, is very uncertain. This is because at low valve lifts the flow through the ports is very low and thereby a small change in the measured torque will greatly affect the swirl number. This can be seen in the plot as the swirl numbers vary widely at 1 mm lift. Since the low valve lift is used during a really short period of the intake stroke this uncertainty has a small effect when calculating mean swirl.

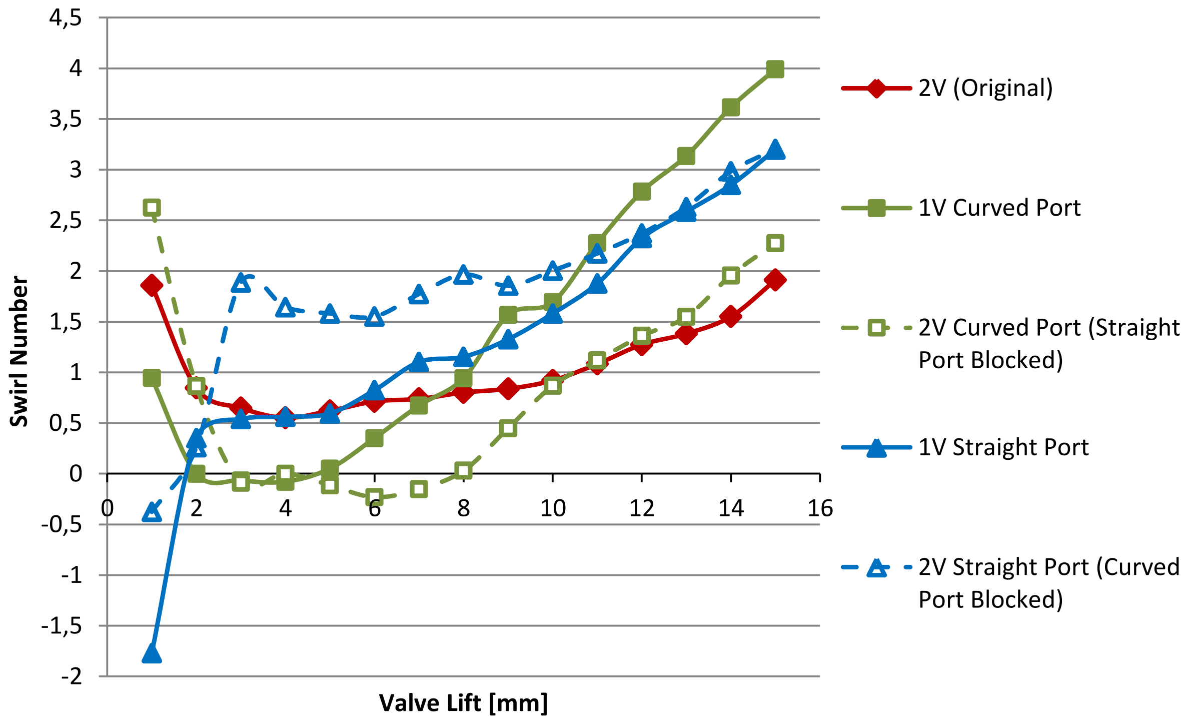

Figure 18. *Swirl Number as a function of valve lift for the case with 2 valves, 1 valve and the case with 2 valves but with one port blocked.*

For the 1V Curved Port case, it can be seen that the swirl generation is really high for high valve lifts, but at low valve lifts it is really small or even negative. A negative swirl number means that the flow in the cylinder is rotating in the opposite direction in respect to the main swirl direction.

If the case 2V Curved Port (Straight Port Blocked) is studied, i.e. with both valves lifted but only a flow through the curved port, it is seen that the swirl number is greatly decreased at high valve lifts. If the layout of the valves and the ports is investigated, see Figure 19, it can be noticed that the valve for the straight port, valve 3, is placed directly after the inlet of the curved port in the flow direction.

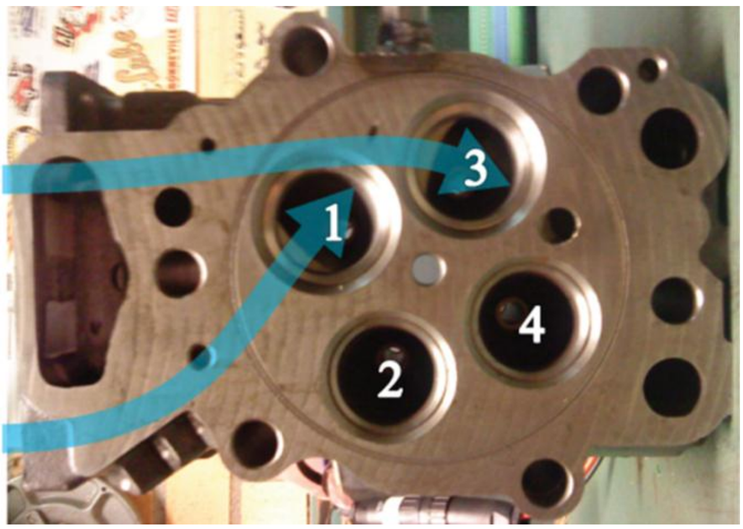

Figure 19. *The layout of the valves and the ports in the cylinder head. The numbering of the valves comes from the Lotus AVT-system. The Curved Port goes to valve 1 and the Straight Port to Valve 3.*

Therefore the valve head and stem at the straight port will greatly affect the flow from the curved port, causing the main flow to be separated into several flows in different directions, and this is the most likely reason for the lowered swirl generation.

If the 1V Straight Port case is investigated it is shown that the swirl generation for high lifts is higher than the 2V (Original) case, but a bit lower than with the 1V Curved Port. For lower valve lifts the swirl is higher than the 1V Curved Ports and about the same as for the 2V (Original) case. If the swirl generation is compared to the 2V Straight Port (Curved Port Blocked), it can be seen that it is increased with lifts on both valves at the lower valve lifts. Again, if the layout of the ports and valves is studied, it can be seen that the valve for the curved port is placed before the inlet of the straight port. At lower valve lifts the valve head chokes the flow and causes a certain amount of flow in the opposite direction of the main swirl, i.e. towards valve 1. If valve 1 is lifted it can disturb this flow, while the flow in the main direction can be built up and continue down the cylinder so it won't be disturbed by the valve head when passing valve 1 after almost one complete rotation. This might be the explanation of why the swirl generation is higher at lower lifts with both valves lifted instead of valve 1 deactivated.

The swirl results from the study of asymmetrical valve lifts can be seen in Figure 20. One interesting observation from this plot is that it's only when one valve is completely deactivated that the swirl number increases greatly at higher lifts. For this figure it should also be mentioned that the white area at lifts from 3-5 mm for only the curved port and for the straight port around 1 mm is because the swirl number at these locations are negative, but the negative values are not plotted in the figure.

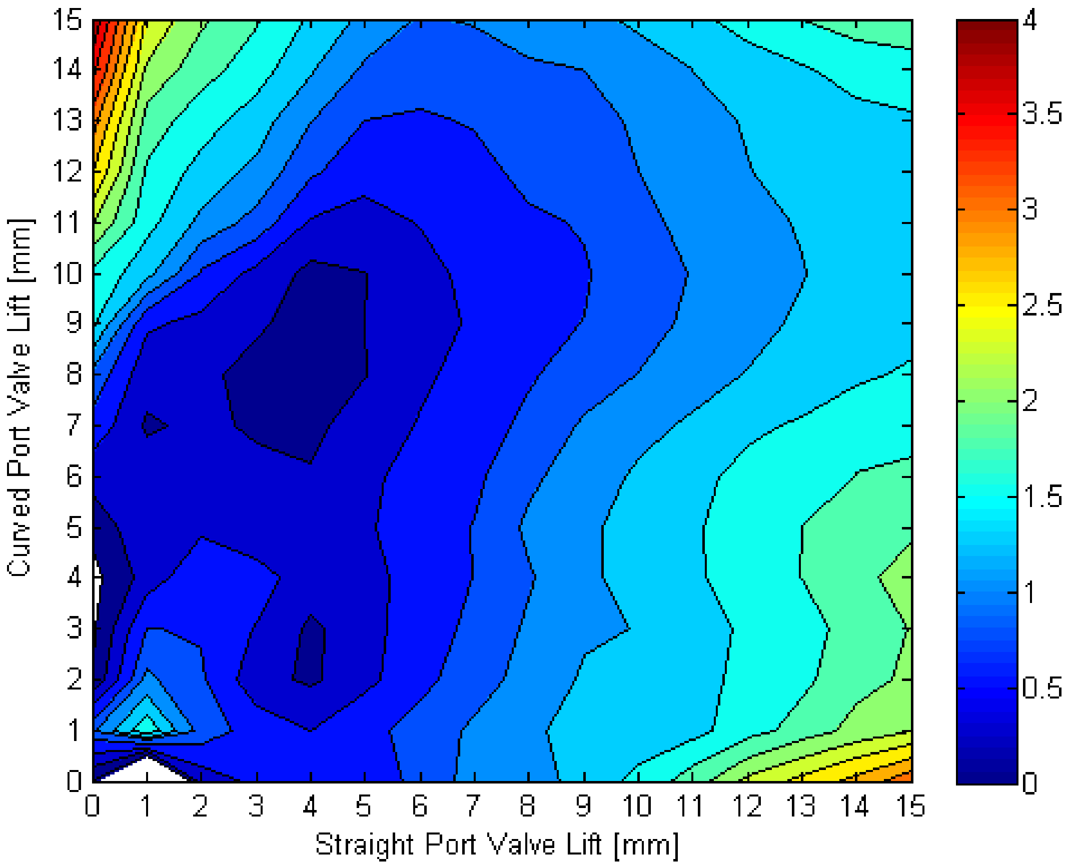

Figure 20. *The Swirl Number as a function of different valve lift combinations.*

6.1.2 Tumble

The tumble measurements in this master thesis have been performed with 15 deg steps for the cylinder head angles. Results from these measurements can be seen in Figure 21 for the 2V (Original) case and the 1V Straight Port case. Here it can be observed that the case with two valves has a much more flat and lower curve than the case with the straight port. The tumble decreases with decreasing valve lift for the 2V case while in the 1V case it greatly increases, causing a peak in the tumble motion at around 5 mm valve lift. Another interesting thing to observe is that there is a minimum value for the tumble motion at around 13 mm valve lift for the 1V case. As in the case with swirl measurements, the tumble number at low valve lifts, especially at 1 mm, is quite uncertain.

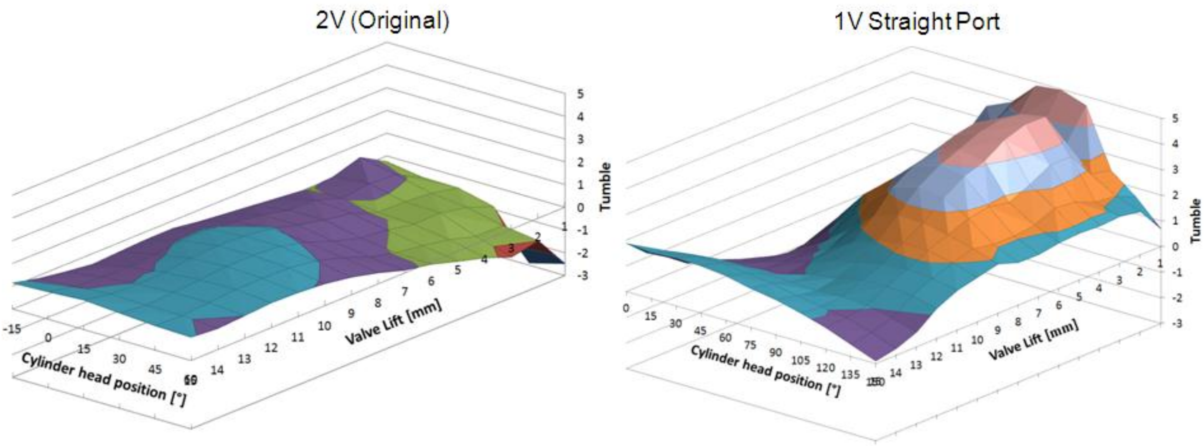

Figure 21. *Tumble Number as a function of valve lift and cylinder head angle for the 2V (Original) case to the left and the 1V Straight Port case to the right.*

As described earlier the maximum tumble for each valve lift were used for the mean tumble calculations in this project. Figure 22 illustrates the maximum tumble for the all the measured cases. From the figure it can be seen that there is much less tumble generation at lower valve lifts for the case with flow through both ports in respect to the cases with flow through one port. Another thing that could be observed is that the tumble motion at low valve lifts, below 5 mm, is negative for the 2V (Original) case.

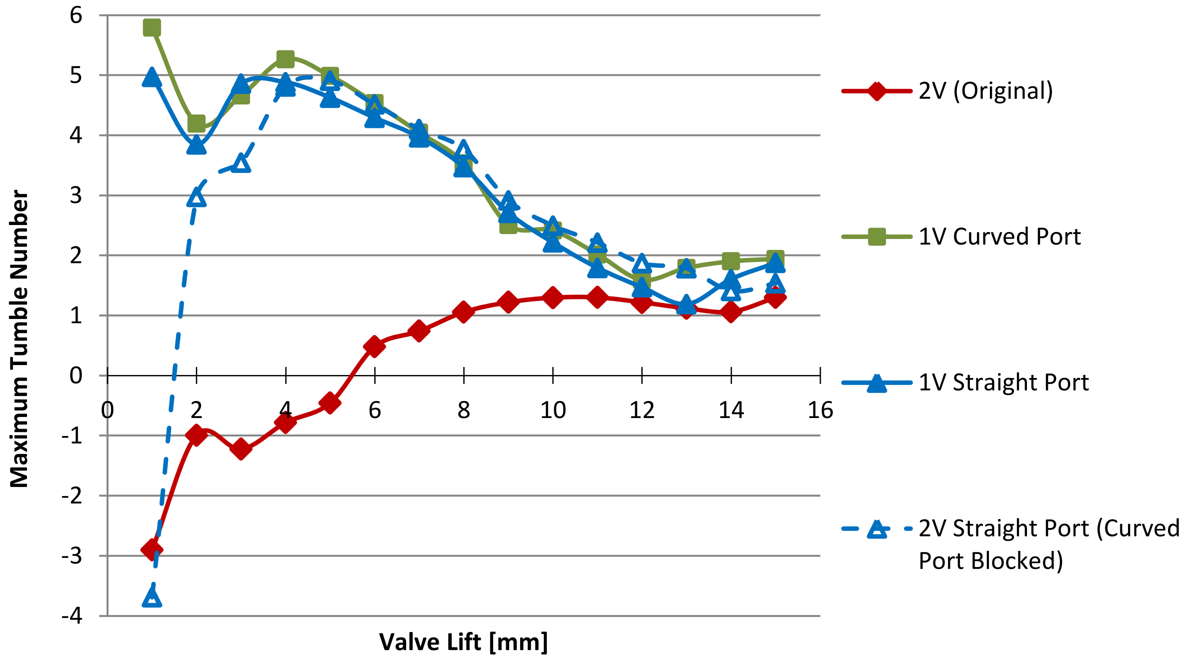

Figure 22. *Maximum Tumble Number as a function of valve lift for the studied cases.*

It is also interesting to see that all cases with flow only through one port has almost the same tumble generation, regardless of which port is used and if the valve is deactivated or if the other port is blocked.

If the cylinder head angle that gives the maximum tumble for each valve lift is studied, see Figure 23, it can be observed that the angles for the 2V (Original) case is between the angles for each port respectively. This is thought to be one of the reasons to why the 2V case have much lower tumble, than the individual ports by them self, as the tumble motion from each port is counteracting each other.

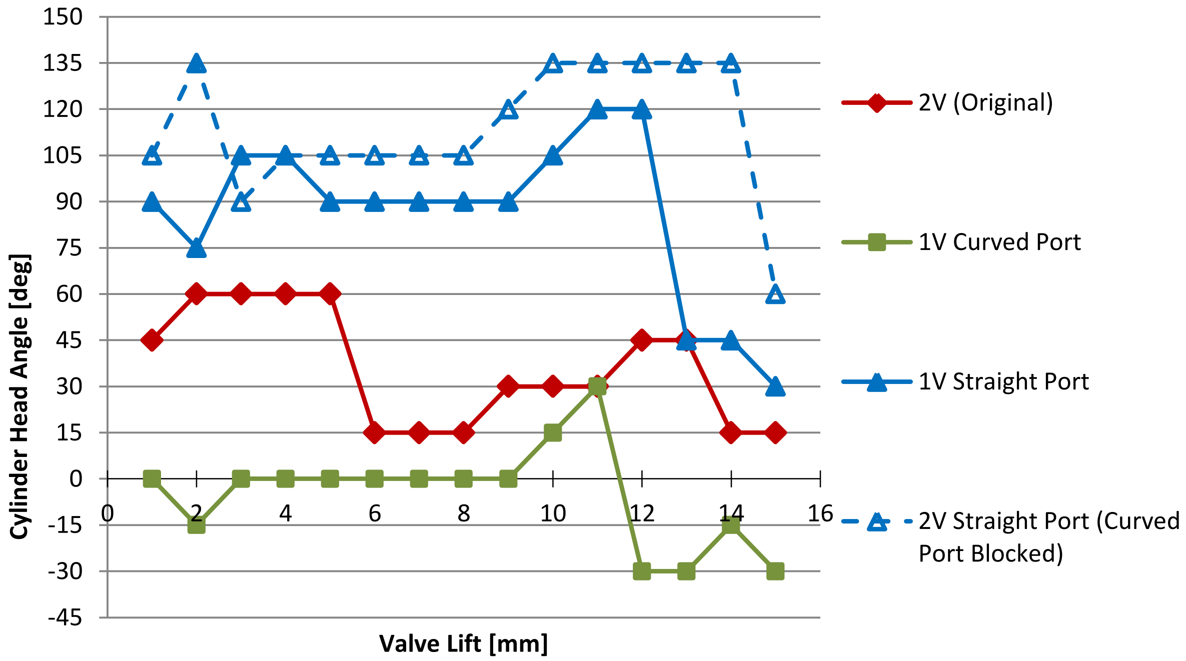

Figure 23. *The Cylinder Head Angle that gives the maximum Tumble Number for each valve lift.*

It can also be seen that there is really small differences between the 1V Straight Port case and 2V Straight Port (Curved Port Blocked), both for the cylinder head angle and for the maximum tumble. This leads to the conclusion that the valve lift at the curved port has really low effect on the tumble generation from the straight port. Another thing that can be seen in the figure is that, for each case, there is quite a small deviation between the cylinder head angles for maximum tumble between the different valve lifts. So even if there should be another way of selecting the tumble number for each valve lift, let's say with the cylinder head angle that gives the highest mean tumble, it wouldn't make a big difference compared to the calculations in this project.

6.1.3 Intake Manifold effects

To investigate the effects from intake manifolds on the measured swirl and tumble, tests have been performed with both the manifold from KTH and from Scania.

Intake Manifold KTH

The intake manifold from KTH was only accessible for flow measurements during a limited time, and at the specific time the cylinder head used in this master thesis wasn't available. In order to be able to investigate the effects of the inlet two other very similar cylinder heads where used. The cylinder heads had been modified to create different swirl numbers, one head had a mean swirl of 1.08 and the other one 3.20, with the original valve profiles. These cylinder heads haven't been used during the engine tests.

For the swirl measurements both cylinder heads were tested with the 2V (Original), 1V Curved Port (Straight Port Blocked) and 1V Straight Port (Curved Port Blocked) cases. These tests can be seen in Figure 24 for the low-swirl cylinder head.

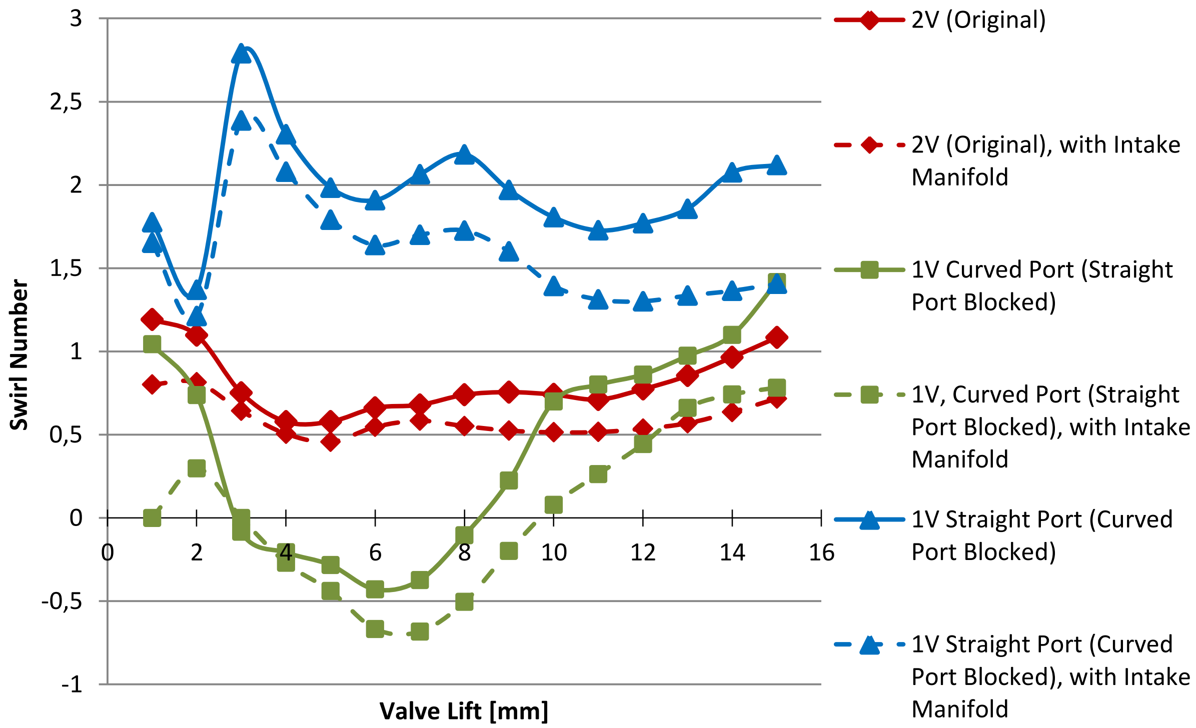

Figure 24. *The effects from the intake manifold from KTH on the measured swirl numbers for the low-swirl head.*

It can be seen that the intake manifold generates swirl in the opposite direction of the main swirl motion for the cylinder head. Therefore the positive swirl values are lowered and the negative swirl values are increased. The trend is also that the swirl is more highly affected at high valve lifts than lower, and this is true for all cases.

The same plot can be seen for the high-swirl cylinder head in Appendix 2. There it can be seen that the trends are the same also with this cylinder head, the swirl numbers are decreased with the intake manifold and the same happens no matter what case that is studied. This leads to the conclusion that intake manifold most likely affects the measured data from the used cylinder head during the rest of the master thesis in the same way, and that no matter what valve strategy used the effect is the same. Because of this conclusion, and the fact that no measurements were performed with the cylinder head used during engine tests, no recalculation of the swirl number was performed for the engine tests at KTH.

The study of the effects from the intake manifold on the tumble generation was performed only at one cylinder head angle, 0 degrees. A wide sweep could not be performed because of limitations in the flow bench cell, as the intake manifold couldn't be fitted on the cylinder head at any other angle. In Figure 25 the effects from the intake manifold can be seen for the low-swirl head for the 2V (Original) and 1V Straight Port (Curved Port Blocked) cases.

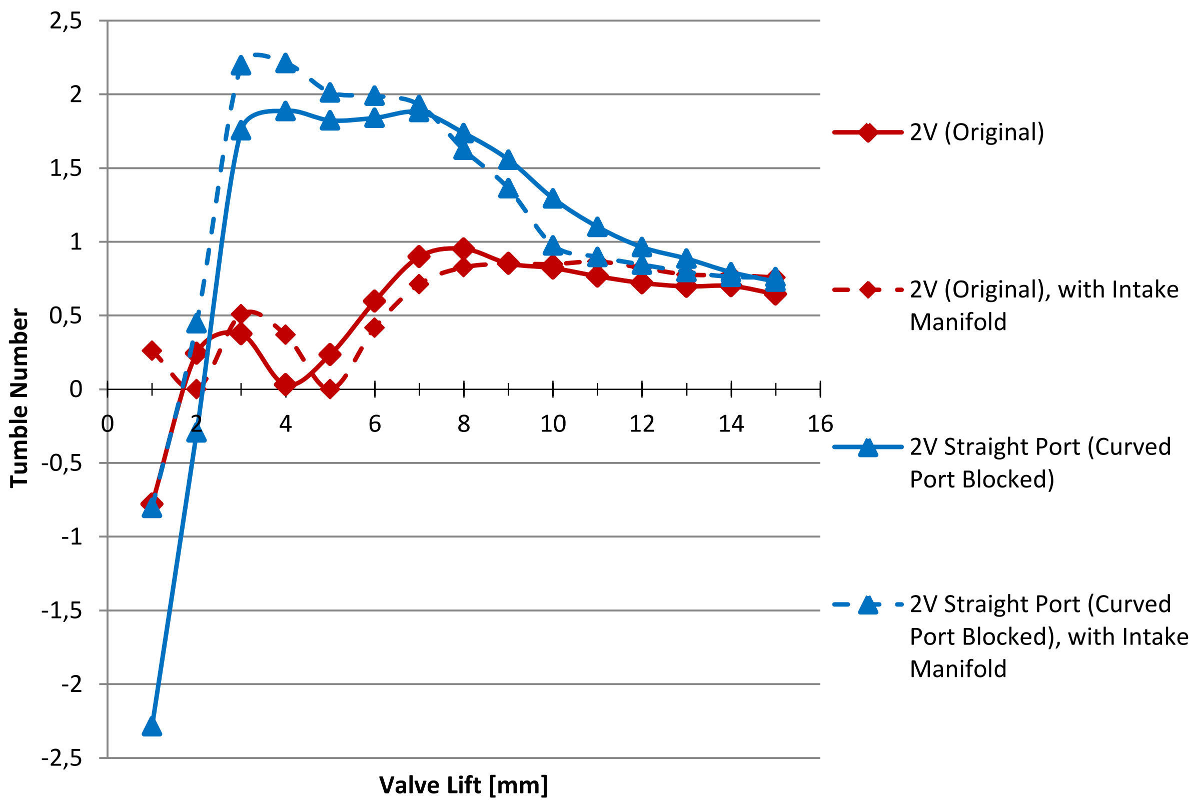

Figure 25. *The effect from the intake manifold from KTH on the measured tumble numbers for the low-swirl cylinder head.*

From this figure the conclusion can be drawn that the intake manifold had a very little effect on the tumble motion, the measured values were almost equal for both the cases with and without the intake manifold, and the differences can as well depend on the measurement accuracy. The same comparison can be observed for the high-swirl head for the 2V (Original) case in Appendix 3, and also here it can be seen that the intake manifold have a very little effect on the tumble motion. Because of this no recalculation have been made for the tumble values for the KTH engine tests.

An investigation was also performed to study the different cylinder heads tumble generation without intake manifold. Tests were done with the 2V (Original) case and 2V Straight Port (Curved Port Blocked) case, cylinder head angle sweeps were performed and the results for the maximum tumble number for each valve lift can be seen in Figure 26. The figure illustrates that no matter what cylinder head that is used, i.e. no matter how much swirl the different ports generate, the tumble motion seems to be the same. From these results the conclusion can be drawn that it is if the flow is through one or two ports that is the important factor for the tumble generation together with the inlet of the ports location.

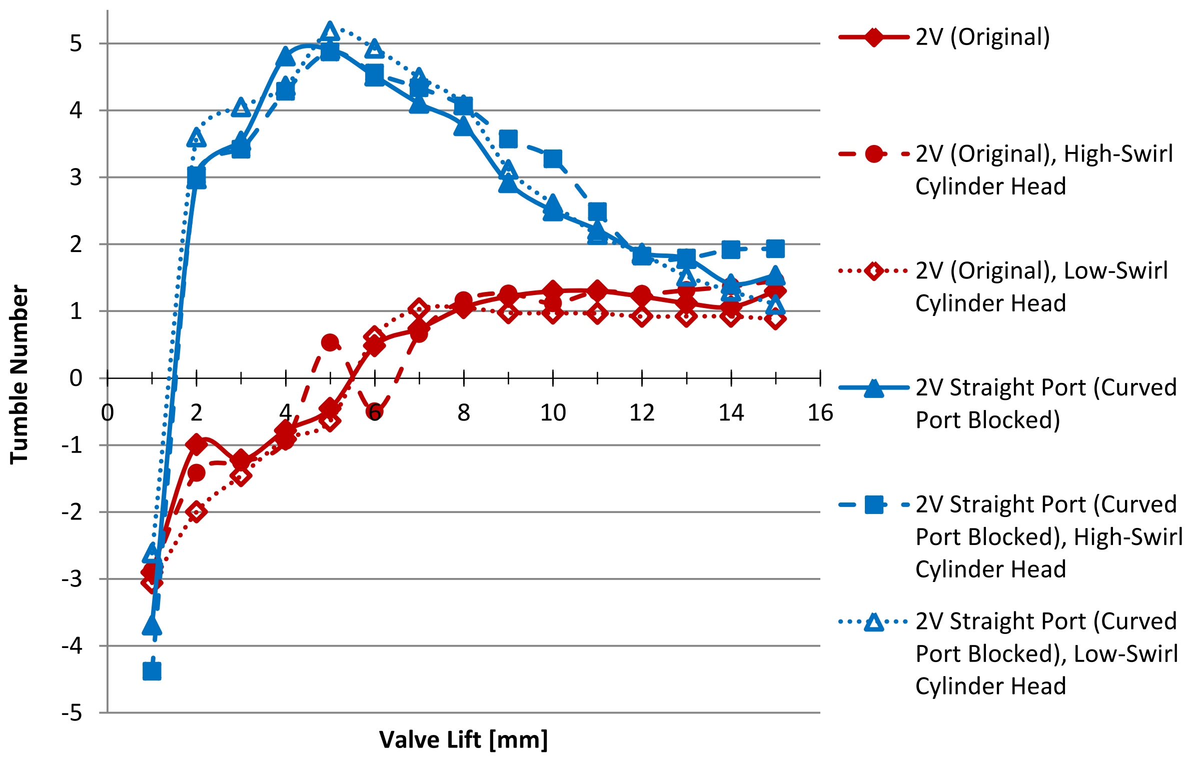

Figure 26. *Tumble number as a function of valve lift for the three different cylinder heads.*

Intake Manifolds Effect Scania

Since the tumble motion seems to be independent to how much swirl different ports generate, and the intake manifold didn't seem to have any effect on it either, no tumble motion study were performed with the intake manifold from Scania. This was partly because of these conclusions, but also because of that it was limited time to do the tests with the intake. First of all a new test were performed with the 2V (Original) case without the intake manifold since the study were performed after the engine tests, this to see how the engine tests had affected the cylinder head. The results can be seen in Appendix 4, at lower valve lifts the results differs slightly because of uncertainties in the measurements, but at higher valve lifts the results are the same.

With the intake manifold from Scania some additional tests can be performed since the side from where the air enters the plenum can be changed. In standard configuration the air enters the plenum from the opposite side compared to the KTH intake manifold. Another test was performed without the plenum, so that only the effect of the two intake runners could be seen. All these tests can be seen for the 2V (Original) case in Figure 27 together with the measured values without any part of the intake manifold.

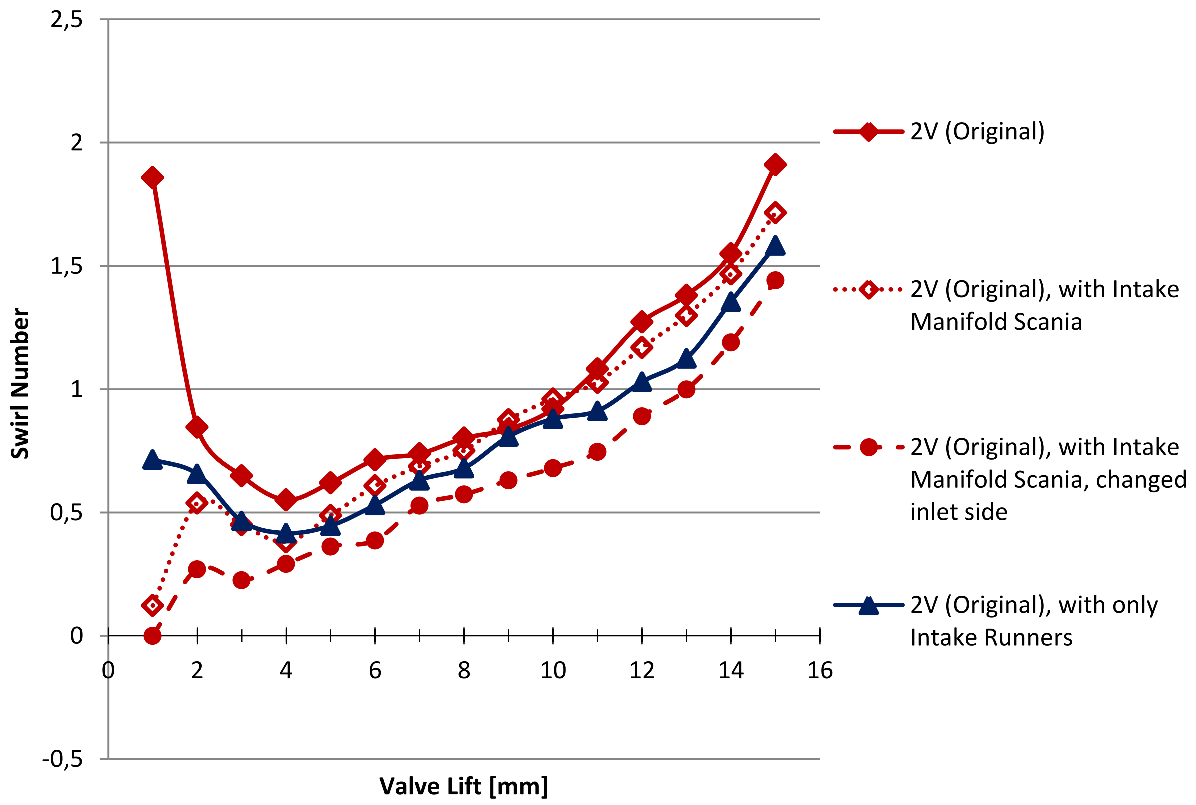

Figure 27. *The swirl measurements with the different applications of the intake manifold from Scania for the 2V (Original) case.*

Here it can be seen that the standard layout of the inlet causes almost no effect in the swirl generation, while the test with the air entering the plenum from the opposite side reduces the swirl generation. The results with opposite inlet side corresponds really well with the ones with the intake manifold from KTH, which also has the inlet from this side, leading to the conclusion that the inlet side has most effect on the swirl generation in the cylinder. The test without plenum shows also on a reduction of swirl, but smaller than the one with the opposite inlet side, i.e. it is in the middle of the two other configurations with the intake manifold. This supports the theory that the side from where the air enters the plenum has great effect, since this case can be said be with the air entering the “plenum” from the middle.

For the 1V Straight port case the Scania intake manifolds effects can be seen in Figure 28. Again it can be seen that the case with the changed inlet side decreases the swirl generation, while the case with the standard appearance of the manifold has quite an unchanged swirl generation, or even a bit higher than without the intake. Since the differences are so small, and the fact that there was no time to study the cases with blocked ports, measurements without the intake manifolds have been used during the evaluation of the engine tests.

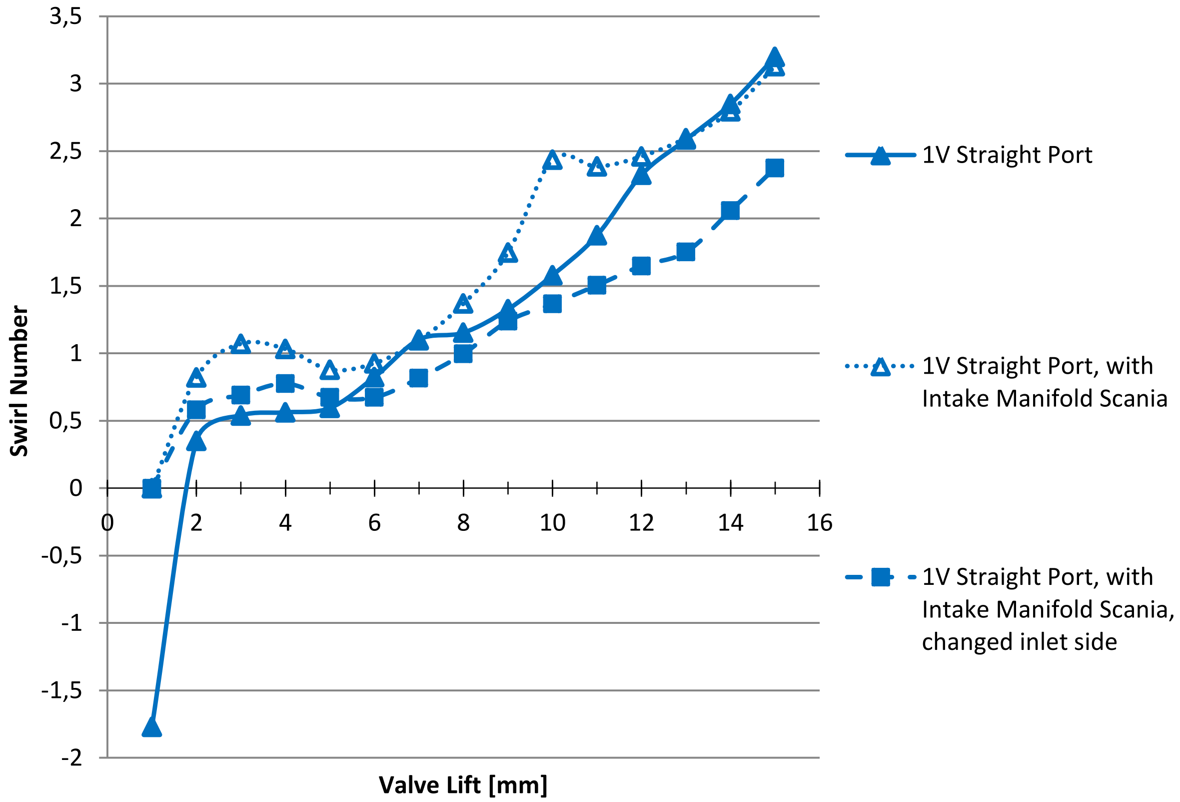

Figure 28. *The swirl measurements with the different applications of the intake manifold from Scania for the 1V Straight Port case.*

6.1.4 $\mu\sigma$

The flow parameter $\mu\sigma$ *is only* studied from the swirl measurements without any intake manifolds. This is because the tumble measurements gives higher flow losses since the 90 degree cylinder liner is used, and if the intake manifold have been used there would also be losses from it and not only from the ports.

Figure 29 illustrates $\mu\sigma$ as a function of valve lift for the cases with symmetrical valve lift, one valve deactivated or one port blocked. This figure shows that $\mu\sigma$ increases when deactivating one valve with respect to blocking one port, and that there are almost the same $\mu\sigma$ no matter if the curved or the straight port is used. Therefore the conclusion can be drawn that the efficiency is decreased if both valves are lifted while the flow only comes from one port. Another interesting thing to observe is how the flow is choked by the valve lift below 8 mm lift, whereas it is limited by the port geometry and the internal valve seat diameter at higher valve lifts.

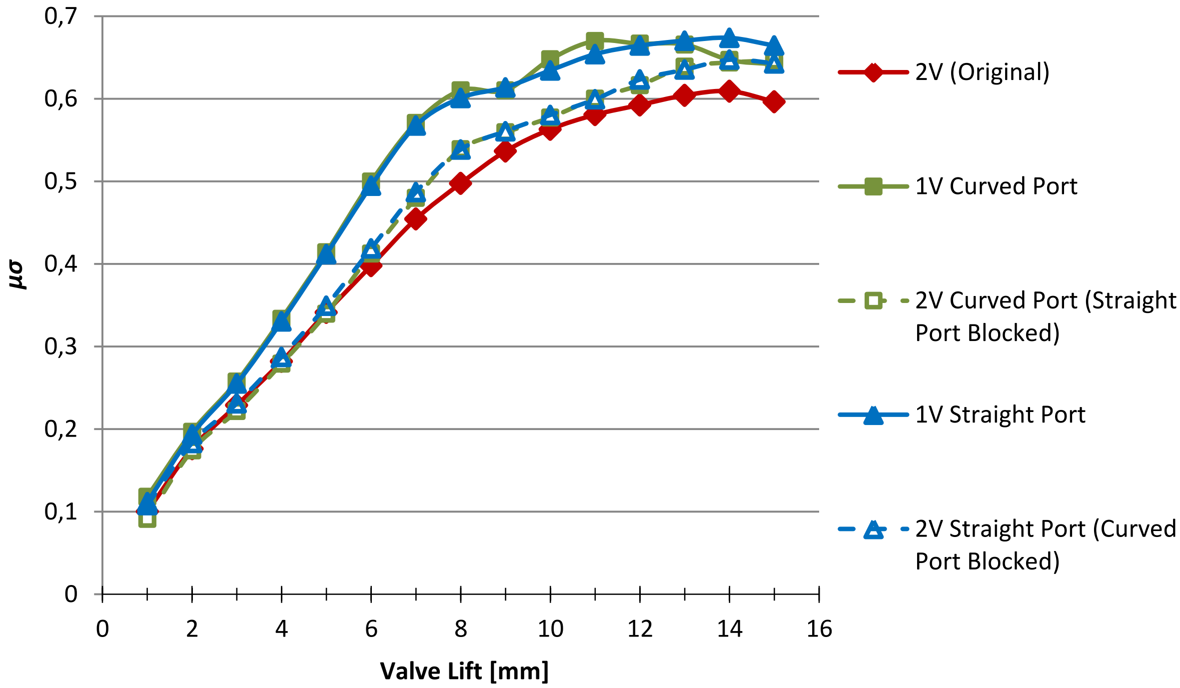

Figure 29. *$\mu\sigma$ as a function of valve lift for the studied cases.*

It can also be seen that $\mu\sigma$ is lower for the 2V (Original) case compared to the other cases. This indicates that the flow is more efficient when it comes only from one port, and that the flow from one port is disturbed when entering the cylinder if it flows from another port.

In Figure 30 $\mu\sigma$ can be seen for the tests with asymmetrical valve lifts.

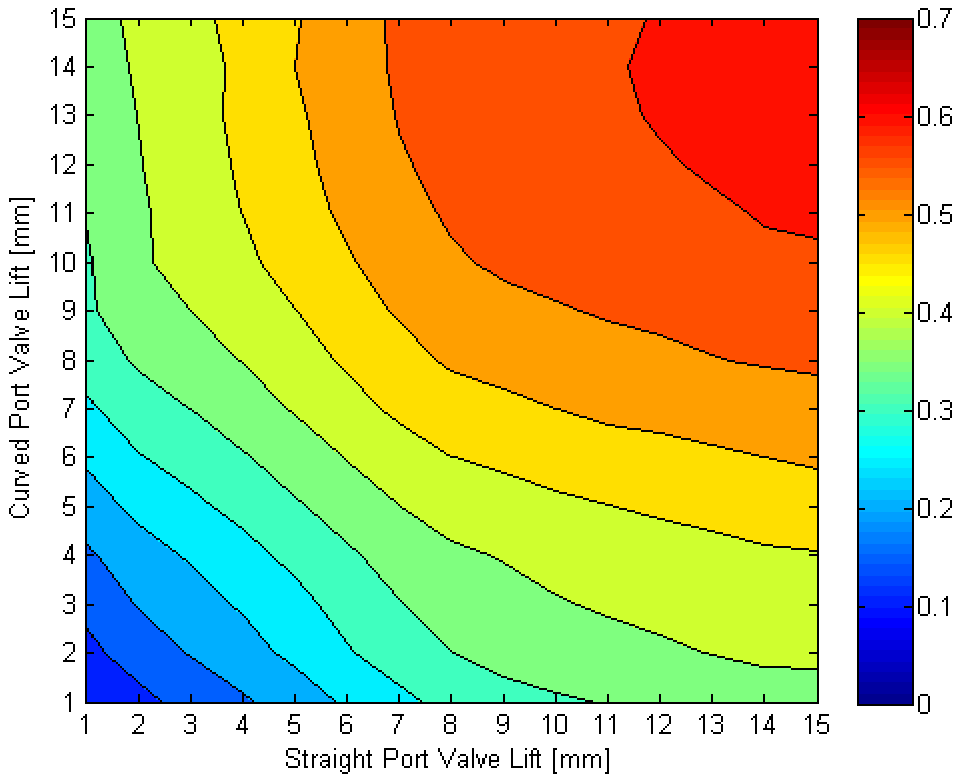

Figure 30. *$\mu\sigma$ for the tests with asymmetrical valve lifts.*

Figure 30 shows that there is quite a symmetric relationship for $\mu\sigma$ around the diagonal with the symmetrical valve lifts. This means that the efficiency of the flow should be unchanged if the curved port have a valve lift of 10 mm and the straight port have 5 mm, or vice versa.

6.2 Comparison between Thien and GT-Power

From the flow bench measurements of swirl and tumble the mean swirl and tumble have been calculated for different valve strategies. Since GT-Power limits the possibility to calculate this only for symmetrical valve lifts or lifts with only one valve, the study of the differences between Thien and GT-Power have been limited to those cases. The data used for this study have been taken from measurements in the flow bench without intake manifolds. To be able to evaluate a number of different valve strategies for Thien mean swirl and tumble, a MatLab script have been created, see Appendix 5.

In Figure 31, the mean swirl can be seen as a function of maximum valve lift for valve strategies with symmetrical valve lifts, and only lift on the valve for the straight port. The profiles with standard appearance have been used for the plotted comparison. Here it can be seen that the different methods of calculating mean swirl gives almost the same values. Though one difference can be observed, the GT-Power calculations gives slightly higher swirl values for low valve lifts for both valve strategies, while at higher mean swirl numbers than 1.5 it gives lower values for both cases. This shows that even if the numbers differs slightly from the different calculations, the same trends will be shown for the mean swirl no matter what method that is used to calculate it. This trend has been seen for all the studied cases, for both the standard and trapezoidal valve profiles.

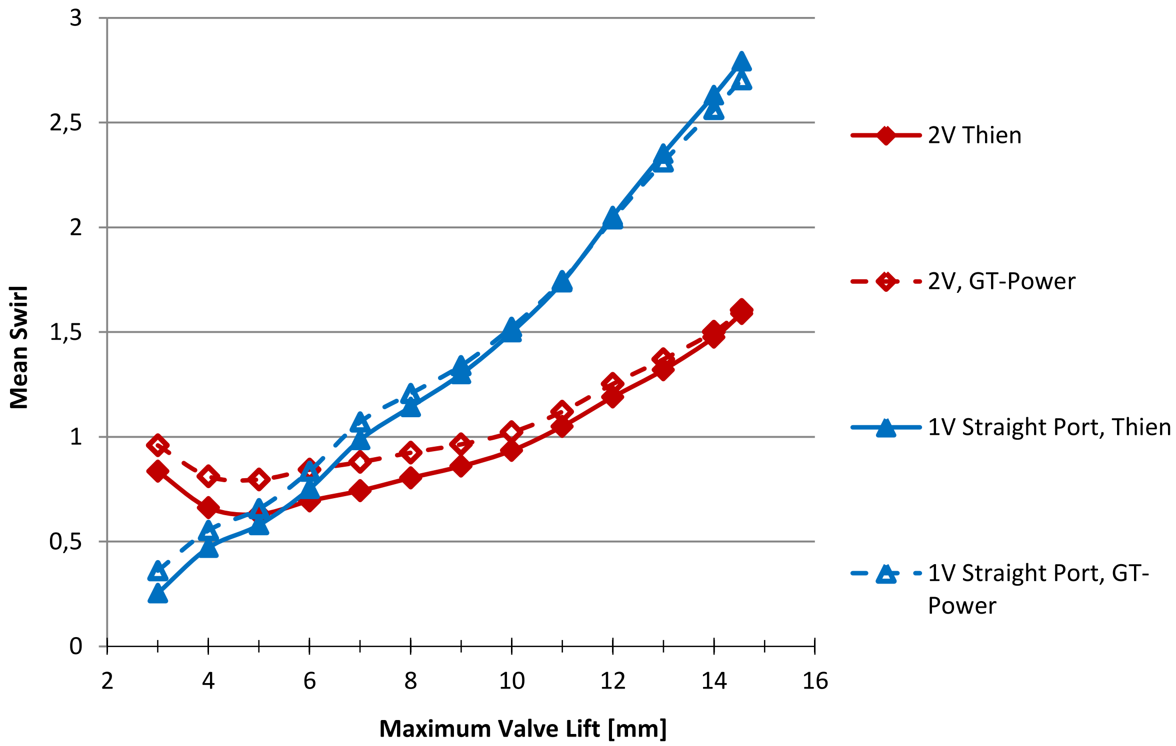

Figure 31. *Mean Swirl according to Thien and GT-Power for the valve strategies with standard appearance.*

To be able to study the difference between the different methods more thoroughly, the soot emissions from the transient load point, see Table 2, have been used. Since the soot emissions are heavily dependent on the swirl motion, Figure 32 and Figure 33 illustrates the smoke emissions as a function of Thien mean swirl and GT-Power mean swirl respectively. If the different plots are studied it can be seen that there are almost no difference between Thien and GT-Power.

As a test, the soot emissions were also plotted as a function of the mean swirl calculated with the intake manifold from Scania, see Figure 34. Here it can be seen that by using these data the correlation between the mean swirl and the soot emissions is even better. It would have been preferable to be able to use this measurement when studying the engine tests. However there haven't been time to redo all the measurements with the intake manifold and therefore it wouldn't be possible to compare all the measured data with this method. Because of this the Thien mean swirl without intake manifold will be used when evaluating the engine tests, but with the knowledge that the intake affects the swirl values slightly.

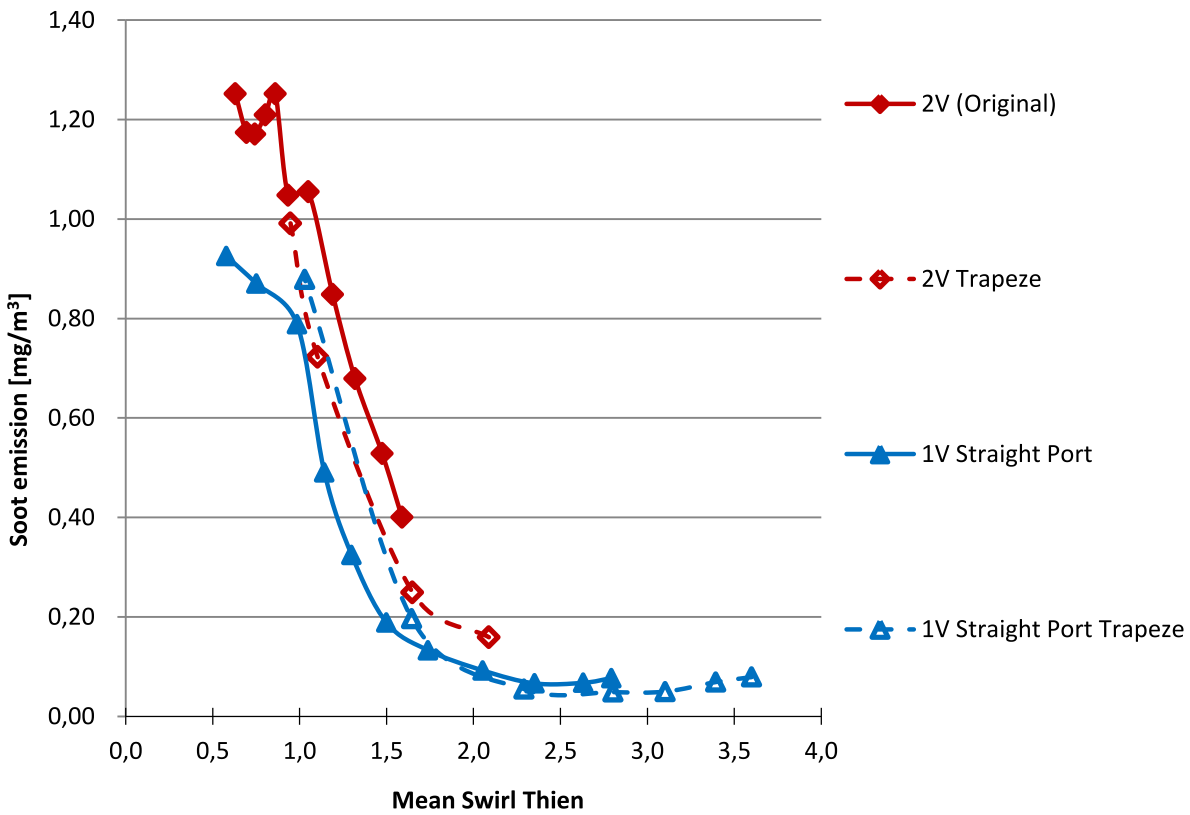

Figure 32. *Soot emission as a function of mean swirl according to Thien for the transient load point.*

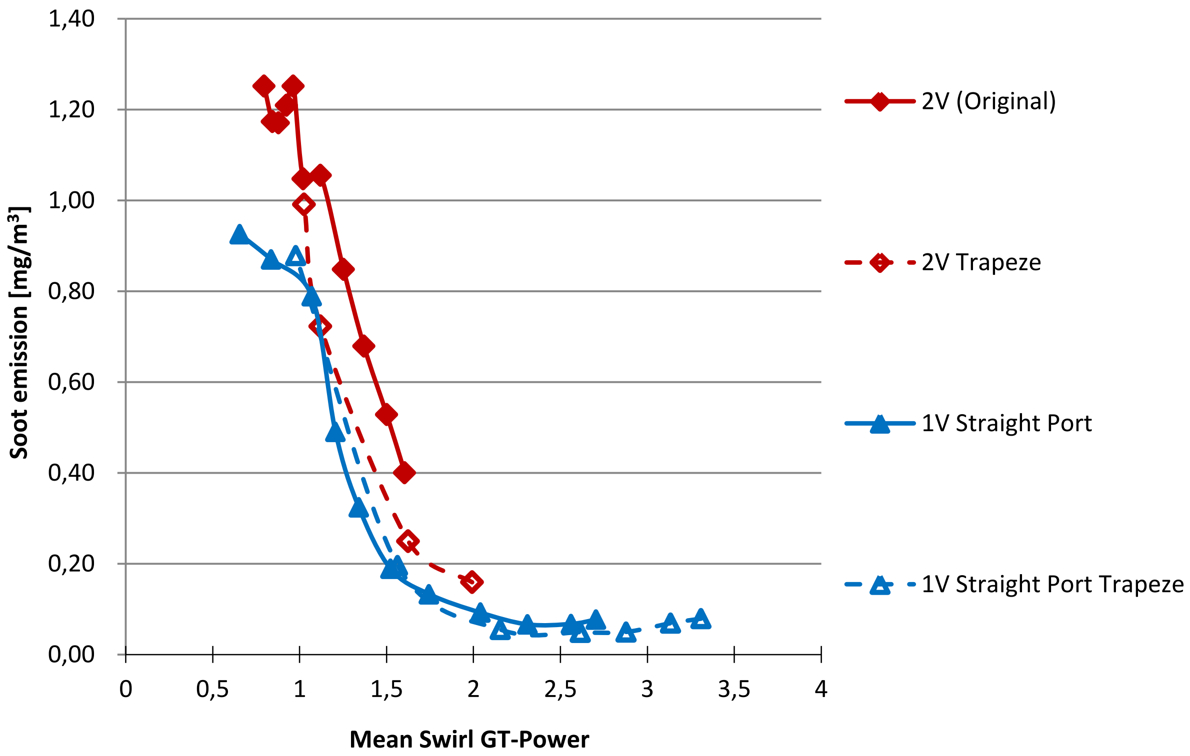

Figure 33. *Soot emission as a function of mean swirl according to GT-Power for the transient load point.*

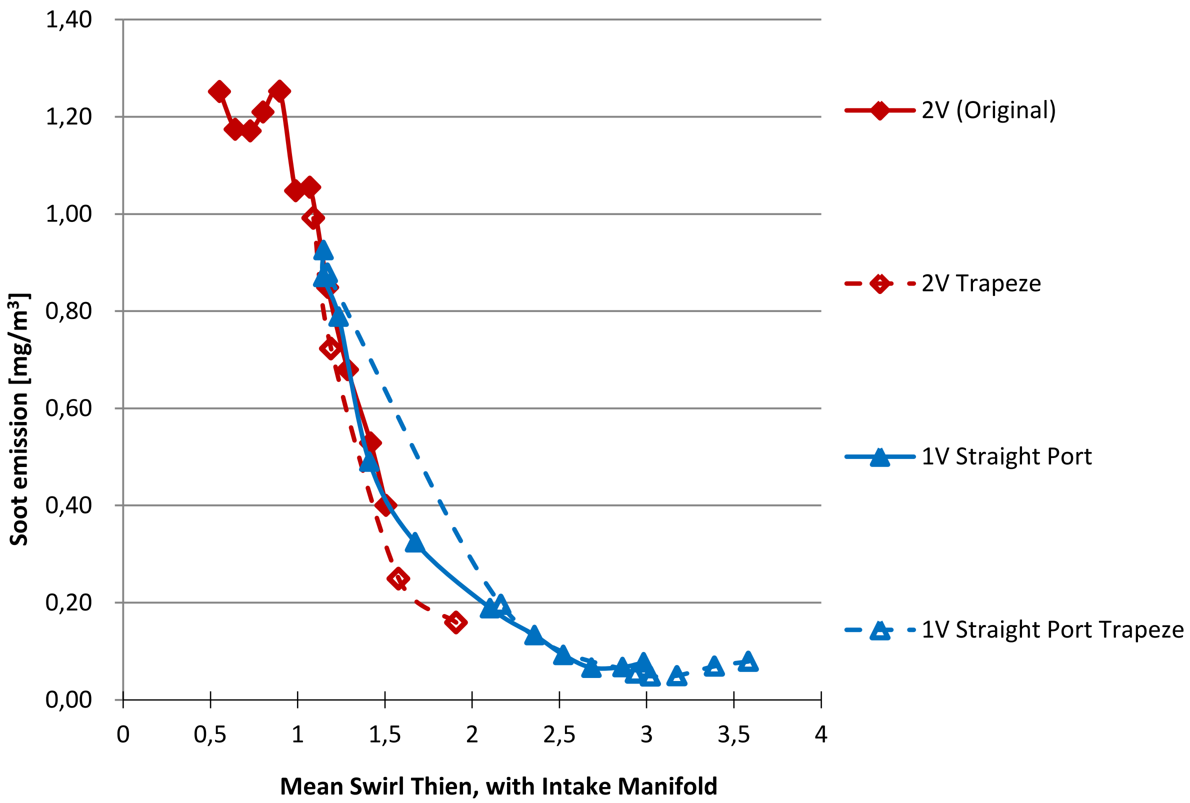

Figure 34. *Soot emission as a function of mean swirl according to Thien with intake manifold for the transient load point.*

For Figure 34, it should also be mentioned that the curve for 1V Straight Port Trapeze seems to follow the trends poorly. This is due to the fact that it lacks measurement points in the area between swirl 1.5-2 and therefore a line is drawn between these measurement points.

The same comparison for Thien and GT-Power tumble can be seen in Figure 35 and Figure 36 respectively. Again it can be observed that the trends are almost identical no matter which method that has been used for the calculation. One even more obvious trend for tumble compared to the swirl is that the Thien calculation gives higher values for the high tumble motions. The maximum value is 5.90 for Thien while it is 4.26 for GT-Power. Observe the different scaling of the x-axis for the two figures.

The fact that the different values differs from each other can be an important aspect if the real value of how much the air rotates in the cylinder is important. However, in this study the important factor is the trend between different valve strategies. Therefore the exact value is of less importance and which method that is used to study the engine tests has less significance. Since the Thien method has been decided to be used for the mean swirl also the mean tumble values that will be used during the engine test study will be evaluated with the Thien method.

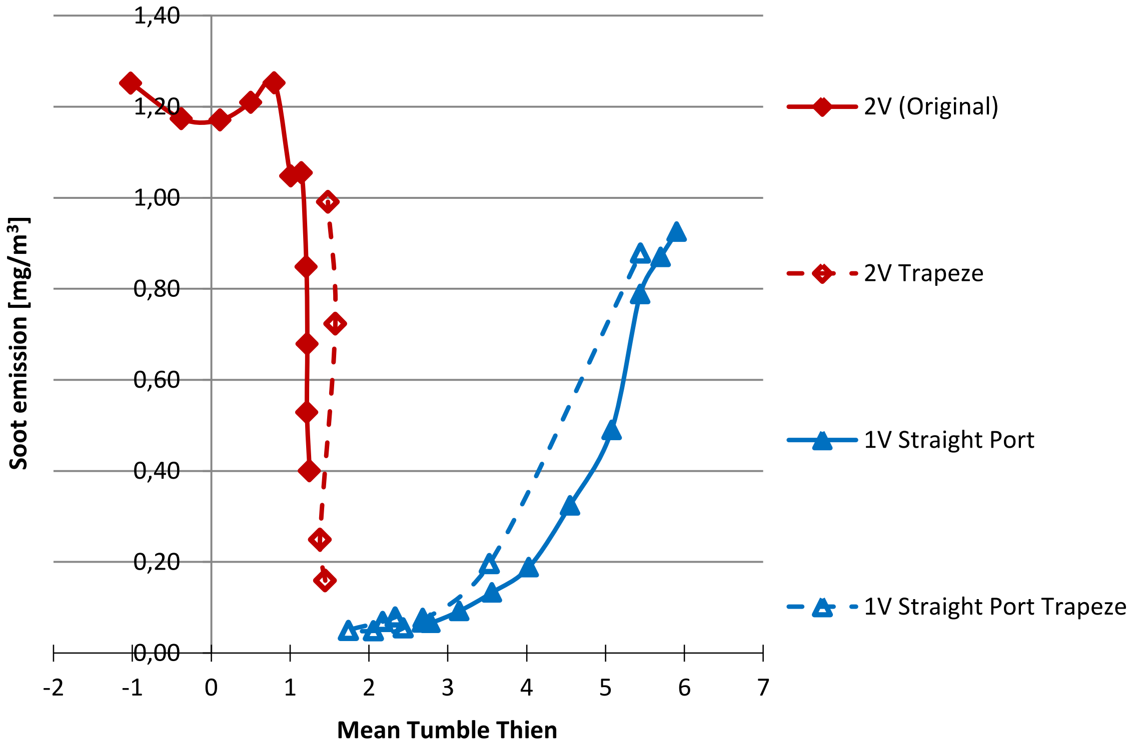

Figure 35. *Soot emission as a function of mean tumble according to Thien for the transient load point.*

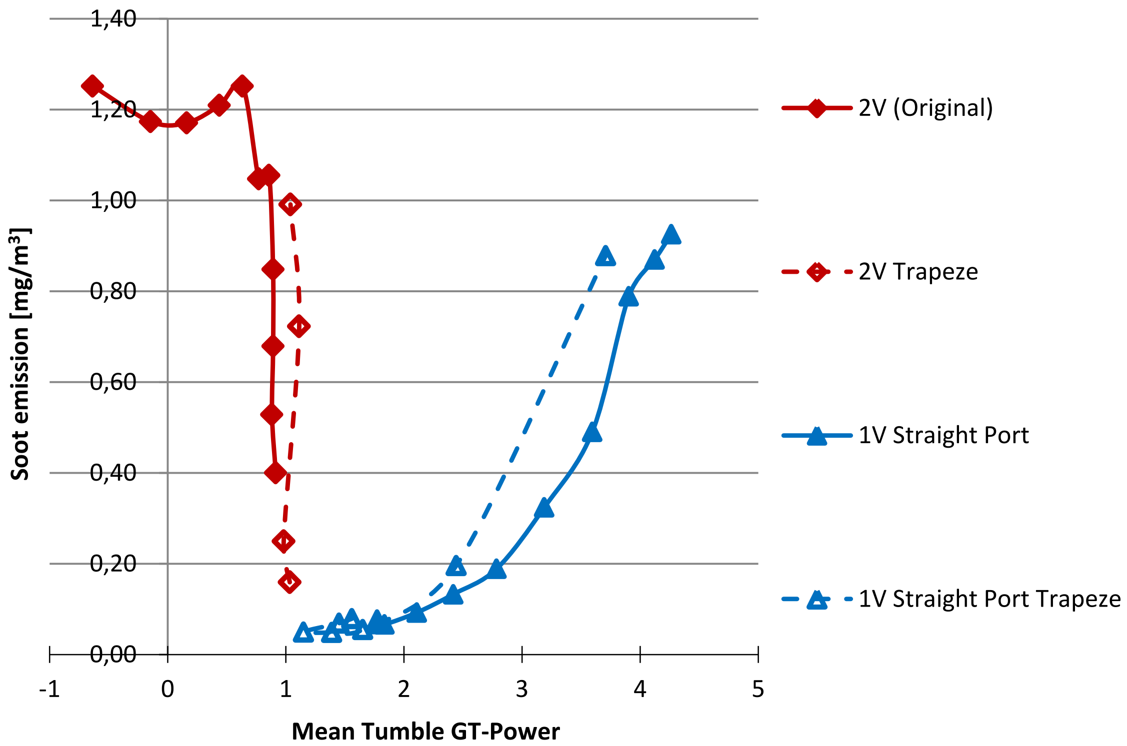

Figure 36. *Soot emission as a function of mean tumble according to GT-Power for the transient load point.*

As mentioned in chapter 5.4 different models were implemented in GT-Power. A study was performed to see what errors occurs if the *2V model* was used for simulating valve strategies with only one valve active, or on the other hand if the *1V model* was used to simulate symmetrical valve lifts. This comparison can be seen in Figure 37, and this shows that the models gives large errors in the calculated mean swirl when used for the wrong cases.

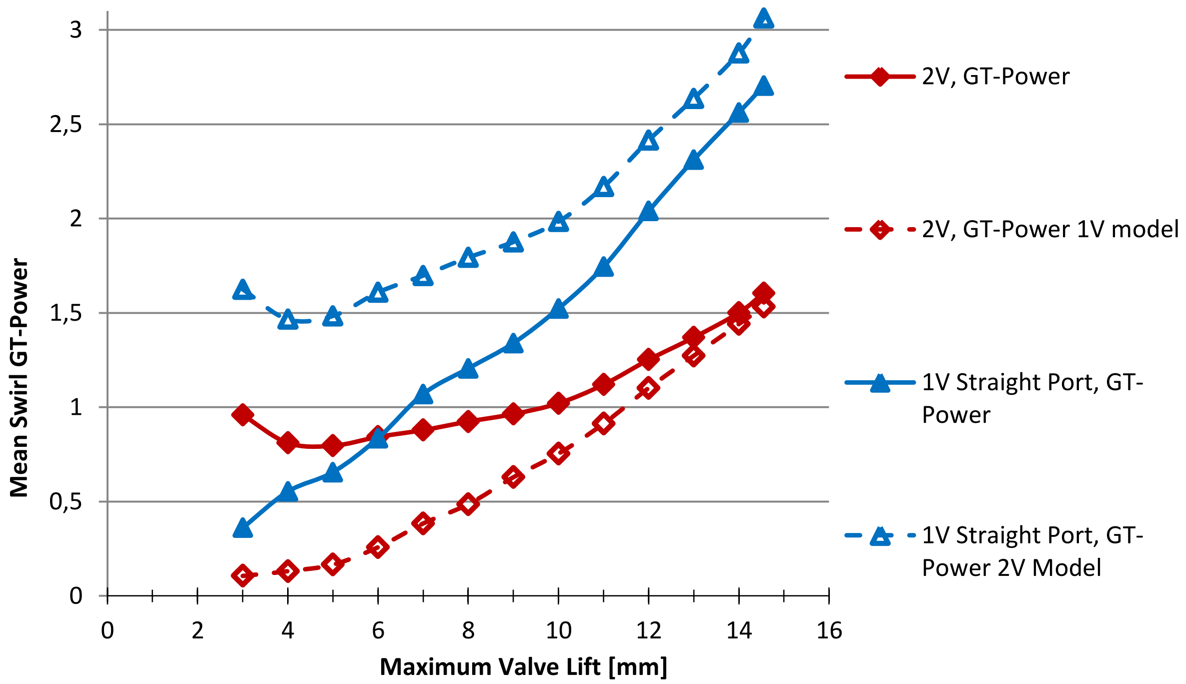

Figure 37. *GT-Power mean swirl when using 1V model for symmetrical valve lifts and 2V model when one valve is deactivated compared to the use of correct model.*

The *1V model* overestimates the symmetrical valve lifts while the *2V model* underestimates the strategy with one valve activated. Because of this, the conclusion can be drawn that none of the models should be used to calculate mean swirl when both valves are used with asymmetrical valve lifts. This gives an even greater advantage when using Thien mean swirl while evaluating engine tests if asymmetrical valve lift is used.

Studies have also been performed with different engine speeds, one according to WHSC mode 9, 1316 rpm, and one at 1000 rpm naturally aspirated. This is plotted for the 2V case and 1V Straight Port case in Appendix 6, where it can be seen that the engine speed has almost no effect on the mean swirl. In the same appendix, a test in GT-Power can be found without the inlet system, i.e. without inlet pipes and intake manifold. This test shows very little effect on the mean swirl.

6.3 Results Engine Tests

In the following chapters the results from the different engine tests performed at Scania and KTH will be presented.

As the possible combinations of valve lifts and valve profiles create too many potential valve strategies for it to be reasonable to test them all, only a select few have been run in the engine test cell. To reduce the number of test cases it was decided to only test asymmetric valve strategies with one of the intake valves completely closed. Since the flow bench results demonstrated that the maximum swirl was found with one valve completely closed, this limitation has a little effect on the ability to vary the swirl.

To provide a frame of reference, the case with two valves using standard valve profiles was run for all load points. Earlier testing also showed limited advantages with regards to smoke emissions provided by the use of trapezoidal valve profiles compared to standard valve profiles. The trapezoidal valve strategies were therefore selected on the basis of matching the swirl number of valve strategies using standard valve profiles. To increase the range of swirl numbers studied, it was also of interest to run the trapezoidal valve profiles with high valve lifts to provide the absolute highest swirl number achievable with this particular cylinder head.

As a cost effective alternative to VVA, the much simpler method of increasing the swirl number by blocking one port was also investigated. The ports were blocked by mounting intake gaskets with opening for only one port. During these tests, symmetric valve lifts are used to study how the valve stem and valve head connected to the blocked port affects the combustion and emissions. The valve strategies run for each load point are defined in the results from the engine testing. For tables with flow parameter data for each of the studied valve strategies see Appendix 7.

6.3.1 WHSC Transient

The Transient load point is defined in Table 4.

Table 4. *The Transient load point.*

Case	Engine Speed	SOI	Inj. Dur.	lambda	P_{CR}	P_{in}	$P_{exhaust}$	T_{in}	EGR
-	rpm	CA°	ms	-	bar	bar	bar	°C	%
Transient	1056	-5.0	2.17	~1.25	1077	0.59 – 0.87	0.55	25	0

The different valve strategies that have been tested can be seen in Table 5. During all these tests, the lambda value has been kept constant for all valve profile strategies by adjusting the inlet manifold pressure. The injected fuel mass and air mass flow have been kept constant. However differences in how the in-cylinder flows have been created affects the engine losses and therefore the fuel consumption. To separate the valve strategies effects on the combustion from the pumping losses, the emissions are plotted in ppm instead of g/kWh. The effects on efficiency from how the in-cylinder flows has been created will be discussed separately.

Table 5. *The valve strategies tested at the Transient load point.*

Valve Strategy	Valve 1 lift	Valve 3 lift
	mm	mm
2V (Original)	5- 14.55 (1 mm step)	
1V Straight Port	0	5-14.55 (1 mm step)
2V Trapeze	9, 10, 13, 14.55	
1V Straight Port Trapeze	0	6, 9, 11, 12, 13, 14, 14.55
2V Straight Port (Curved Port Blocked)	5-14.55 (1 mm step)	
2V Straight Port (Curved Port Blocked) Trapeze	13, 14.55	

In Figure 38 the soot emissions can be seen as a function of the swirl motion for the studied cases. Here it can be seen that the soot emissions decreases with an increased swirl motion. This is mostly dependent on that an increased swirl motion increases the after oxidation of the soot particulates. The increased swirl motion can be achieved either by deactivation of the valve for the curved port or by blocking the port and it can be seen that both the strategies effects the soot emissions in a similar way. The different soot emissions at the same swirl number between the strategies, depends largely on the fact that the plotted swirl numbers originates from measurements without the intake manifold. If the intake manifolds effects had been taken into account the mean swirl number and soot emissions would probably correlate very well. However as the flow bench measurements with the intake manifold weren’t performed for all cases, it was deemed more interesting to see the trends for all valve strategies.

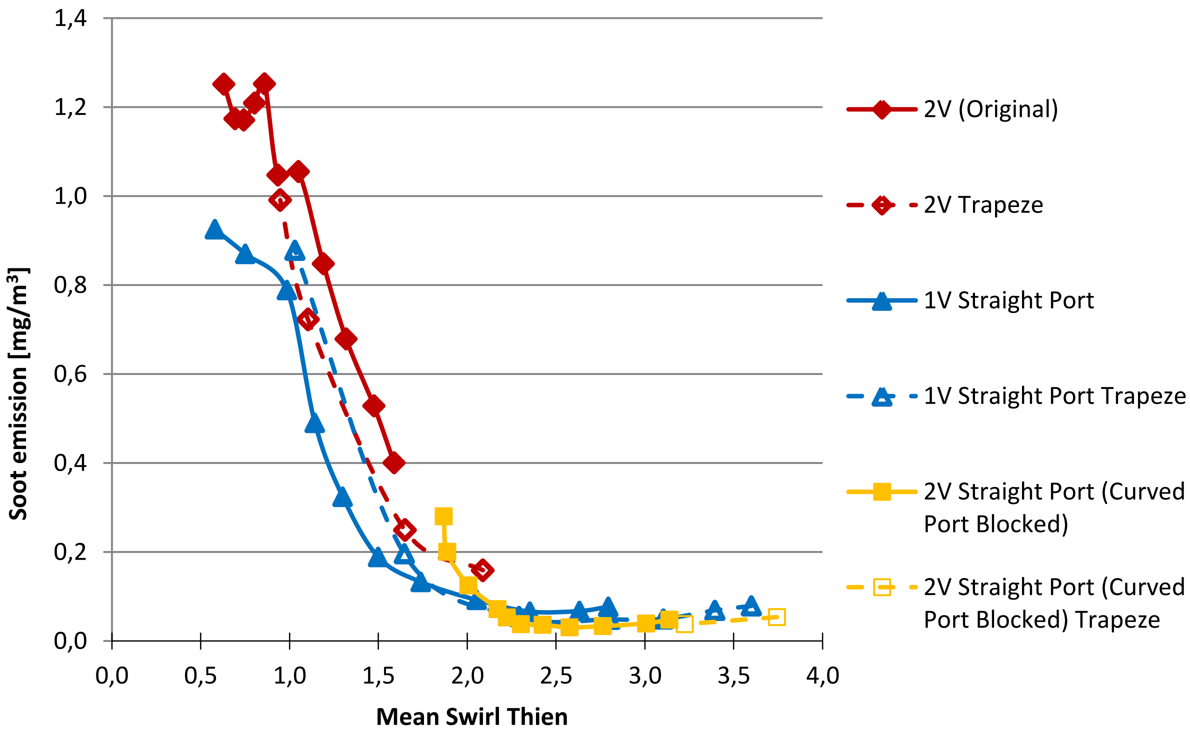

Figure 38. *Soot emissions as a function of mean swirl according to Thien.*

The CO emissions can be studied in Figure 39. An increased swirl motion increases the possibility for CO to react with the oxygen causing a higher level of transition to CO_2 at the end of the combustion.

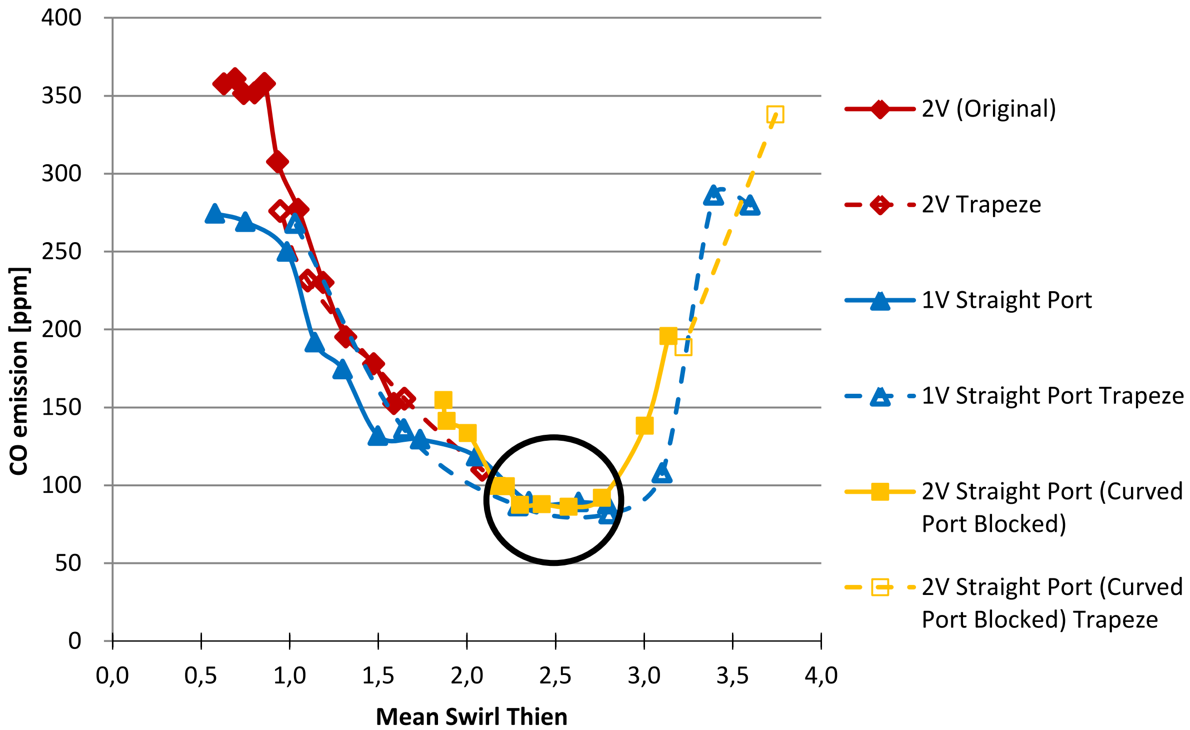

Figure 39. *CO emissions as a function of mean swirl according to Thien, the black circle illustrates where also the soot emissions are lowest.*

But at high swirl number, over 3, the CO emissions increases greatly again. This might be caused by the strong air motion that makes the fuel sprays intersect each other, which leads to a more incomplete combustion. An even higher swirl number could affect the combustion so much so that even the soot emissions would increase. A slight tendency of this phenomenon can be seen in the soot emission figure for the highest swirl numbers. The lowest soot emissions is obtained around a mean swirl of 2.5, and this corresponds well to the CO emissions, see black marker. Because of this the conclusion can be drawn that the CO-emission is the first indicator for an unfavorable air motion.

The soot emissions can also be seen in Figure 40, but here as a function of both swirl and tumble. This plot shows that the soot emission primarily are dependent on swirl, and not so much on the tumble motion.

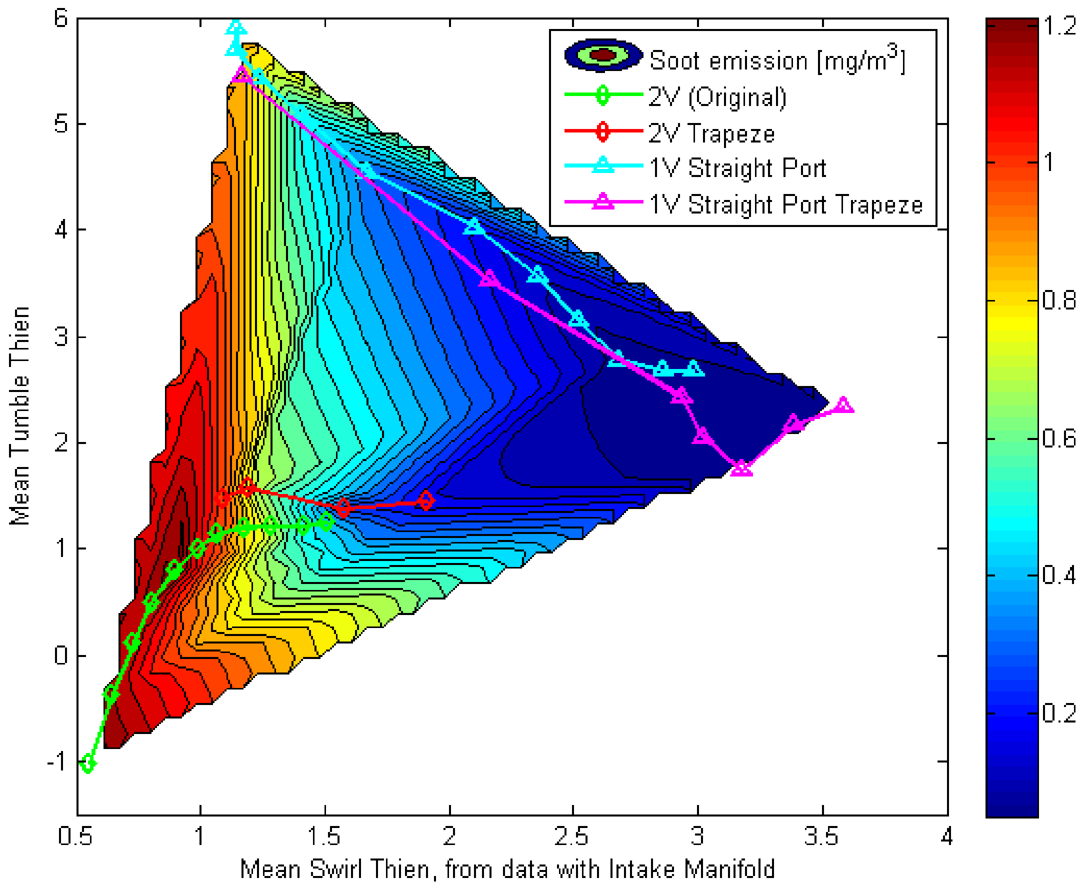

Figure 40. *Soot emissions as a function of swirl and tumble.*

While studying this plot, it should be observed that the mean swirl is calculated from the measured data with the intake manifold from Scania and not without it as in all the other plots. The reason for choosing this data for the plot is because otherwise a misleading trend would be shown, since the swirl motion is overestimated for the 2V case and underestimated for the 1V case. It should also be noticed that the line colors for the different cases are changed compared to the other plots in order to be visible in the color graph. One problem with plotting the emissions in this way is that small changes are really hard to be seen, only the big trends can be noticed.

To be able to study the tumble motions effect on the soot emissions more deeply also 2D graph is shown in Figure 41. Here it seems like a tumble number of around 1.5-2.5 gives the lowest smoke emissions, but this is due to the fact that the highest swirl numbers are obtained for this tumble values. For the 2V (Original) case, with valve lifts of 5-9 mm, tumble values of around -1 to 1 for approximately the same swirl motion is obtained. This area is marked with a blue circle in the plot, and it indicates that a lower tumble motion can give lower soot emissions. The trend though is quite small and to be able to explain it with heat release graphs is difficult.

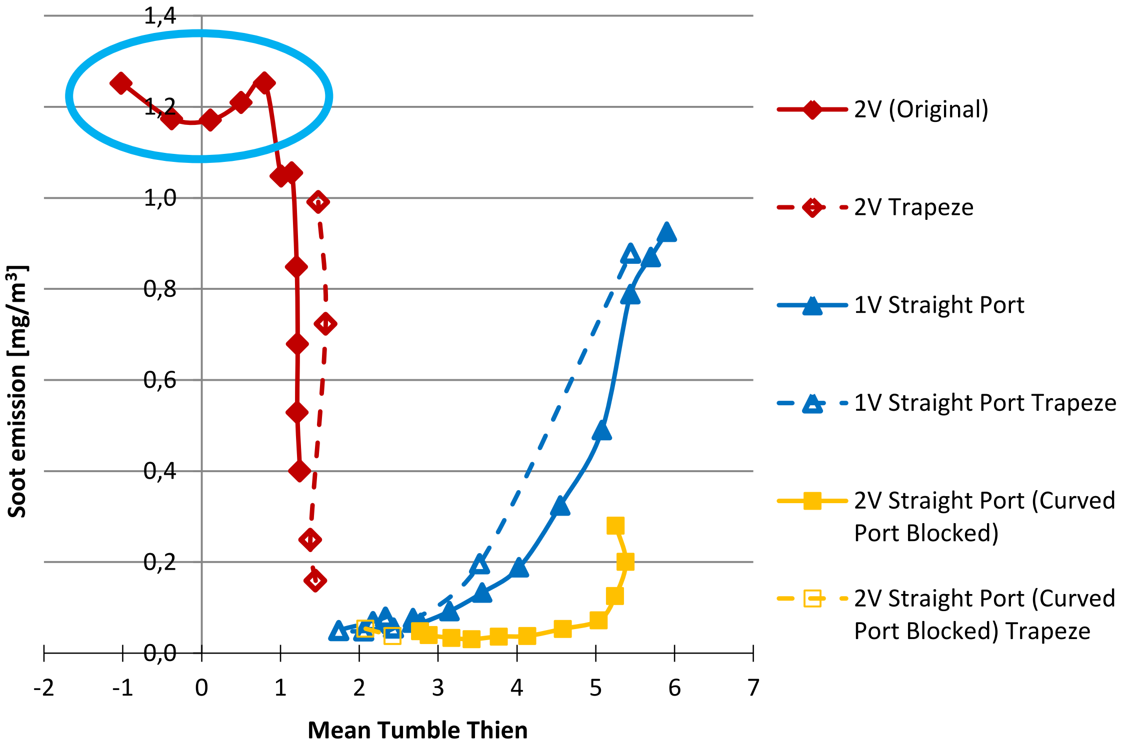

Figure 41. *Soot emissions as a function of tumble, where the blue circle indicates that a lower tumble motion, within the marked area, could decrease the soot emissions.*

If the cylinder pressure is analyzed for different cases, a quite interesting phenomenon can be seen. Figure 42 illustrates this for some of the valve strategies tested, where it can be observed that different compression pressure is obtained even though lambda is kept constant by adjusting the inlet manifold pressure for all the strategies. The compression pressure increases when one valve is deactivated, and it also increases with lower maximum valve lift. The trend that it decreases when using a trapezoidal profiles instead of profiles with standard appearance can also be seen in the figure.

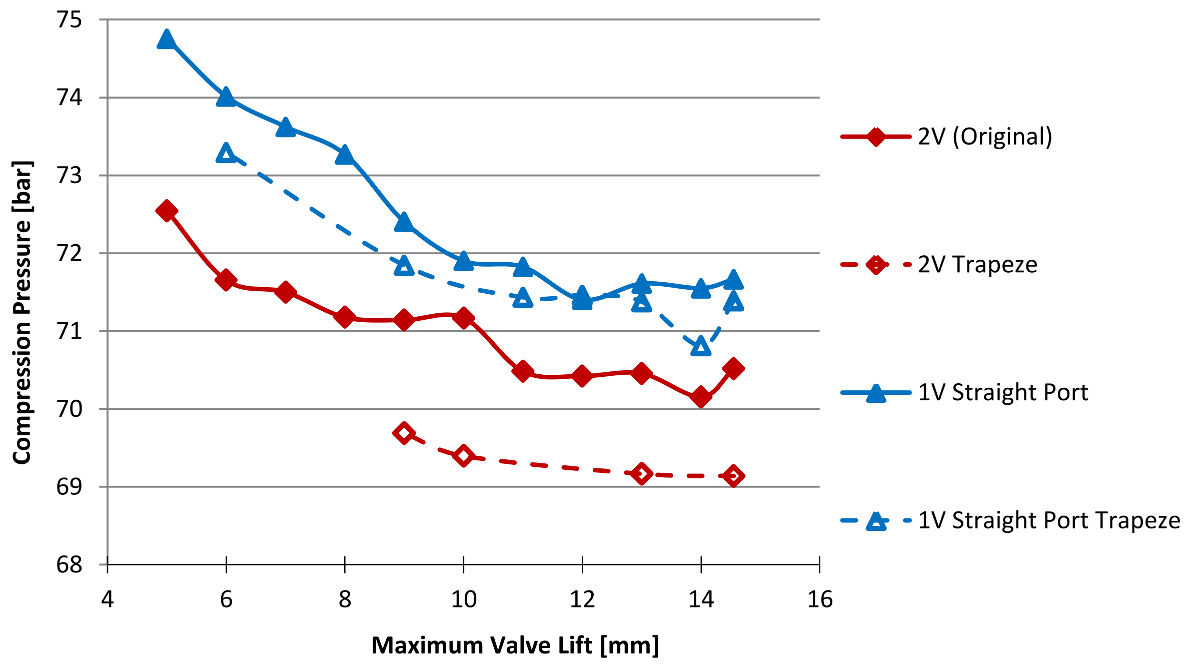

Figure 42. *Compression pressure as a function of valve lift.*

Since the mass flow is constant for all the studied strategies the only factor that can explain the differences in pressure is the temperature. In order to study this, the temperature has been calculated from the pressure trace and the air mass flow assuming adiabatic compression with one of Concertos templates. From the GT-Power simulations the normalized turbulent intensity has been used to see the relationship between this factor and the temperature, which can be seen in Figure 43. At lower valve lifts the turbulent intensity increases since the velocity of the flow past the valves is increased, the same phenomena occurs when deactivating a valve. A higher turbulent intensity gives a higher compression temperature.

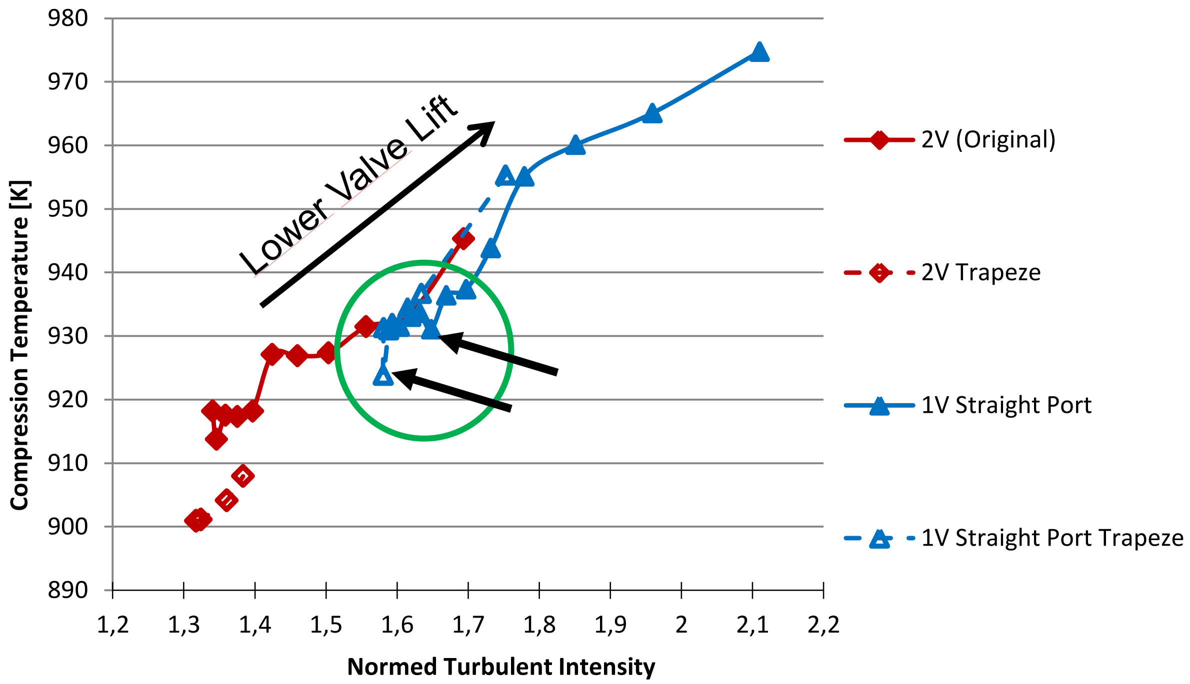

Figure 43. *Compression temperature as a function of normalized turbulent intensity, where the arrows indicates points with minimum tumble for a given valve profile.*

That the higher turbulent intensity gives a higher compression temperature can be explained by two factors. One explanation is that an increase in turbulent intensity can cause a higher heat transfer between the gas in the cylinder and the cylinder wall during the intake stroke. Since the inlet air is colder than the cylinder during the intake stroke, this heat transfer will increase the temperature of the gas in the cylinder. The small scale turbulence, that turbulent intensity is a measure of, is thought to decrease quite rapidly after passing into the cylinder. Therefore the turbulent intensity only has a small effect on the heat transfer during the compression stroke. Because of this the compression temperature is increased with a higher turbulent intensity. The effect is even greater since a change in temperature before compression gives a higher temperature change after compression.

Another explanation can be that since the turbulent intensity decreases rapidly because of viscous losses, and thereby the kinetic energy is transformed into heat. The strategies with higher turbulent intensity during the intake stroke can thereby get an increase in the gas temperature. In order to study this phenomenon a rough estimation of the total potential energy in the air flow was performed. From GT-Power the air flow velocity, *v*, and mass flow rate past the intake valves was obtained as a function of crank angle. From these values the kinetic energy in the air flow, *E*, was calculated with the equation

$$E = \frac{1}{2} m v^2 \tag{32}$$

$m =$ mass transported into the cylinder at a given crank angle

for each crank angle. With only one valve active and 5 mm lift, a flow velocity of over 200 m/s was obtained compared to 50 m/s for the standard case, 2 valves and original valve profiles. Therefore a much higher total kinetic energy of the air flow was obtained for the 1 valve strategy. If all this energy can be transformed into heat in the gas, given a specific heat capacity of 1 J/gK for air, a gas temperature increase of almost 20 degree can be obtained before the compression stroke. From this calculation the conclusion can be drawn that neither of the factors can be disregarded. With a higher air flow velocity past the valves the local pressure and thereby the temperature in the gas is lower, leading to a higher temperature difference between the gas and the valve. Therefore the heat transfer to the gas might be increased, which also can be one explanation to the higher compression temperature.

Another conclusion that might be drawn from Figure 43 is that the tumble motion can have some effect on the temperature. Marked in the plot are two points taken from the case with only the valve for the straight port activated, and with a valve lift around 13-14 mm where it have been noticed that there are a valley in the tumble generation. The tumble values are lowest around this value, it increases with both higher and lower valve lift, and a lower tumble value seems to decrease the temperature slightly. However the trend is really small and it should not be stated that this must be the case, it can also be other phenomenon's causing this trend. But an increase in tumble motion might cause an increase in the heat transfer during the intake stroke and intensify the effect of a higher temperature together with the turbulent intensity. Also the tumble motion is decreases due to viscous losses and transforms into heat, and again this can be another factor that explains this phenomena.

Concerto has also been used to analyze the start of combustion, SOC, for the different valve strategies. The definition of SOC have been the crank angle where the unfiltered heat release first is positive during the combustion, this have been analyzed for every cycle and then the mean value of the 100 logged cycles have been the used SOC. Since the SOI has been kept constant during the test, SOC is a measure of the ignition delay. In Figure 44 it can be seen that the compression temperature has a great effect on SOC, where a lower temperature causes a longer ignition delay. It can also be seen that there is a step between the 2V (Original) case and the 1V cases at the same temperature, where the 2V strategy has a longer ignition delay. This might be caused by the increase in tumble motion for the 1V cases compared to the 2V case.

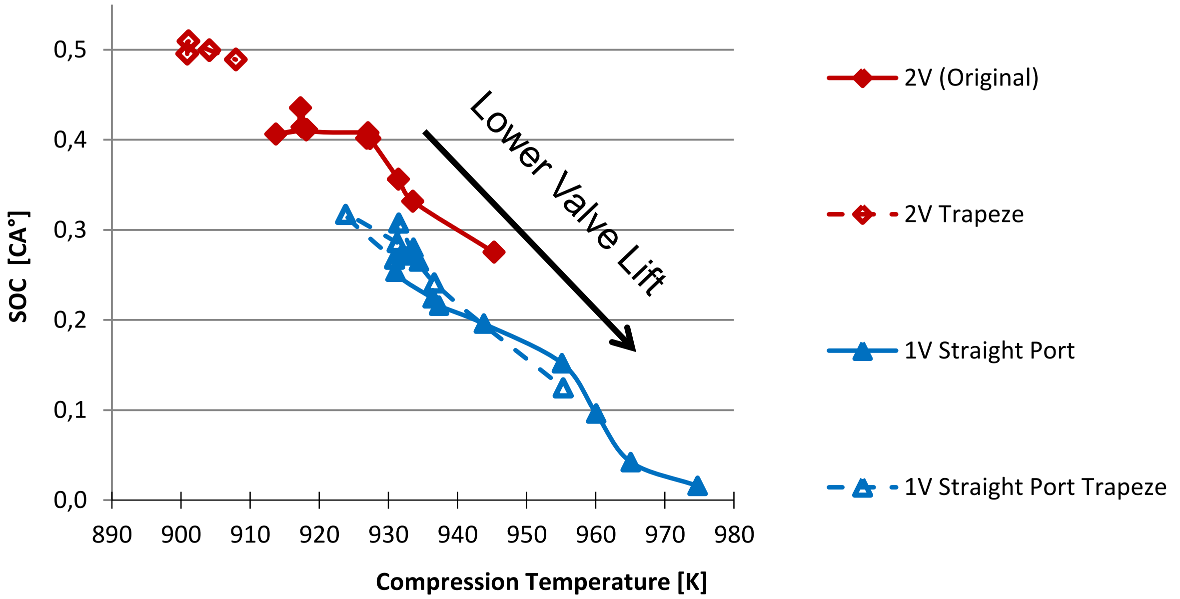

Figure 44. *Start of combustion as a function of compression temperature, the arrow illustrates the direction of a lower valve lift.*

The start of combustion affects the combustion phasing, which can be seen in Figure 45 where the heat release is plotted as a function of crank angle. The heat release is low pass filtered with 3000 Hz in Concerto. A shorter ignition delay, i.e. an earlier SOC, results in a smaller premixed combustion which can be seen as the lower first peak with the earlier SOC. Because of this great effect from the temperature, it is hard to investigate what difference the higher tumble levels, with low lifts and only one valve active, makes on the combustion.

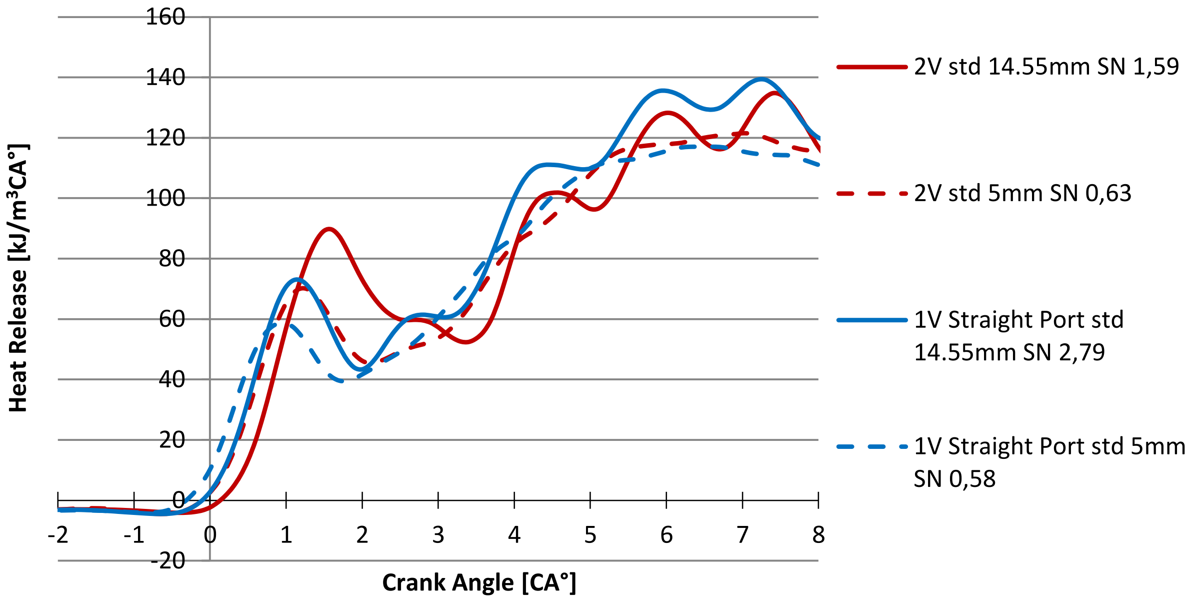

Figure 45. *Heat release as a function of crank angle for some of the valve strategies.*

The reduction in premixed combustion gives longer diffusion combustion, and since the soot emissions mostly are produced during the diffusion combustion this can increase the soot emissions for a fix swirl number. If the tumble motion can affect the temperature and thereby SOC, which is one of the possible conclusions from Figure 43, this can be an explanation to the trend marked in Figure 41, where a higher tumble motion seems to be giving a higher soot emission. For these valve strategies the swirl number is almost unchanged.

From the heat release plot, the conclusion also can be drawn that an increased swirl motion is increasing the heat release rate for the diffusion combustion, at the later crank angles in the plot, in other words it is increasing the intensity of the combustion. An increase in the intensity of the diffusion combustion should mean a higher combustion temperature and thereby higher NO_x emissions, since the NO_x production is heavily dependent on temperature. On the other hand, a decreased premixed peak should lower the NO_x production since a lot of NO_x is produced during the premixed combustion.

Since the NO_x production is heavily dependent on the temperature, an increased compression temperature can also increase the NO_x emissions. From this it can be concluded that there are several factors that have the potential of affecting the NO_x emissions. In Figure 46 the NO_x emissions are plotted as a function of the mean swirl for the studied valve strategies. All the different factors are needed to try to explain the trends in this case. First it can be said that one of the main differences for the case with flow only through one port in respect to two ports is that the flow is more choked for these cases causing a higher compression temperature and thereby increased NO_x emissions. But at swirl numbers above 2.7 the NO_x emissions suddenly decreases, above this swirl number the combustion is affected negatively, which has been seen as higher CO emissions in Figure 39. This causes a lower combustion temperature and lower NO_x emissions.

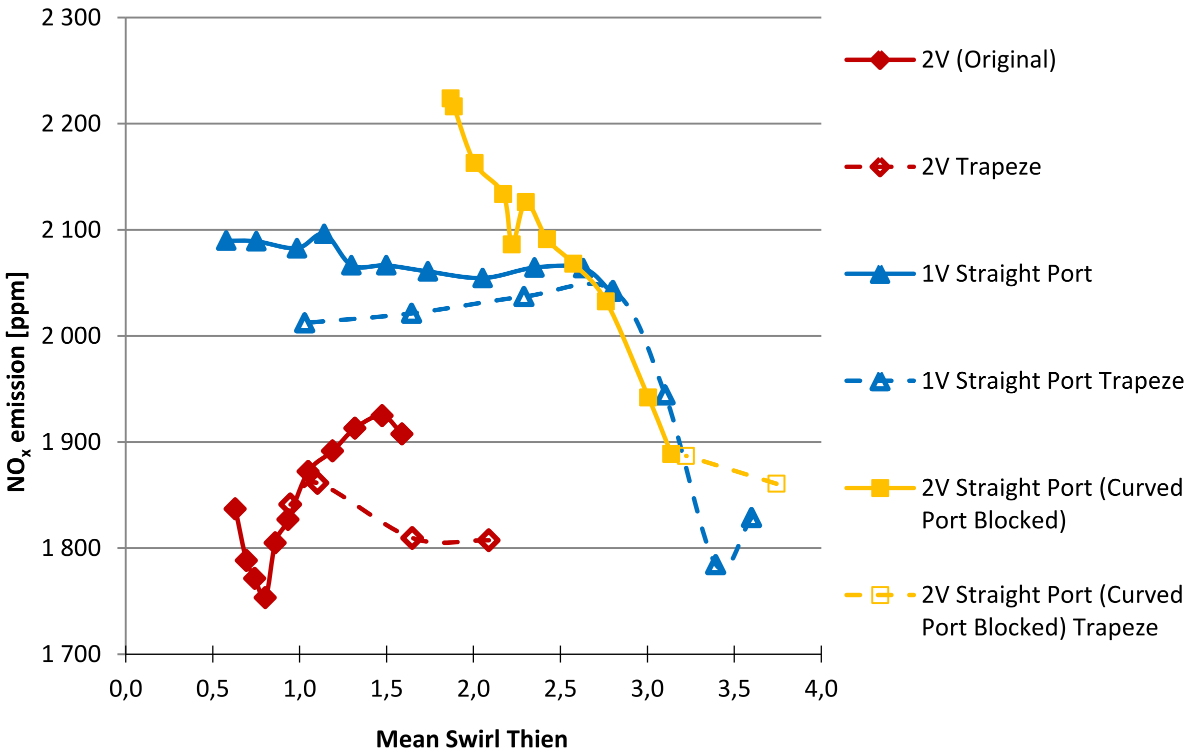

Figure 46. *NO_x emissions as a function of mean swirl.*

At the lowest swirl numbers the emissions are increasing even though the intensity of the diffusion combustion is lower and the fact that the premixed combustion is lower due to the earlier SOC, which can be seen for both the 2V (Original) case and the 1V Straight Port case. This can be due to the fact that here the choking of the flow is really high because of the low valve lifts, causing the temperature to increase significantly and thereby increasing the NO_x emissions. For the 2V (Original) case the emissions are higher at higher swirl numbers because of the increased diffusion combustion intensity. Highest NO_x emissions are obtained with low valve lifts with the curved port blocked, where both the temperature increase and the higher diffusion combustion intensity is increasing the NO_x emissions.

If the HC emissions are studied, see Figure 47, it can be seen that they are kept at a fairly constant and low level for all the studied cases. Since there are so small differences between the cases it is hard to see any trends on the HC emissions for different in-cylinder flows, however a small trend suggests that HC increases with increased swirl.

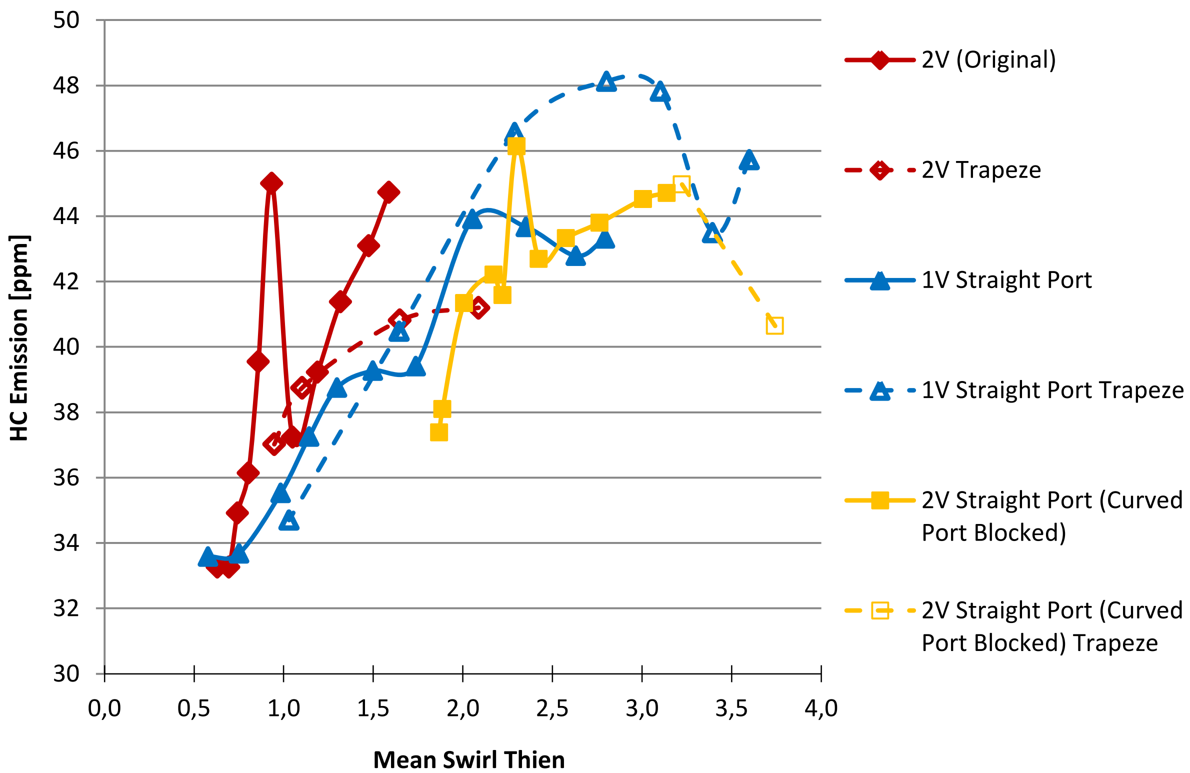

Figure 47. *HC emissions as a function of mean swirl according to Thien.*

In Figure 48 the volumetric efficiency can be seen for the different valve strategies as a function of valve lift. Here it can be seen that the volumetric efficiency is higher for the 1V case than the cases with flow through both ports from maximum valve lift down to approximately 10 mm valve lift. It can also be seen how the trapezoidal profiles slightly increases the volumetric efficiency from the 2V (Original) case, but increases it a lot for the 1V Straight Port case and is even higher than for the 2V (Original) case for all the tested valve lifts.

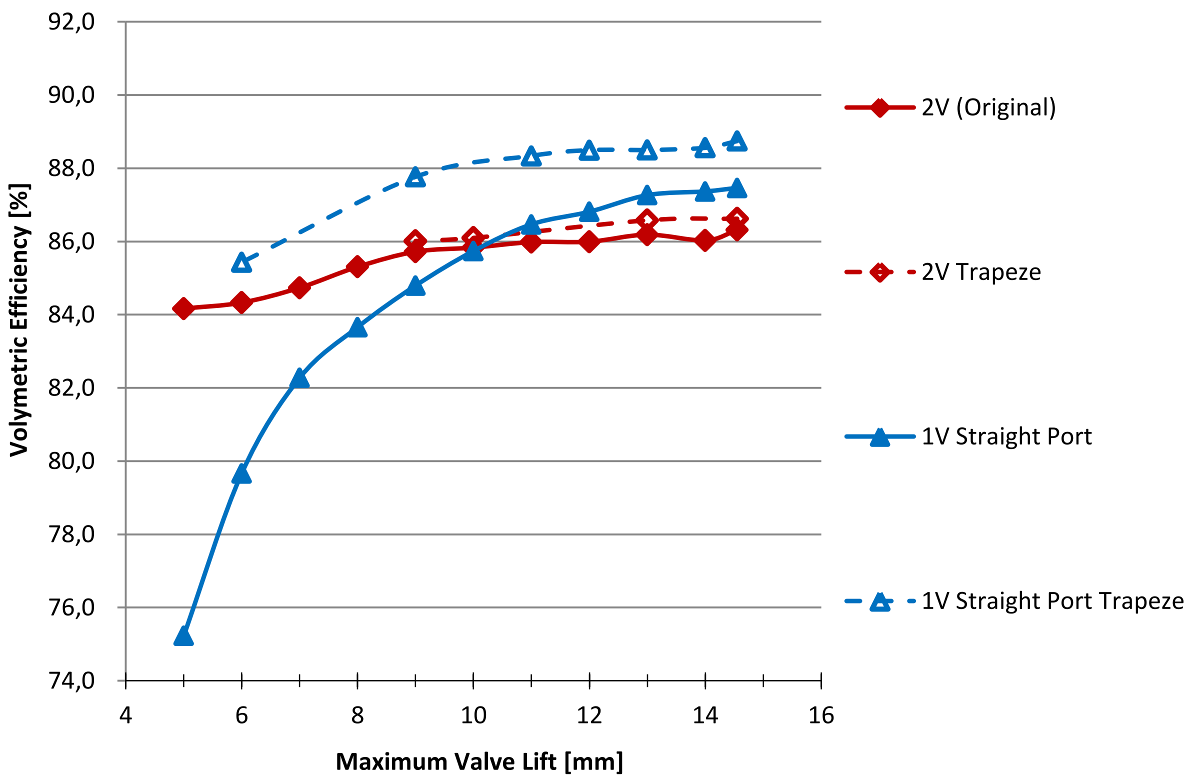

Figure 48. *Volumetric efficiency, calculated from the density in the intake manifold, as a function of maximum valve lift for the different cases studied at the Transient load point at 1056 rpm.*

If a PV diagram is studied, see Figure 49, the reason for the higher volumetric efficiency for the case with flow through one port compared to the case with flow through both ports can be explained. If the two strategies are studied with maximum valve lift it can be seen that the pressure in the cylinder decreases a lot more for the 1V case than the 2V at the beginning of the intake stroke, and this is because of the more choked flow with one valve instead of two valves activated.

However, with the 1V strategy the speed of the flow gets higher in order to compensate for the pressure difference, and at the end of the intake stroke this higher speed causes an even higher filling ratio. When studying this particular graph it should be remembered that the inlet manifold pressure has been adjusted for all the cases so that lambda is kept constant. This can be seen in the legend were the absolute pressure is noted. The reason for the higher pressure after the inlet stroke in this plot is due to the explained phenomena with a higher temperature with the more choked flow.

The reason for the different pressure traces during the exhaust stroke, despite that the exhaust back pressure is kept constant, is assumed to be because of a slight pegging error of the cylinder pressure trace. This error could be caused by the decay of the turbulent intensity which adds heat to the cylinder gas during the assumed adiabatic compression when pegging. Though the pressure difference is very small, around 0.1 bar for the worst cases, compared to the difference in compression pressure.

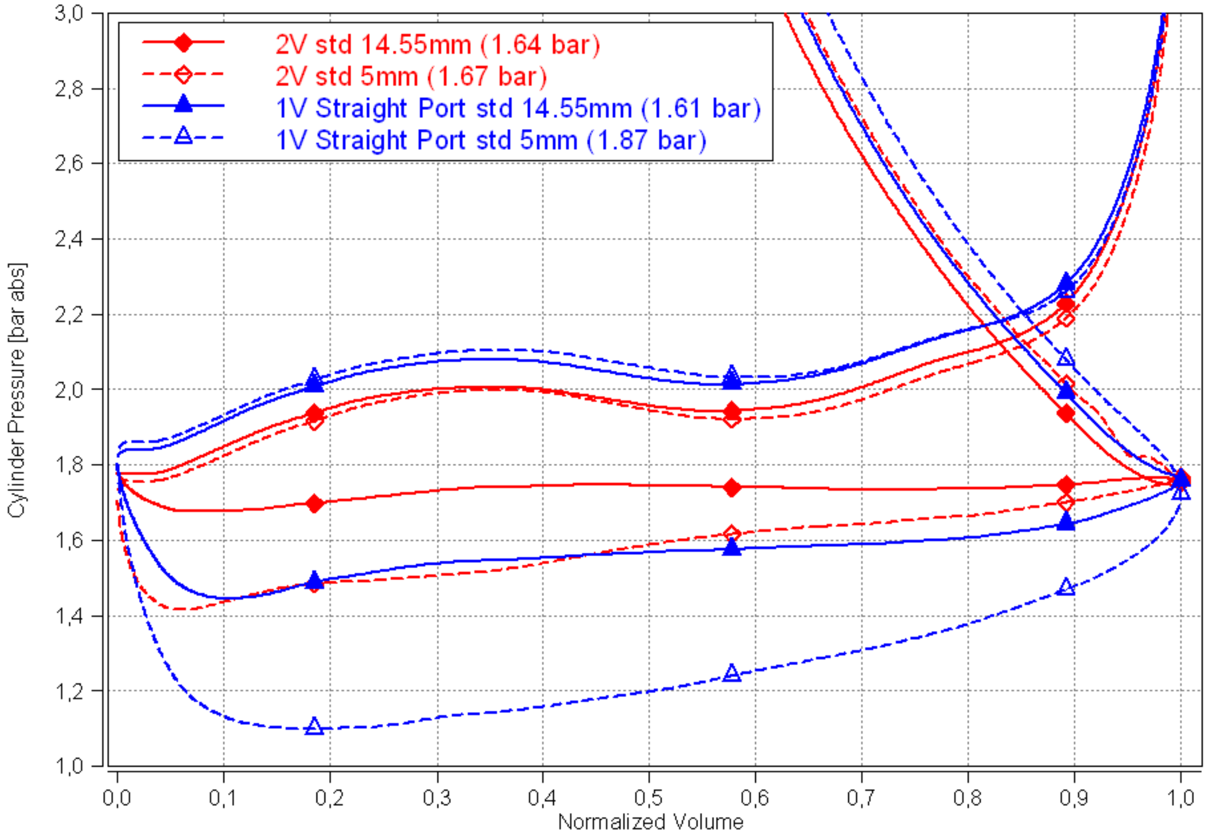

Figure 49. *PV diagram for four of the tested valve strategies.*

For the lower valve lifts, especially for the 1V strategy, the lower volumetric efficiency has to be compensated with a higher inlet manifold pressure, and in the figure it can be seen that even when doing so the pressure is heavily decreased at the beginning of the intake stroke. The lower cylinder pressure during the intake stroke causes higher pumping losses. These losses are described by the Pump Mean Effective Pressure, PMEP, plotted in Figure 50 for the studied cases. The figure illustrates how the pumping losses increases while deactivating or blocking one port in respect to the case with flow through both ports. A higher negative value means higher pumping losses. It can also be seen how the pumping losses heavily increases with the lowest valve lifts with only one port or one valve active. Again it should be remembered that the boost pressure have been lowered for the high valve lifts with one valve or one port deactivated in order to compensate for the higher volumetric efficiency. This causes comparatively higher pumping losses for the deactivated valve or blocked port cases compared to if the same inlet manifold pressure has been used. On the other hand, at lower valve lifts, the inlet manifold pressure has been higher for these cases and thereby the pumping losses are lower than they should be with the same inlet manifold pressure.

One slight trend can also be seen that the pumping losses for the cases with blocked port are slightly higher than the cases with one valve deactivated, at least for the higher valve lifts. This can be due to the fact that the valve for the deactivated port disturbs the flow from the straight port. However, the differences are really small and it should not be stated that this must affect the pumping losses. It can also be seen that there is a trend of slightly higher pumping losses with the trapezoidal profiles than with the standard ones. Again, though the differences are quite small.

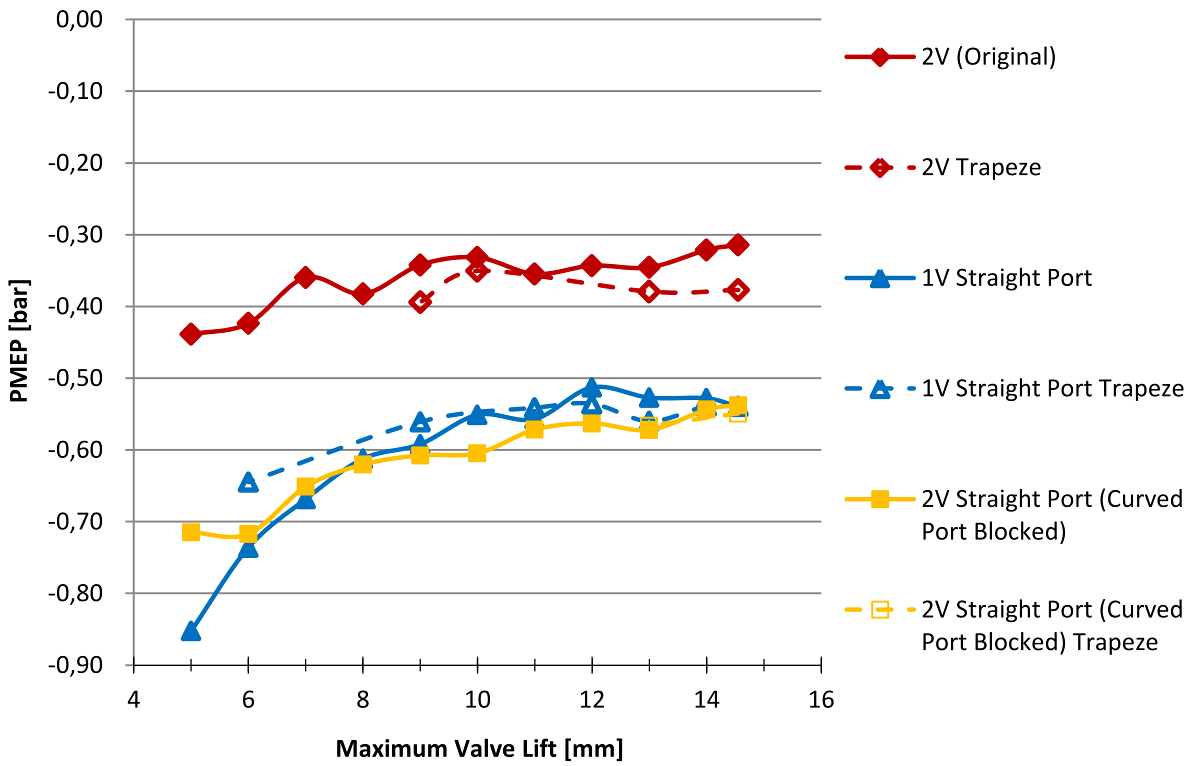

Figure 50. *PMEP as a function of valve lift.*

The Brake Specific Fuel Consumption, BSFC, is plotted in Figure 51 for the studied cases. The injected fuel mass is kept constant for all the strategies.

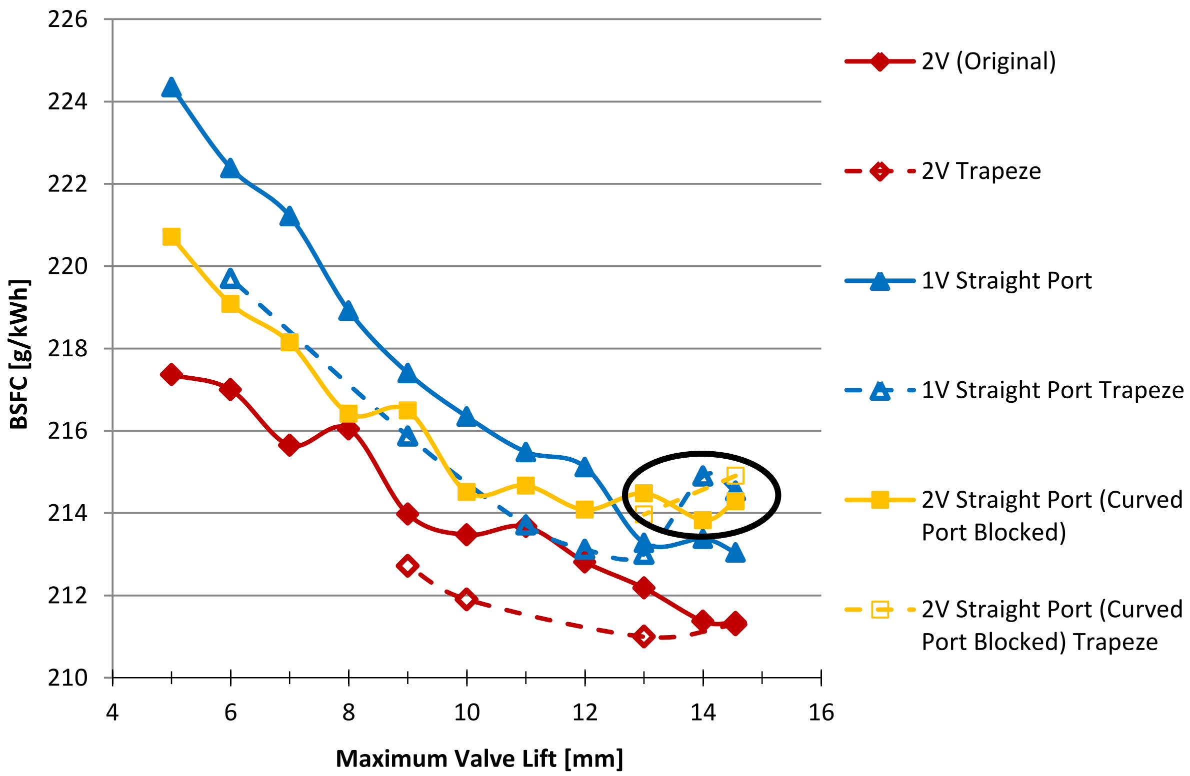

Figure 51. *Brake Specific Fuel Consumption as a function of valve lift for the studied cases, where the black circle shows the valve strategies with a swirl number over 2.7.*

It can be seen in Figure 51 that BSFC increases for the cases with on valve or one port deactivated, and the largest reason for this behavior is thought to be because of the higher pumping losses. The marked area corresponds to the strategies with a swirl number over 2.7, which has been shown to have negative effects on the combustion since the CO emission increased. This also increases BSFC which is seen in Figure 51. Once more it should be remembered that the boost pressure have been adjusted for the different cases in order to match the same lambda. For the high valve lifts with one port blocked and one valve deactivated the boost pressure has been lowered, giving higher pumping losses and thereby a higher BSFC. If the different cases had been tested with the same inlet manifold pressure, then maybe the efficiency had been quite equal for the different strategies at high valve lifts. On the other hand the higher boost pressure at low lifts with these strategies is making the BSFC lower than what would be the case on the same inlet manifold pressure as for the standard cases.

Other factors that influence the efficiency are for example the phasing of the combustion. The SOI has been kept constant for this tests, but the change in amount of premixed combustion with respect to the diffusion combustion and also the intensity of the combustion is changed causing different combustion angles for 50% burned, CA50%. A higher swirl motion also means a higher heat transfer during and after the combustion, with an increased amount of heat transferred from the cylinder gas to the wall. Thereby a higher amount of energy is transferred to the cylinder wall instead of to the piston movement and because of this the amount of work that can be taken out from the expansion stroke is reduced. This lowers the efficiency of the engine and thereby BSFC increases.

6.3.2 WHSC SCR mode 9

The load point emulating a SCR equipped production engine at WHSC mode 9 can be seen in Table 6.

Table 6. *The WHSC SCR mode 9 Load Point.*

Case	Engine Speed	SOI	Inj. Dur.	lambda	P_{CR}	P_{in}	$P_{exhaust}$	T_{in}	EGR
-	rpm	CA°	ms	-	bar	bar	bar	°C	%
SCR	1316	-7.0	1.38	~2.04	1186	0.81 – 1.44	0.83	25	0

The valve strategies used at this load point are found in Table 7.

Table 7. *The valve strategies tested in at the WHSC mode 9 SCR load Point.*

Valve Strategy	Valve 1 lift	Valve 3 lift
	mm	mm
2V (Original)	5- 14.55 (1 mm step)	
1V Straight Port	0	5-14.55 (1 mm step)
2V Trapeze	9, 10, 13, 14.55	
1V Straight Port Trapeze	0	6, 9, 11, 13, 14, 14.55
2V Straight Port (Curved Port Blocked)	14.55	
2V Straight Port (Curved Port Blocked) Trapeze	14.55	

The soot emissions for the studied valve strategies are shown in Figure 52. Here it can be seen that the trends are very similar to the ones observed for the load point simulating a transient, but that the soot emissions generally are much lower. Especially for the low swirl numbers, and this is because of the much higher lambda on this operating point causing the combustion to be less sensitive and not form as much soot, and also a more efficient after oxidation can take place.

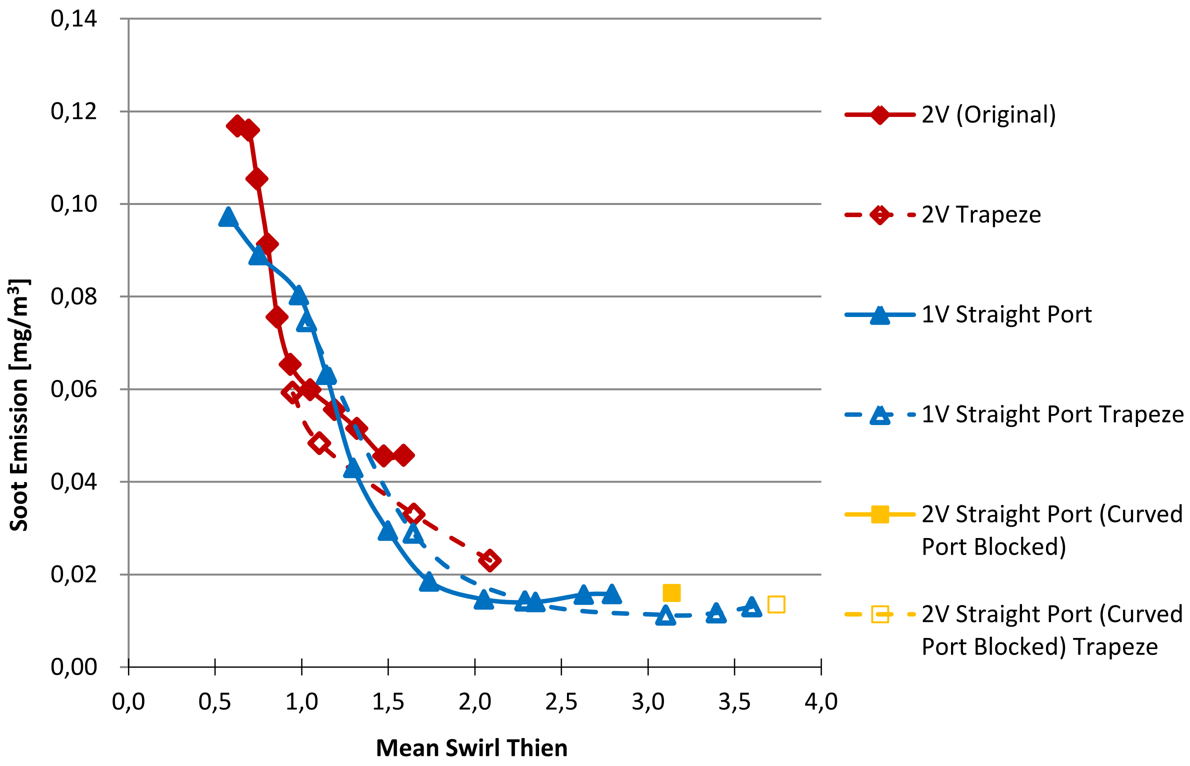

Figure 52. *Soot emissions for the selected valve strategies as a function of mean swirl for the SCR mode 9 load point.*

If the CO emissions are studied, which can be seen in Figure 53, the same trends can be seen again compared to the transient load point. Also here the CO emissions are much lower because of the increased lambda making oxygen available for CO_2 conversion in a larger extent.

However, for really high swirl numbers the CO emissions doesn't increase at all in the same extent as they do for the transient load point, and again this is thought to be because of the higher lambda causing the combustion to be less sensitive for the swirl increase. This can also be seen in the soot emission plot as the emissions are kept quite constant at higher swirl numbers.

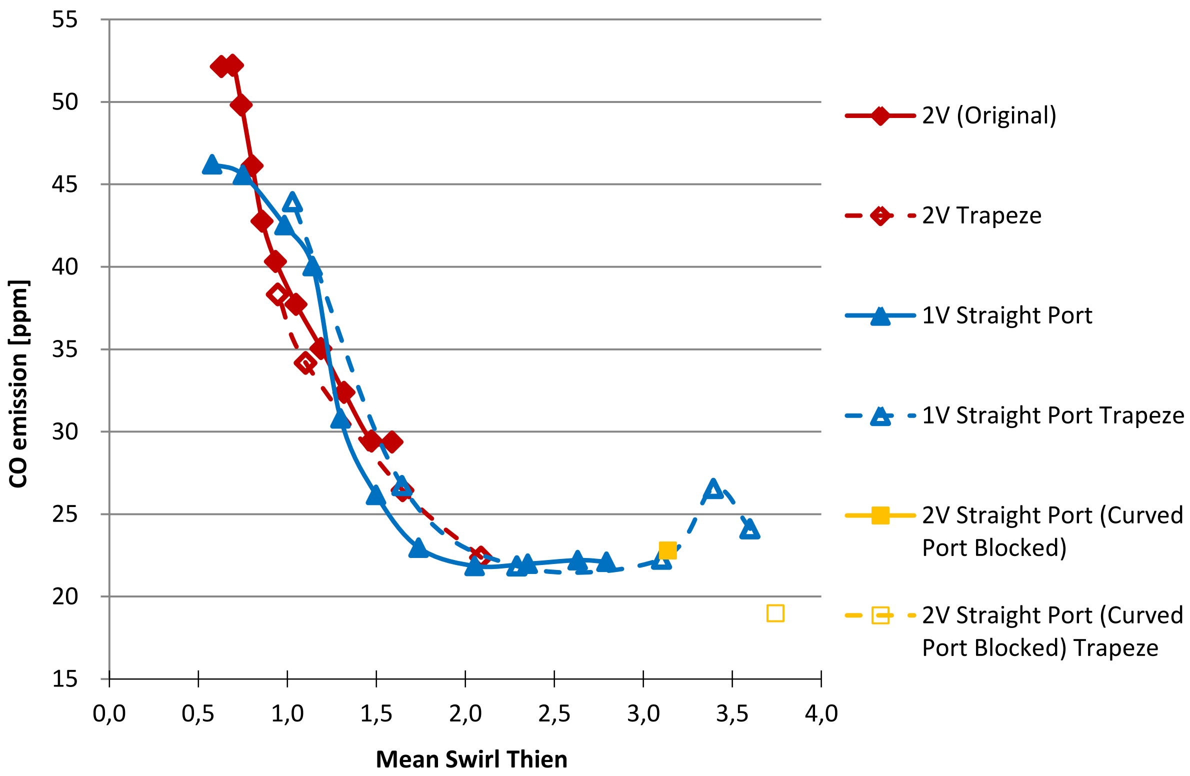

Figure 53. *CO emissions as a function of mean swirl.*

In Figure 54 the NO_x emissions can be seen and for the 2V (Original) and 2V Trapeze cases the trends are once again the same as for the transient load point. But when deactivating one port or on valve, the different load points differs from each other. Here, the NO_x emissions increases with increased swirl even though the compression temperature is much higher on the low valve lifts with low swirl. From this the conclusion can be drawn that the NO_x emissions are more heavily dependent on the swirl motion at higher lambda values because of the higher oxygen content in the cylinder, while at lower lambda values the temperature increase is a factor that affects the NO_x emissions in a greater extent. It can also be seen that the trapezoidal profiles for the 1V cases gives lower NO_x emissions, which is thought to be dependent on a lower compression temperature since the flow is less choked. Once again the trend that the CO and NO_x emissions are connected to each other can be seen, where points with higher CO emission corresponds to points with lower NO_x emissions.

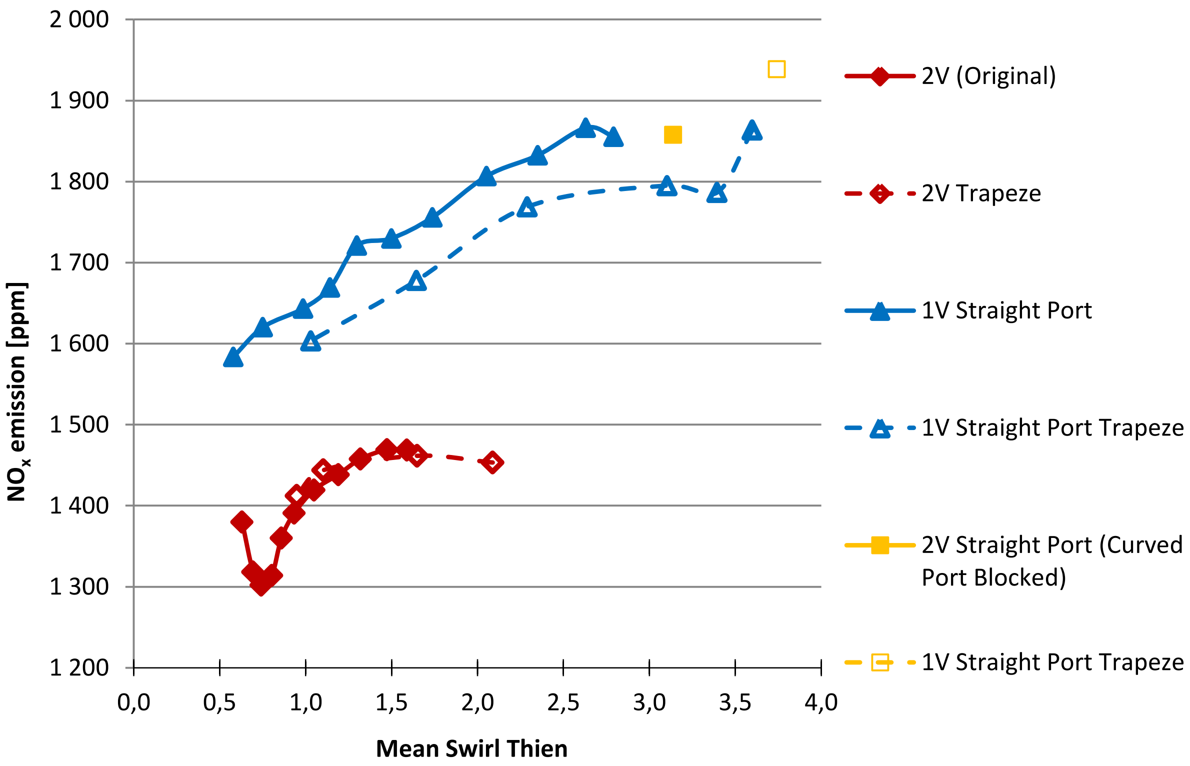

Figure 54. *NO_x emissions as a function of mean swirl for the studied valve strategies.*

For HC it can be mentioned that the variation of the emissions are very low for the different cases in the same way as at the transient load point. If the volumetric efficiency is studied, see Figure 55, similar trends as for the transient load points can be seen.

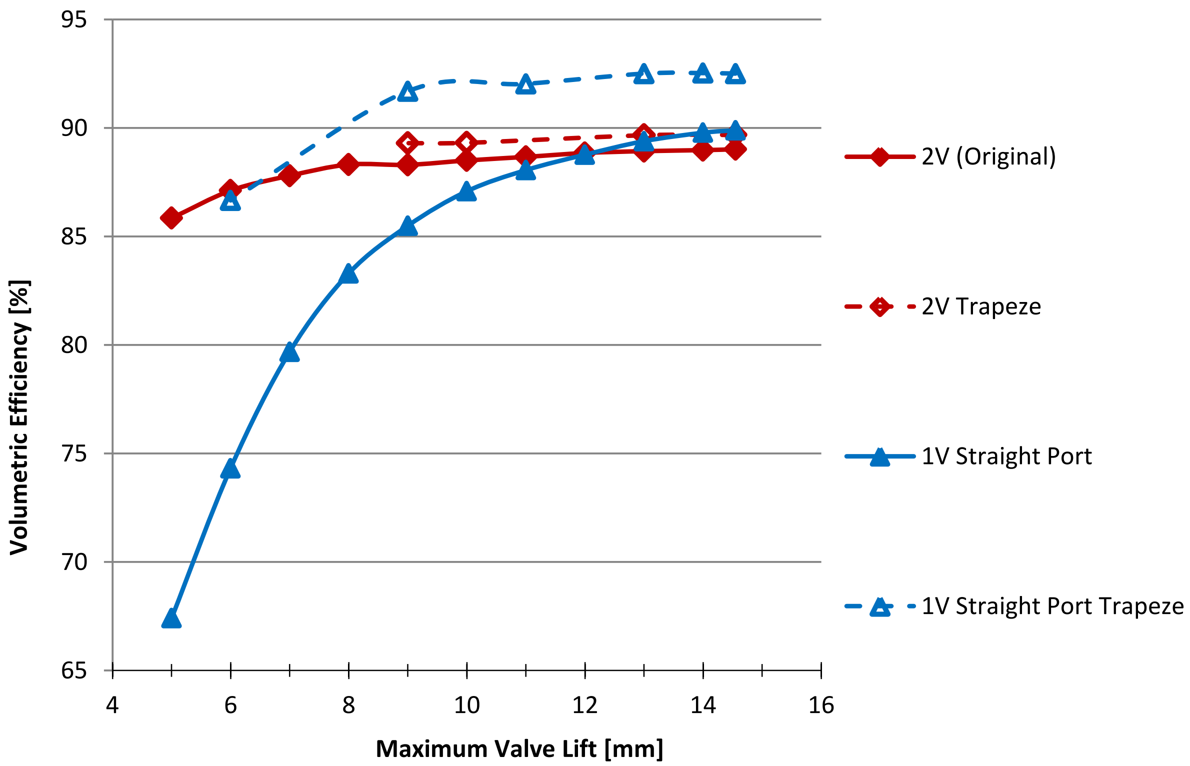

Figure 55. *Volumetric efficiency as a function of maximum valve lift.*

One difference though is that the case with only one valve activated has lower volumetric efficiency already for maximum valve lifts from 12 mm and lower, instead of from 10 mm for the transient load point. This is thought to be mostly because of the higher engine speed at this load point, causing the restriction of the flow to be more noticeable.

The pumping losses are illustrated in Figure 56, where PMEP is plotted as a function of valve lift. Even for PMEP the same trends can be observed, but the pumping losses are higher at this load point because of the higher engine speed even though the set exhaust back pressure is lower than the boost pressure for this specific load point. The differences between the case with flow through one port in respect to flow through both ports are also higher for this load point, showing that it is more inefficient to deactivate or block one port at higher engine speed. Please note that the 2V Straight Port (Curved Port Blocked) Trapeze case has almost the same PMEP as the 2V Straight Port (Curved Port Blocked), and therefore the Trapeze case is hidden behind the other case in Figure 56.

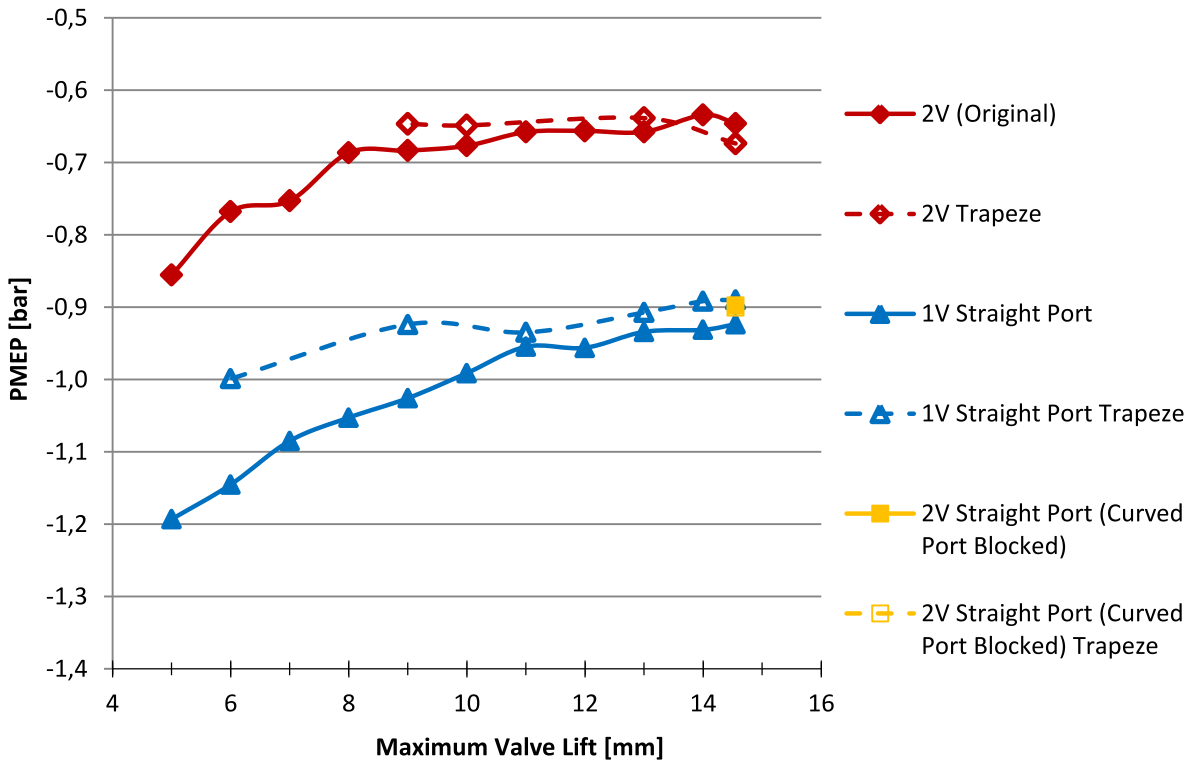

Figure 56. *PMEP as a function of maximum valve lift for the tests at WHSC mode 9 SCR. Note that the yellow data points are placed almost on top of each other.*

This effects the total efficiency of the engine and this is shown in Figure 57 in form of the BSFC. At this load point the cases with one valve deactivated or one port blocked is no way near as efficient as the case with flow through both ports. Once again it should be stated that the pumping losses are not the only factor that influence the brake specific fuel consumption. A higher swirl motion means higher heat transfer and thereby less possible work to be applied to the piston. Also differences in the combustion phasing because of different compression temperature and thereby different SOC, and different intensity of the combustion due to different in-cylinder motions are affecting the efficiency of the engine, in similar ways as for the transient load point.

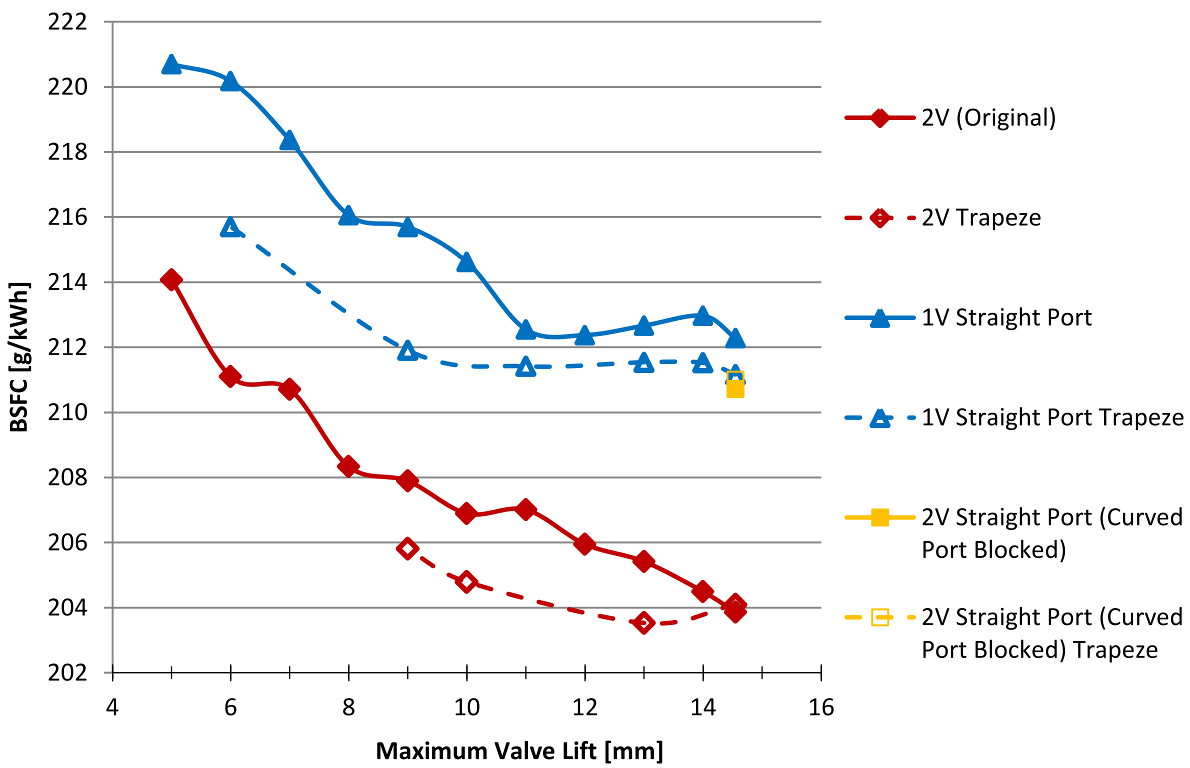

Figure 57. *BSFC as a function of maximum valve lift.*

For this load point the different cases with high valve lifts were tested with small differences in boost pressure because of the very similar volumetric efficiency between the strategies, and thereby the comparison between the different BSFC is quite fair. But for the lower valve lifts the boost pressure have been increased for the cases with one port blocked or one valve deactivated, and the BSFC would be even worse for these cases on the same inlet manifold pressure as for the standard case.

6.3.3 WHSC EGR mode 9

The WHSC EGR mode 9 load point is defined in Table 8.

Table 8. *The WHSC EGR mode 9 load point.*

Case	Engine Speed	SOI	Inj. Dur.	lambda	P_{CR}	P_{in}	$P_{exhaust}$	T_{in}	EGR
-	rpm	CA°	ms	-	bar	bar	bar	°C	%
EGR25	1316	-7.7	1.15	~1.57	1224	1.18 – 1.55	1.28 – 1.65	42	25

To investigate whether the trends seen for the valve strategies during the transient and SCR load points remain the same when introducing EGR, the mode 9 EGR load point were run with the valve strategies defined in Table 9.

Table 9. *The valve strategies tested in this chapter.*

Valve Strategy	Valve 1 lift	Valve 3 lift
	mm	mm
2V (Original)	10, 11, 14.55	
1V Straight Port	0	7, 8, 10, 13, 14.55
2V Trapeze	9, 10, 13, 14.55	
1V Straight Port Trapeze	0	6, 9, 11, 13, 14, 14.55
2V Straight Port (Curved Port Blocked)	13,14.55	
2V Straight Port (Curved Port Blocked) Trapeze	13,14.55	

The WHSC mode 9 EGR load point shows very similar trends for the soot emissions, see Figure 58, as the SCR case. But as seen during the earlier load point simulating a transient, the highest swirl numbers do not produce the lowest soot emissions, rather the minimum soot emissions are located around a maximum valve lift of around 12-13 mm and a swirl number of around 2.5. Also the CO emissions has the same trend as the transient load point with an increase of emissions at to high swirl numbers, which can't be seen in for the WHSC SCR point. This seems to suggest that the combustion is more sensitive for higher swirl numbers both with lower lambda values and with EGR.

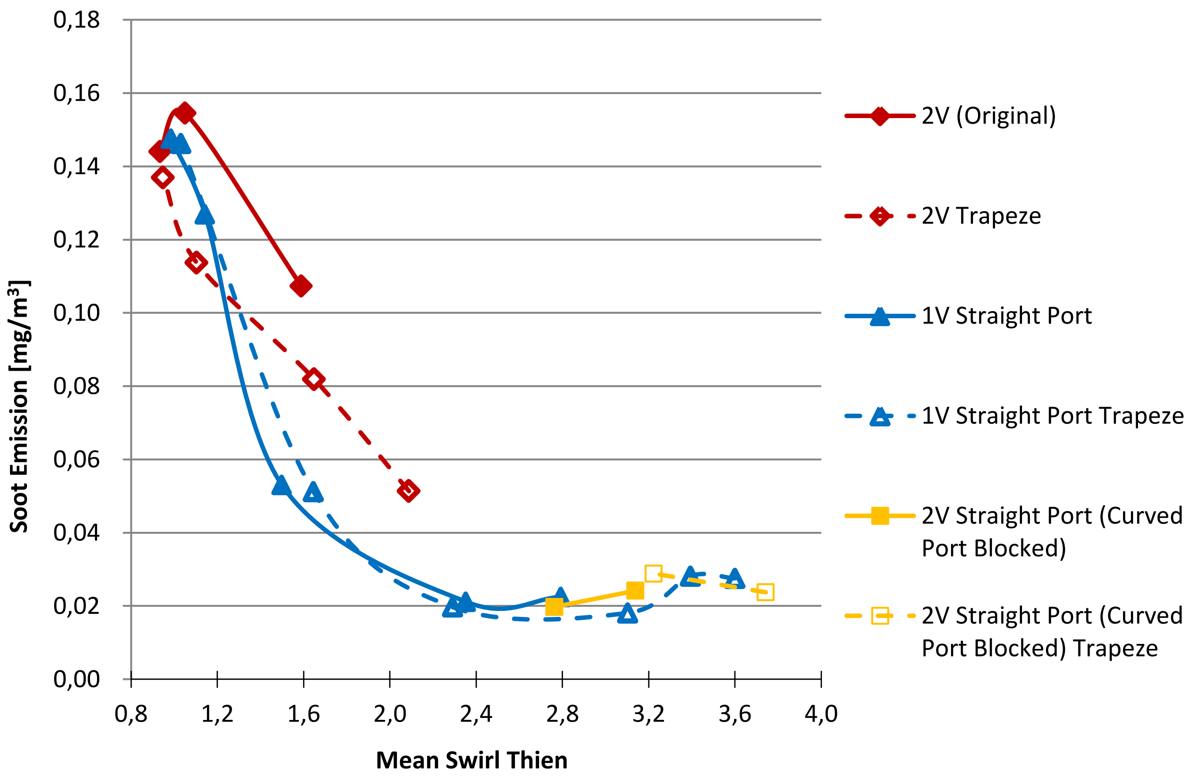

Figure 58. *The Soot Emissions for the selected valve strategies as a function of Swirl Number.*

While the soot emissions display a clear connection to the swirl number, the NO_x emissions, which can be seen in Figure 59, do not show such a connection. Once again the trends are very similar to the SCR case.

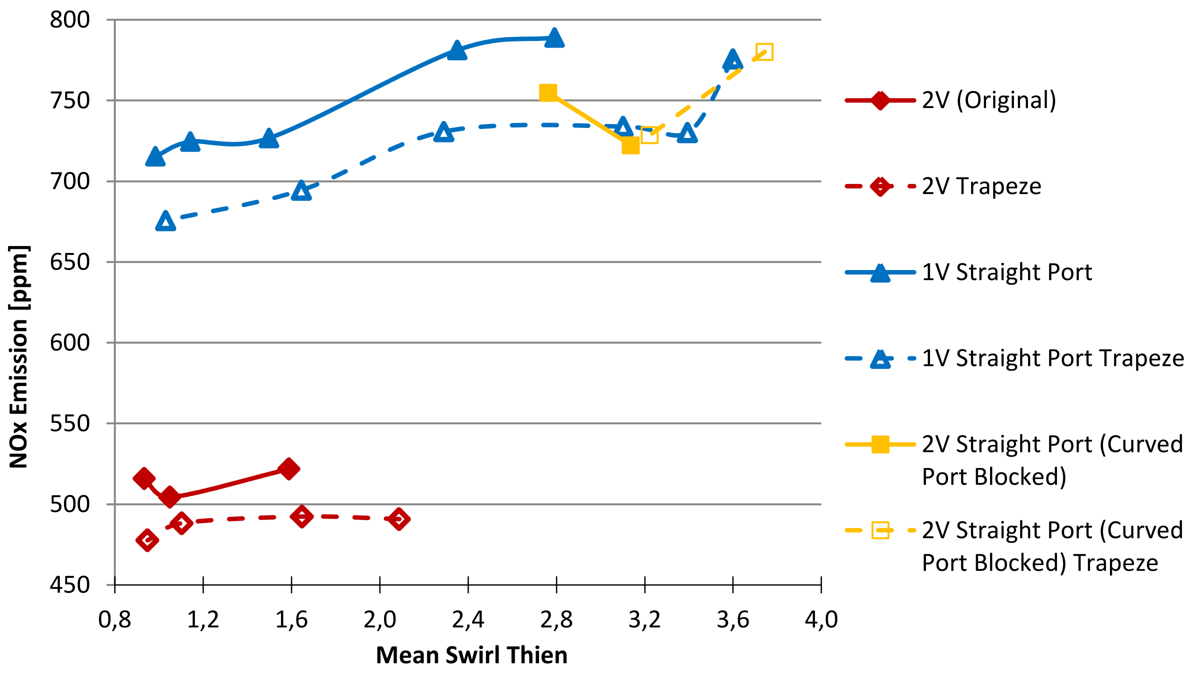

Figure 59. *The NO_x emissions for the valve strategies as a function of Swirl Number.*

The major difference in NO_x emissions between the valve strategies are when going from two valves open to one deactivated or a port blocked. Again this is thought to be because of the increased compression temperature with the more choked flow. Once again the NO_x emissions doesn't decrease at the highest swirl numbers, in a similar way as for the SCR case. However, the CO emissions increases at the highest swirl numbers, see Figure 60, which doesn't follow the same trend as for the SCR load point, rather it is more like the transient point. This suggests that the connection between the CO and NO_x emissions isn't as clear when EGR is introduced.

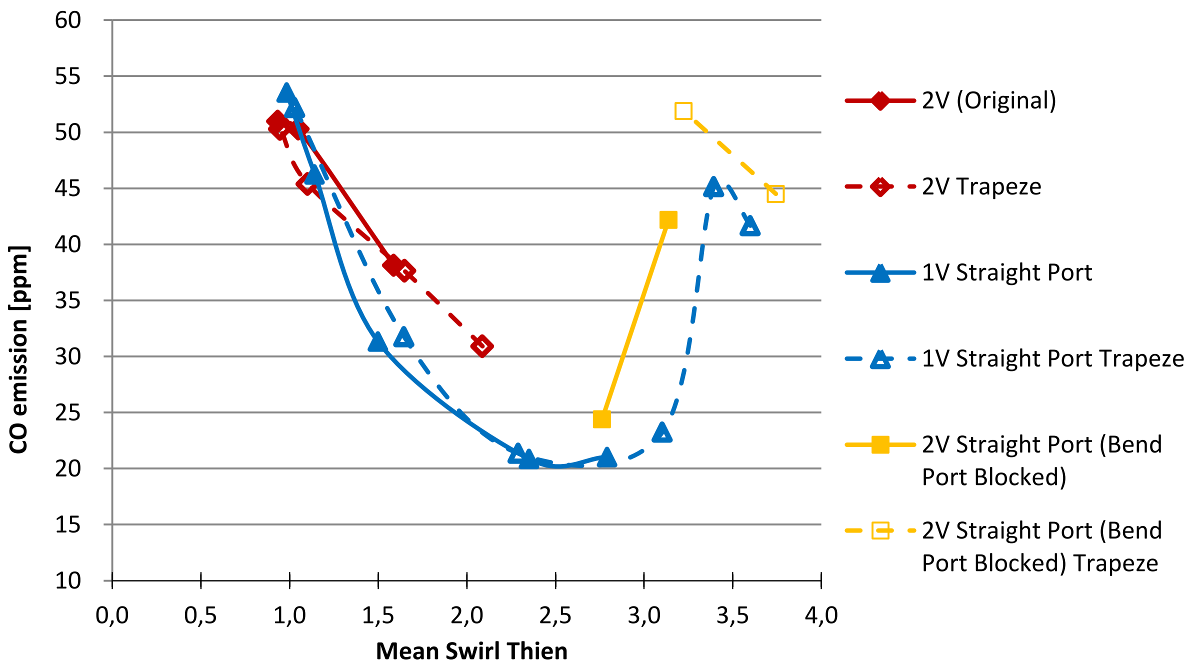

Figure 60. *The CO emissions as a function of mean swirl according to Thien.*

If the pumping losses is investigated with PMEP, as can be seen in Figure 61, also here very similar trends occurs. One difference is that there are higher pumping losses in general for the EGR case compared to the SCR case. This is thought to be because of the higher temperature of the inlet gases with EGR causing lower volumetric efficiency and thereby higher pumping losses.

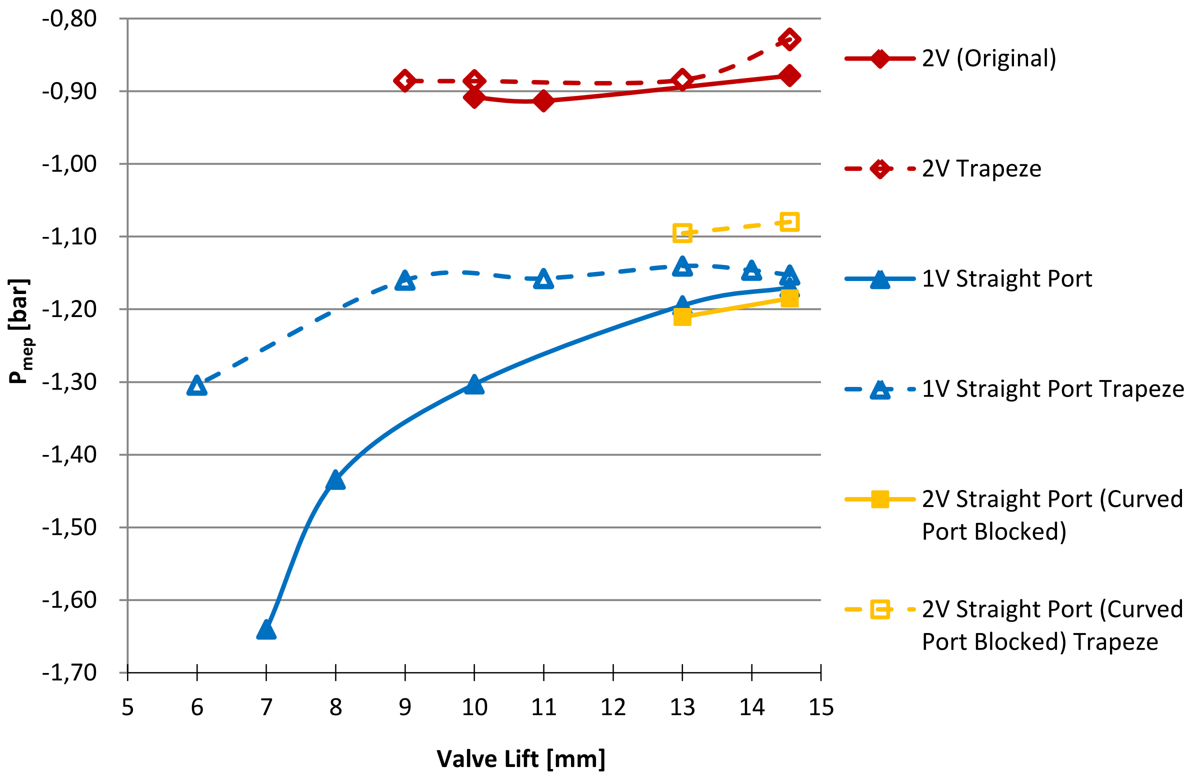

Figure 61. *The pumping losses for the valve strategies as a function of valve lift.*

Compared to the transient load point at 1056 rpm the differences in pumping losses between the 2V cases and the 1V cases have increased significantly, in the same way as for the SCR point. Especially for the most restrictive strategy, 1V Straight Port, Std. Profile, where the pumping quickly increase as the valve lift is lowered.

It is generally assumed that a higher swirl increases the heat losses significantly which should imply a higher fuel consumption, but as can be seen in Figure 62 the fuel consumption for this load point doesn’t increase with the swirl number. Instead the dominant factor seems to be the pumping losses which in turn increase when the valve lift is lowered.

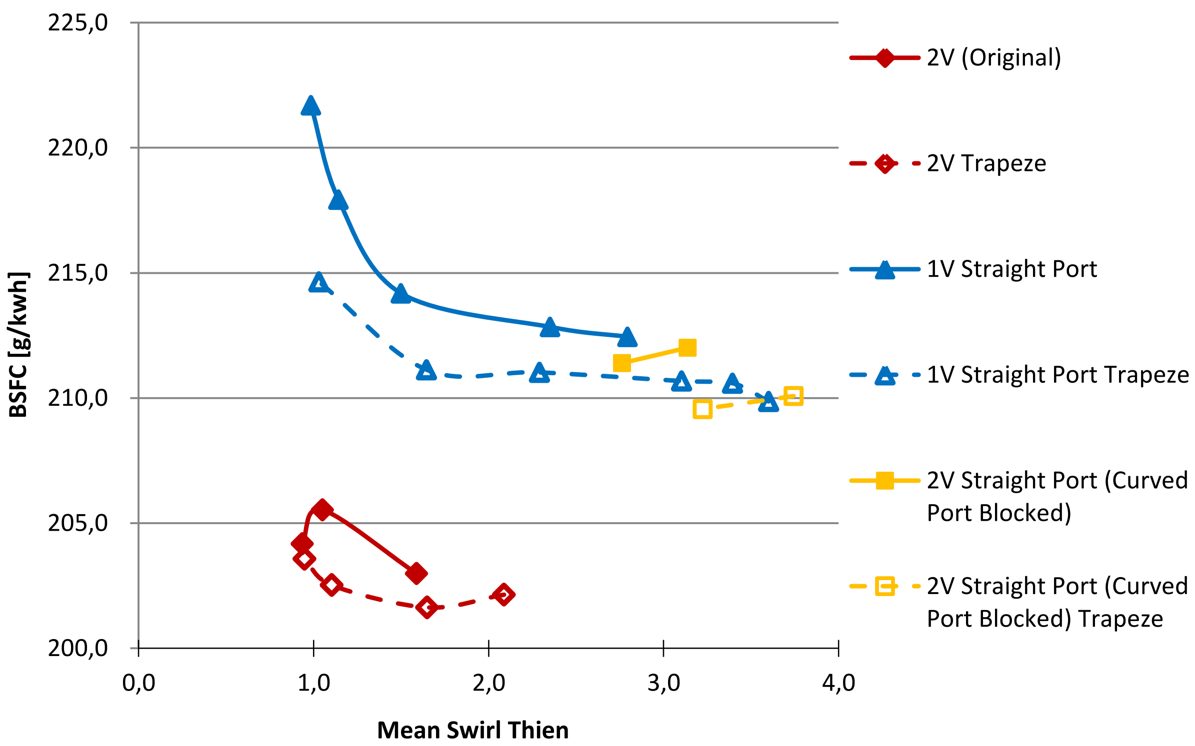

Figure 62. *The BFSC for the different valve strategies as a function of Swirl Number.*

6.3.4 EGR Sweep

To test the EGR sensitivity of the selected valve strategies shown in Table 10, the EGR levels were increased in two steps from the 25% in the load point for WHSC mode 9 to 30 and 32.5%. The load points can be seen in Table 11.

Table 10. *The tested valve strategies in this chapter.*

Valve Strategy	Valve 1 lift	Valve 3 lift
	mm	mm
2V (Original)	14.55	
1V Straight Port	0	13,14.55
1V Straight Port Trapeze	0	13,14.55
2V Straight Port (Curved Port Blocked)	13,14.55	

Table 11. *The three load points with different EGR levels.*

Case	Engine Speed	SOI	Inj. Dur.	lambda	P_{CR}	P_{in}	$P_{exhaust}$	T_{in}	EGR
-	rpm	CA°	ms	-	bar	bar	bar	°C	%
EGR25	1316	-7.7	1.15	~1.57	1224	1.18 – 1.55	1.28 – 1.65	42	25
EGR30	1316	-7.7	1.15	~1.44	1224	1.23 – 1.31	1.33 – 1.41	42	30
EGR32.5	1316	-7.7	1.15	~1.37	1224	1.22 – 1.34	1.32 – 1.44	42	32.5

The trends for the soot emissions are shown in Figure 63. Please observe that the emissions are plotted against the calculated engine out EGR according to the PDP and not the indicated values from the Horiba. In other words, an EGR level of 25%, 30% and 32.5% according to the Horiba correspond to around 26%, 32% and 35% from the PDP.

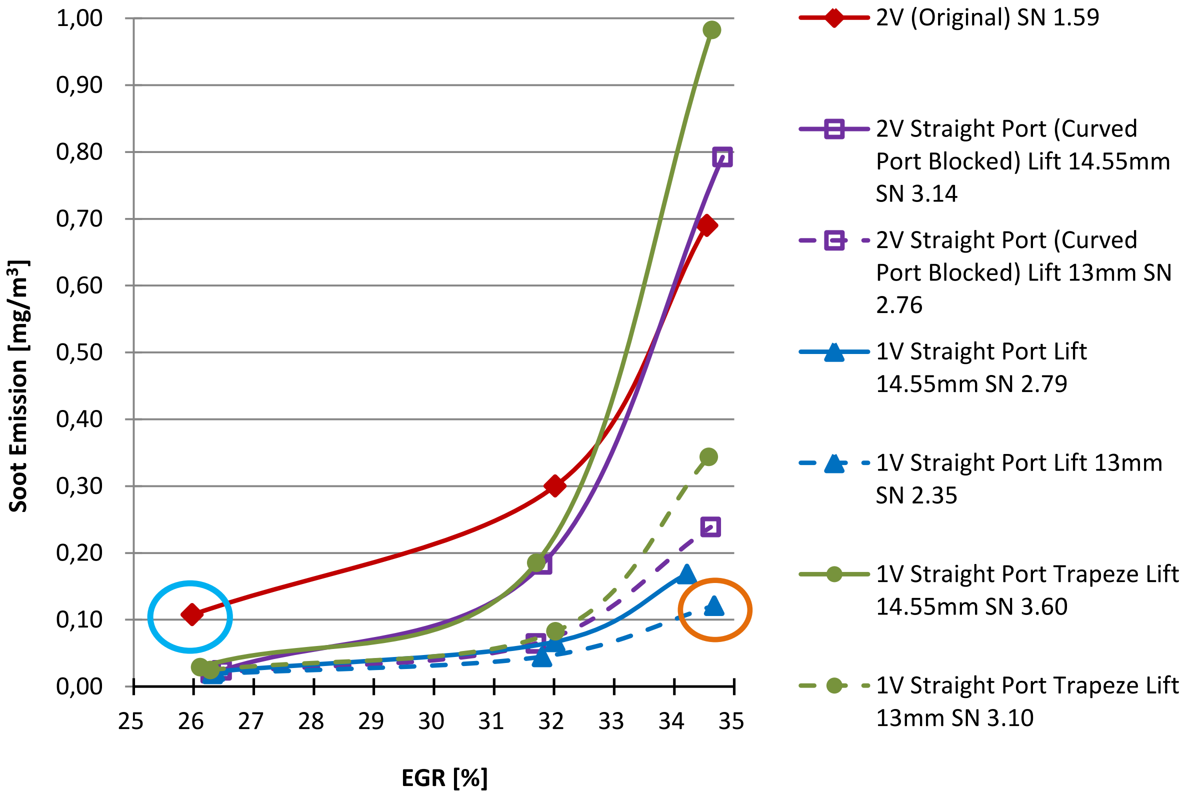

Figure 63. *The soot emissions for different valve strategies when the EGR level is swept, two interesting points with similar soot emissions at different EGR levels is marked by circles in the figure.*

As can be seen in the figure the valve strategies with the highest swirl numbers produce more soot than the 2V case above a certain EGR level at around 33-34%. At the lower EGR levels all the valve strategies selected in this test produced lower soot emissions than the standard 2V case. At the highest EGR level it is assumed that the increased soot emissions are caused by over-swirling for the higher swirl numbers, which decreases the combustion quality in a similar way as for the transient load point. At this EGR level the lowest soot emissions is obtained changing from the standard valve strategy to the 1V Straight Port Lift 13 mm case, with a swirl number of 2.35. This point is marked with a orange circle in the figure and it is interesting to see that it has similar soot emissions as the standard strategy at 26% EGR, marked with a blue circle. The soot emissions increases with higher swirl numbers than 2.35 and at the level of 3.14 and above the soot emissions is higher than the standard case for the highest EGR level.

Support for the theory of over-swirling can be found by studying the CO emissions in Figure 64, which shows a almost perfect scaling with the swirl number if the 2V case is disregarded. The same points are marked in this figure as for the soot emissions and again similar emission levels are obtained.

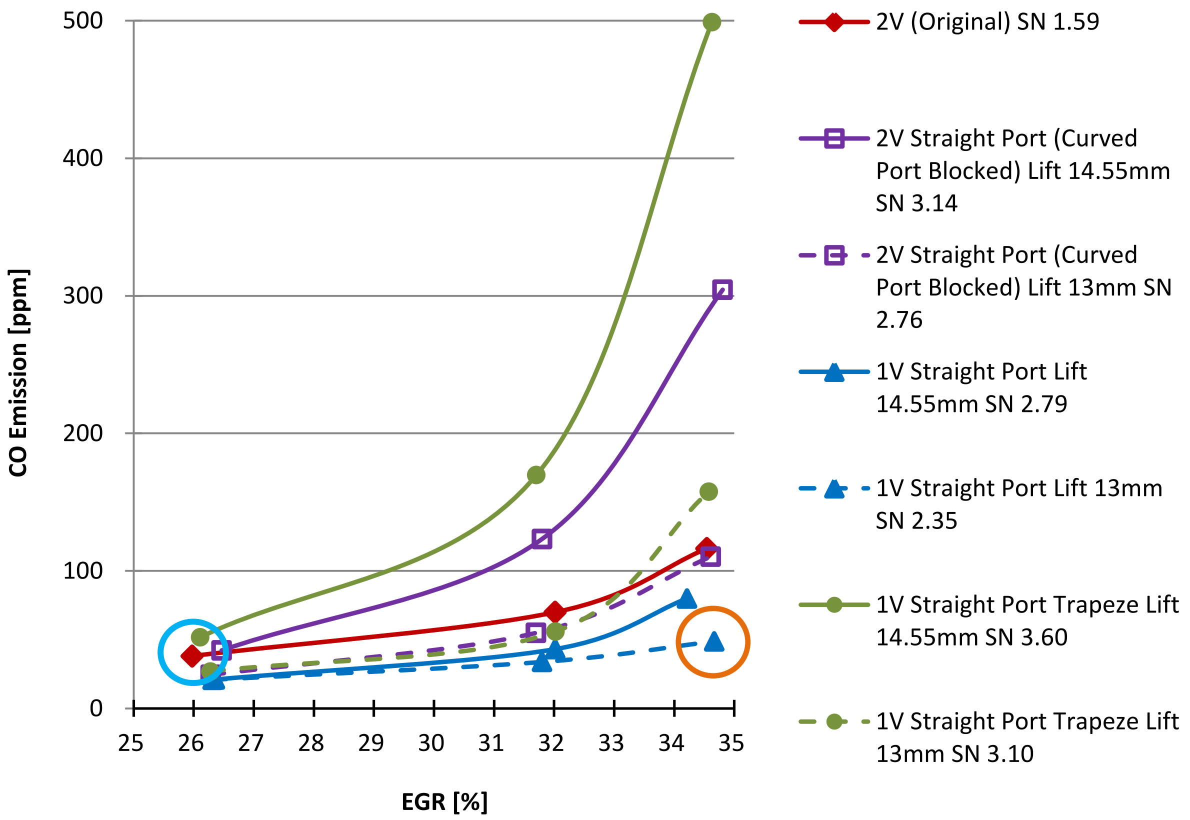

Figure 64. *The CO emissions with different valve strategies when the EGR level is swept, two interesting points with similar CO emissions at different EGR levels is marked by circles in the figure.*

While the reduction in soot emissions is important, the purpose of EGR is to lower the NO_x emissions. As can be observed in Figure 65, all the selected valve strategies increase the NO_x emissions in comparison with the 2V (Original) case, which is thought to be primarily caused by the increase in compression temperature when deactivating or blocking a port. This is of course not desirable, but after a deeper analysis the advantages of these valve strategies become apparent. As for a given soot level, the NO_x emissions can be lowered significantly. Especially if comparing the soot emissions for the best case, 1V Straight Port Lift 13 mm at 35% EGR, see orange circle, with the 2V (Original) case at 26% EGR, see blue circle, where the 1V case produces similar soot and CO emissions while the NO_x emissions are reduced by 60%.

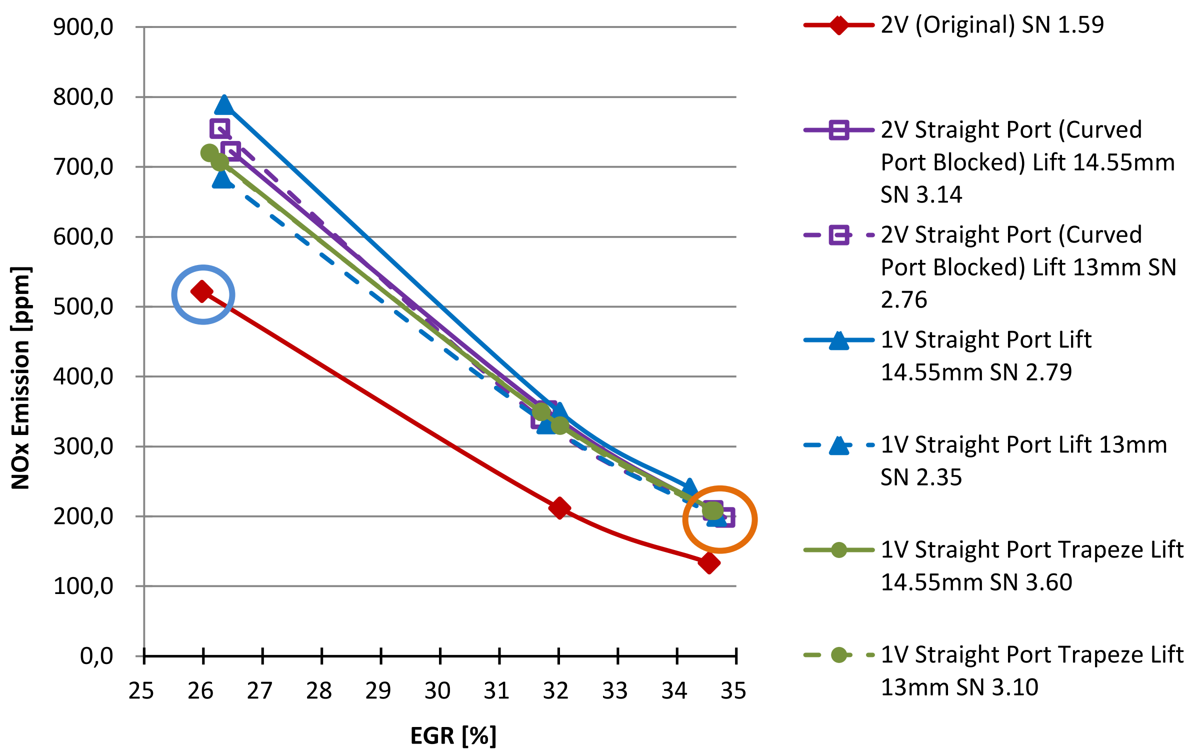

Figure 65. *The NO_x emissions with different valve strategies when the EGR level is swept. The same points as for the soot and CO emissions are marked by circles in the figure and here a reduction of the NO_x emissions could be seen.*

Of course there is a cost attached to lowering the NO_x emissions by this method. This can be seen by studying the BFSC in Figure 66. As the injected fuel mass is kept constant for all the valve strategies, the differences in fuel consumption depends on the combustion quality, heat losses and pumping losses.

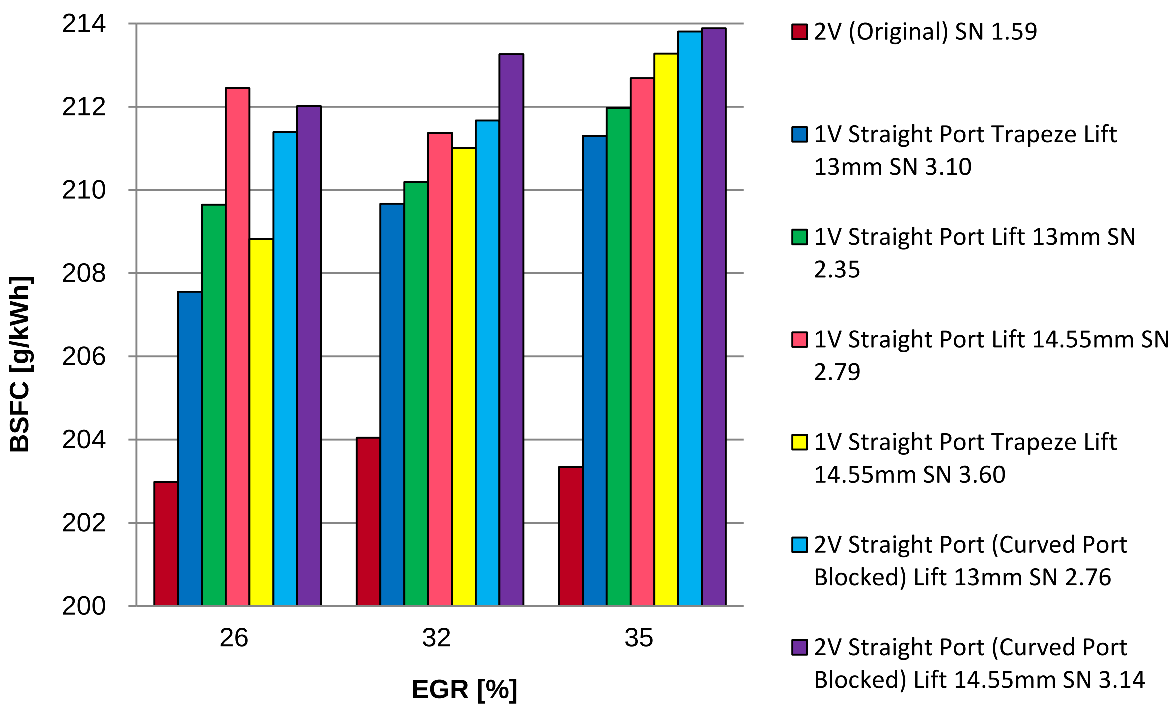

Figure 66. *The BSFC with different valve strategies when the EGR level is swept.*

The fuel consumption for the 2V case is not significantly affected by the different EGR levels, while the trend for the alternative valve strategies is an increase in fuel consumption with higher EGR levels. The valve strategies with 13 mm lift provide the best fuel consumption of the alternative valve strategies, with a slight advantage for the trapezoidal profile.

To analyze this further, the pumping losses for the different valve strategies are plotted in Figure 67. As can be observed in the figure the major differences in pumping losses is a result of deactivating one valve or port. This is the major factor explaining the higher BSFC with one valve deactivated or one port blocked.

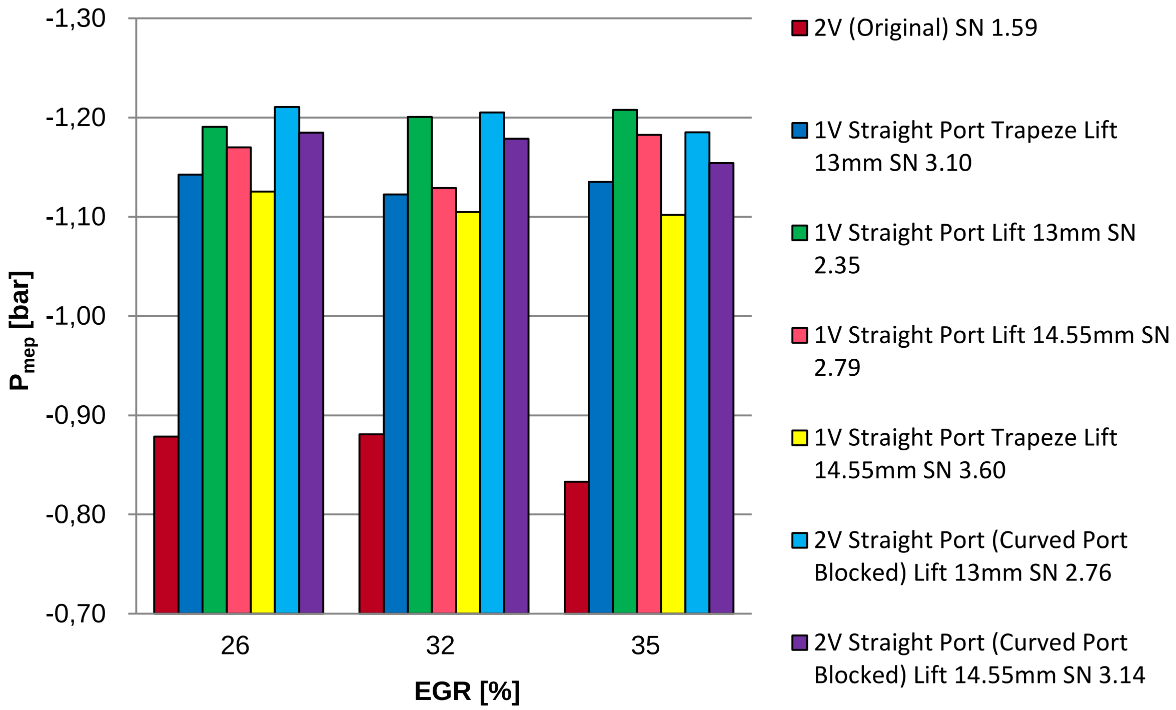

Figure 67. *The pumping losses with different valve strategies when the EGR level is swept.*

It is worth pointing out that the values of the pumping losses are not directly comparable as the intake manifold pressure was slightly modified for each valve strategy to match the reference lambda of the 2V case. Another factor which influences the pumping losses is the exhaust back pressure. As the EGR-pump requires a pressure differential of 0.1 bar between the intake and exhaust manifolds to function, the exhaust back pressure is therefore modified along with the intake manifold pressure.

6.3.5 Engine Speed Sweep

The load points for the engine speed sweep can be found in Table 12.

Table 12. *The load points for the engine speed sweep.*

Case	Engine Speed	SOI	Inj. Dur.	lambda	P_{CR}	P_{in}	$P_{exhaust}$	T_{in}	EGR
-	rpm	CA°	ms	-	bar	bar	bar	°C	%
Engine Speed Sweep	1700 – 800	-10 to -3	1.4	~1.25	1500	0.12 – 0.34	0	25	0

From the engine speed sweep an investigation of how the valve strategies affect the engine's volumetric efficiency can be performed. Unfortunately the engine test cell at KTH had problems measuring the air mass flow and also logging the cylinder pressure, therefore the set inlet manifold pressure is used for this comparison. All valve strategies have been run with the standard maximum valve lift of 14.55 mm. The starting point for the sweep was a engine speed of 1700 rpm for the 2V case, where a suitable injected fuel mass was found, which achieved a lambda value of 1.25 at a intake manifold pressure of 0.12 bar. As the injected fuel mass was kept constant throughout the sweep, the inlet manifold pressure had to be increased as the engine speed was lowered in steps of 100 rpm. A constant lambda value of 1.25 was maintained regardless of valve strategy. The variation of the inlet manifold pressure as a function of engine speed for the different valve strategies can be seen in Figure 68.

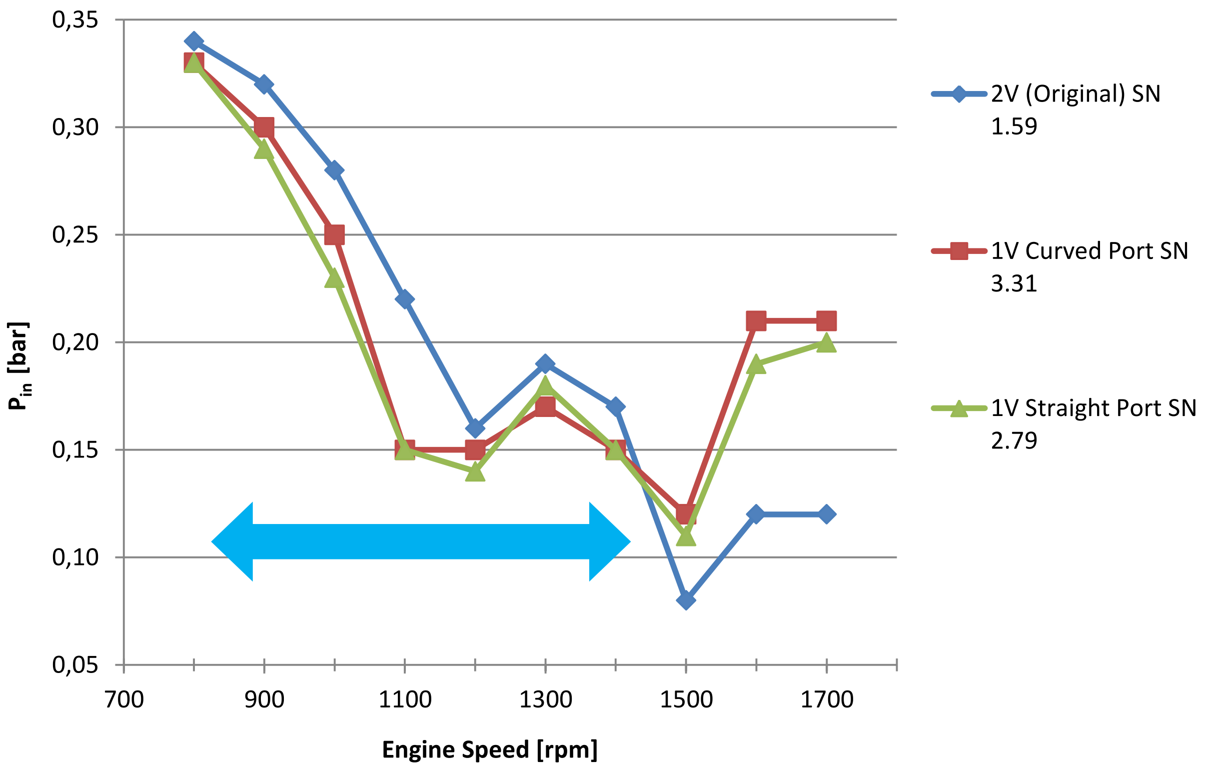

Figure 68. *The intake manifold pressure required for constant lambda value at engine speeds from 800-1700 rpm shown for a selection of valve strategies. The blue arrow illustrates the engine speed for which the 1V cases have a better volumetric efficiency.*

As can be observed the inlet manifold pressure for the 1V cases is lower than for the 2V case up to around 1400 rpm, this suggests that the volumetric efficiency for these cases are better than with standard 2V case. This area is illustrated with a blue arrow in the figure. This might be caused by a larger amount of backflow for the 2V case. Another interesting observation that can be made is the similar trends for the 1V cases, therefore it doesn't matter which valve is deactivated from a volumetric efficiency standpoint. This was also shown earlier in the flow bench results as the $\mu\sigma$ values were quite equal for both cases. It should be noted when seeing this result that the pumping losses are still increased when deactivating a valve, at least at higher engine speeds. This couldn't be studied for this sweep because of the deficiencies in the logging of the cylinder pressure. The intake ports do affect the flow very differently though as can been seen in Figure 69, which shows the smoke emissions as a function of engine speed for the different valve strategies.

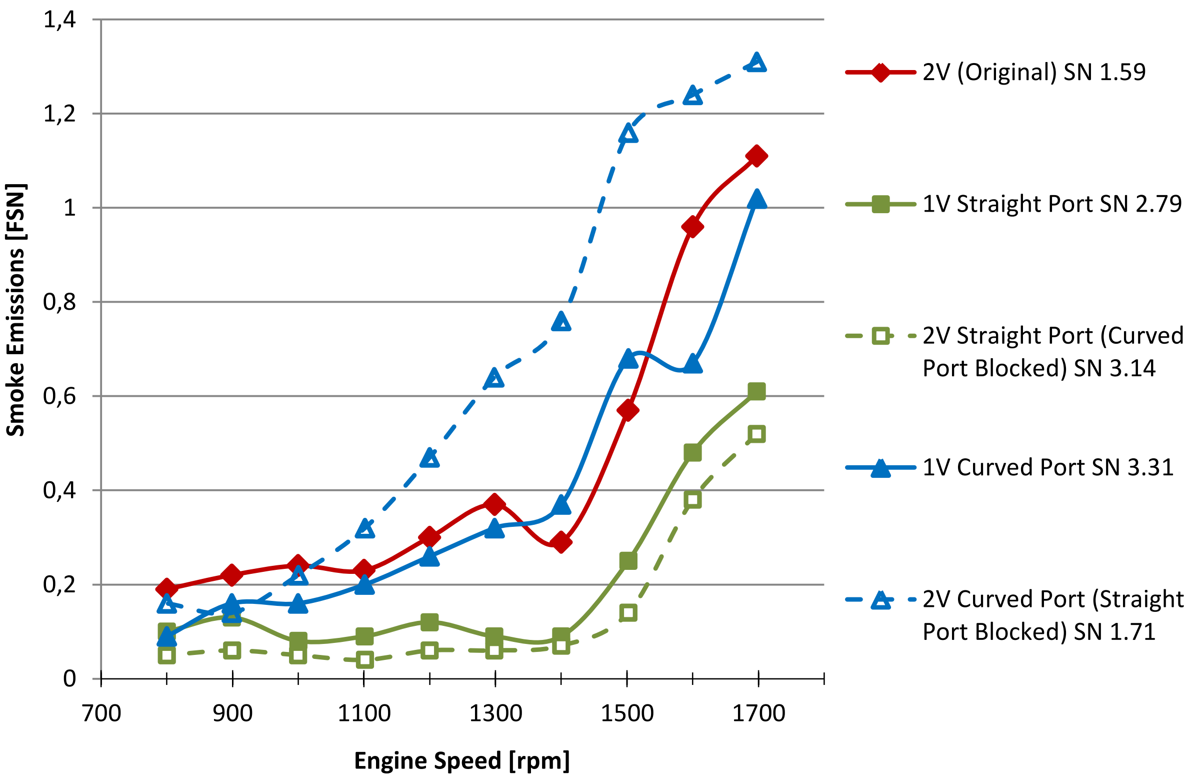

Figure 69. *Smoke emissions as a function of engine speed for a different valve strategies.*

Figure 69 shows that the 1V Straight Port valve strategy has an advantage in smoke emissions compared to the 2V case for all engine speeds. This was unexpected as it was assumed that the higher swirl would be an disadvantage at high engine speeds, since this was the trend with the high-swirl cylinder head of the project [2] prior to this master thesis. However it might have been the discontinuity formed by the masked valve seats with the high-swirl head which caused this trend or that the swirl number was simply too high for good smoke performance at high engine speeds.

When studying the valve strategies with the curved intake port it is clear that the swirl number doesn't describe the results very well. The poor smoke characteristics of the curved port is assumed to be caused by the change of direction that takes place for the swirl motion as described in the flow bench measurements. The result of this varying swirl direction is a valve strategy with a measured swirl number of 3.31 to perform on par with the standard 2V case with a swirl number of 1.59. A possible explanation for this phenomena is that it takes more energy to slow down and reverse the in-cylinder air flow than it would take to just continue to increase the air flow in the same direction. Neither the Thien calculation method for the mean swirl number or the GT-Power simulation, which shows the same trends, takes this into account and this results in a likely erroneous value.

The valve strategies which simply blocked one of the intake ports amplified the trends seen for the cases when the corresponding valve was deactivated. When the curved port was blocked the lowest smoke emissions were reached. This is assumed to be because of the valve of the blocked port acts as a guide, which directs the air flow at low valve lifts in the main swirl direction. In the flow bench measurements this effect was seen as a higher swirl number at low to medium valve lifts and as can be seen in Figure 69 this has a beneficial effect on the smoke emissions. On the other hand when blocking the straight port the valve head and steam blocks the build-up of the air motion in the main swirl direction. The effect of this in the flow bench was even more negative swirl motion in addition to a lower maximum value. Despite only lowering the swirl number to 1.71, the smoke emissions display a much worse trend then the 2V case with a swirl number of 1.59. The conclusion drawn from this is the same as when deactivating the valve to the curved port, that the swirl number is not correctly predicted.

6.3.6 Lambda Sweep

To illustrate the potential benefits of lowering the smoke emissions, a sweep from lambda 3 to lambda 1 was performed, see Table 13.

Table 13. *The load points for the lambda sweep.*

Case	Engine Speed	SOI	Inj. Dur.	lambda	P_{CR}	P_{in}	$P_{exhaust}$	T_{in}	EGR
-	rpm	CA°	ms	-	bar	bar	bar	°C	%
Lambda Sweep	1000	-2	0.72 – 1.86	3 – 1	2000	0.5	0	25	0

All valve strategies have been run with the standard maximum valve lift of 14.55mm. The smoke and NO_x emissions for different valve strategies as a function of the lambda value are shown Figure 70.

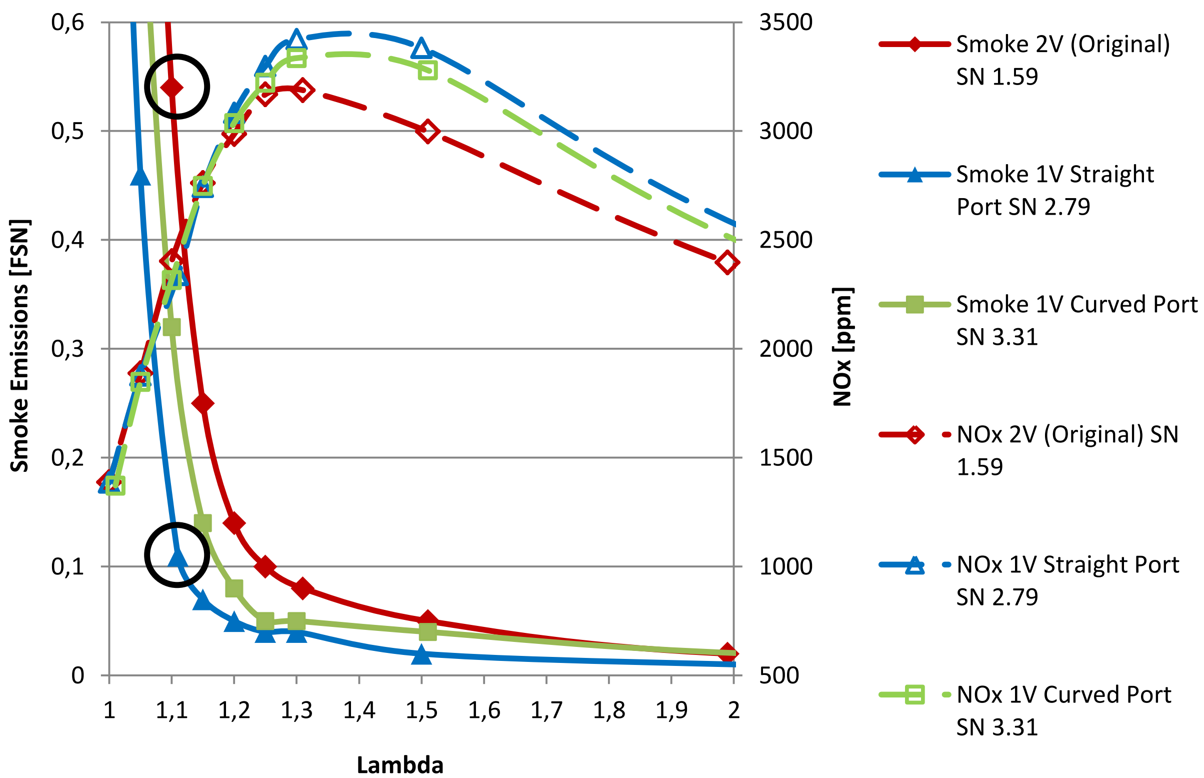

Figure 70. *The smoke and NO_x emissions for different valve strategies as a function of lambda value. The two black circles mark a significant smoke reduction at lambda 1.10.*

As can be observed in the figure it is possible to run the engine at a significantly lower lambda value for a given smoke limit using valve deactivation. For example the smoke reduction between the standard 2V case and the 1V Straight Port strategy is reduced by around 80% at lambda 1.10, from 0.54 to 0.11 FSN. Yet again it is possible to see that the soot emissions for the case with the curved port doesn’t correspond well to the calculated swirl number. At the lower lambda values, below 1.20, all three cases converge towards the same NO_x emissions regardless of the swirl number and a lower lambda value gives lower NO_x emissions. At these low lambda values the air excess is so small that it effects the NO_x formation.

7 Discussion and Conclusion

The master thesis has shown that the in-cylinder flow can be greatly affected by different valve strategies with both symmetrical and asymmetrical valve lifts. This has also been shown to affect the emissions. By only adjusting the valve lifts on the inlet valves, swirl numbers between 0 and 4 according to Thien can be achieved, and also swirl in the opposite direction to the common rotational direction can be achieved for flow only through the curved port at low lifts with the studied cylinder head. If the swirl motion is generated in one direction at low valve lifts, and in the opposite direction at higher valve lifts, the calculated mean swirl correlates poorly with measured emissions. This is because both the Thien and GT-Power method doesn't describe the phenomenon that occurs, when the air motion has to change direction in the cylinder, in an accurate manner. This has to be further investigated and if swirl measurements display this behavior, knowledge of this phenomenon is of great importance.

Also the tumble motion can be greatly affected by different valve lifts. With a two valve strategy the tumble motion is highest at maximum valve lifts, with tumble values from around 1.5 to 0 and also negative values at the lowest lifts, i.e. the motion is in the opposite direction. The tumble motion for the strategies with only one valve activated or one port blocked were very similar to each other. The highest tumble values were obtained at low valve lifts, with a value of almost 6 at 5 mm lift compared to around 1.5 at the maximum valve lift.

The study of the tumble motion showed the importance of measuring tumble for several cylinder head angles on every valve lift, since the angle of the maximum tumble is affected by the strength of the swirl motion. If a traditional tumble study is performed, where a single valve lift sweep is performed for the cylinder head angle that gives most tumble at the maximum valve lift, valuable information on the tumble motion's behavior at lower valve lifts is lost.

If the curved port is blocked, the valve stem and valve head of this port have been proven to be able to increase the swirl motion compared to the case with the valve of the curved port deactivated, without any great effects on the flow efficiency. On the other hand, if the straight port is blocked, the valve stem and head from the straight port greatly decreases the swirl motion. For both the cases the tumble motion is almost unaffected.

From the investigation of the different methods to calculate mean swirl and tumble it can be concluded that, for the case with unchanged valve timing from the standard Scania D12, the methods gives almost the same trends. For swirl the values are almost identical, while Thien gives somewhat larger tumble values than GT-Power, but still the trends are very similar when comparing different valve strategies with each other. Therefore, which one of the investigated methods to be used for calculating the mean flow characteristics when performing a study like the one in this master thesis is of less importance. But if for example a miller strategy would be used with late inlet valve closing, the GT-Power method would be preferable since the calculations are performed even after BDC of the intake stroke. On the other hand the Thien method would be preferable, if both valves are lifted but asymmetrical lifts are used, since the valves are described separately in GT-Power and therefore makes it difficult to implement flow coefficients for asymmetrical valve strategies.

From the engine cell tests the in-cylinder flow has been seen having great effects on the emissions. An increase in swirl motion reduced the soot emissions. For the load point simulating a transient, with a lambda value of 1.25, the soot emissions can be reduced from

0.40 mg/m^3 for the original case to 0.08 mg/m^3 with the valve to the curved port deactivated, and to 0.06 mg/m^3 with the curved port blocked. Though with higher NO_x emissions as a result when deactivating a valve or blocking a port. With trapezoidal valve profiles a further increase of swirl motion can be obtained, resulting in similar soot emissions and reducing the NO_x emissions to the same levels as the original case, but with an increase in CO emissions.

For the tests performed at higher lambda values the same trends were observed for the soot emissions. The NO_x emissions for these tests were constantly higher with the strategies of deactivating the valve or blocking the straight port, compared to the 2 valve strategy. On the other hand the CO emissions can be kept at low values even with the highest swirl numbers tested.

With the introduction of EGR to WHSC mode 9 very similar trends arises compared to the SCR mode. From the EGR sweep it can be seen that the case with a maximum valve lift of 13 mm for only the straight port with 35% EGR, has similar soot emissions compared to the standard case at 26% EGR. With the higher amount of EGR the NO_x emissions decreases, and in this case they were lowered by 60% compared to the standard case at 26% EGR.

The tumble motion’s effect on the combustion hasn’t been possible to isolate in this study. This is due to the fact that the increase in tumble motion at lower valve lifts coincides with an increase in compression temperature when the flow past the intake valve is choked. The higher compression temperature substantially affects the start of combustion and thereby the proportion of premixed combustion in relationship to diffusion combustion. Since the temperature increase is thought to have a much greater effect than the tumble motion, no real conclusion of the tumble motions effect on the combustion can be drawn from this study.

However there are not only benefits with deactivating a valve or blocking a port. Even though the volumetric efficiency have been found to be higher than the standard strategy up to an engine speed of about 1400 rpm, the pumping losses increases, especially at higher engine speeds. Therefore the overall efficiency of the engine is decreased at high engine speeds, and the strategy with valve or port deactivation can only be justifiable for engine speeds around the tested 1056 rpm or lower with respect to the brake specific fuel consumption.

As a final conclusion it can be said that different valve strategies can greatly affect the in-cylinder flow and thereby the emissions and performance of the engine. However, since no VVA system is ready for production in heavy duty diesel engines, it is difficult to compare the benefits for such a system in relation to the cost. If a VVA system would be available several strategies can be used to enhance the performance of the engine. But on the other hand, the more cost effective method with a throttle in the curved inlet port can be used to block the port and reduce the soot emissions to the same levels as with one valve deactivated.

8 Further Work

From this master thesis some things can be singled out as suggestions for further work.

First of all it would be desirable to do further engine tests with the different valve strategies, but contrary to the performed tests during the master thesis it would be preferable to also adjust the inlet temperature so the same compression temperature, i.e. the same compression pressure, is achieved for all strategies. If the same compression temperature is achieved, the effects of the different tumble motions hopefully can be studied in a much better way.

Running engine tests with the low- and high-swirl cylinder tests would also be of interest to generate both high and low swirl numbers while keeping the tumble motion at the quite low levels achieved with the standard valve strategy.

To perform studies of the different strategies in an optical engine or with help of computational fluid dynamics, CFD, can be of interest to deeper analyze the different in-cylinder flows. It can especially be of interest to study the phenomena's that occur when a valve strategy generates swirl in two different rotational directions during the same intake stroke. It can also be used to study the tumble motion more thoroughly, and through this create a better understanding and maybe a better model for calculating mean tumble can be found than using the maximum tumble values for every lift.

Studying the potential of varying the in-cylinder flow while using a throttle in the curved inlet port can also be of interest if this more simple and cost effective system would be desirable instead of a VVA system.

9 Abbreviations

VVA – Variable Valve Actuation
VVT – Variable Valve Train
AVT – Active Valve Train
FFVA – Fully Flexible Valve Actuation
IVO – Inlet Valve Opening, Crank Angle
IVC – Inlet Valve Closing, Crank Angle
LIVC – Late Inlet Valve Closing, Crank Angle
CAD – Crank Angle Degree
SI – Spark Ignited
HD – Heavy Duty
TDC – Top Dead Centre
TDCF – Top Dead Centre Fire
SOI – Start Of Injection, Crank Angle Degree after TDCF
SOC – Start Of Combustion, Crank Angle Degree after TDCF
BDC – Bottom Dead Centre
EGR – Exhaust Gas Recirculation
SCR – Selective Catalyst Reaction
AFR – Air Fuel Ratio
BSFC – Brake Specific Fuel Consumption
PMEP – Pump Mean Effective Pressure
CO – Carbon monoxide
CO_2 – Carbon dioxide
NO_x – Nitrogen Oxides
HC – Hydro Carbon
FSN – Filter Smoke Number
DGV – Doppler Global Velocimetry
CFD – Computational Fluid Dynamics
WHSC – World Harmonized Stationary Cycle
Inj. Dur. – Injection Duration, milliseconds
P_{CR} – Common-Rail Pressure, bar absolute
P_{in} – Intake Manifold Pressure, bar relative
$P_{exhaust}$ – Exhaust Back Pressure, bar relative
T_{in} – Inlet Temperature, Degree Celsius

10 References

1. Wilson. N. D. et al., *"Asymmetric Valve Strategies and Their Effect on Combustion"*, SAE 930821

2. Holmberg, T., Ottosson, S. et al., *"Fria Ventiler – Ventilprofilsstrategier för momentoptimering med emissionsbegränsningar vid transienter", Förbränningsmotorteknik Projektkurs, MF2017, 2010*

3. He, X. et al., *"Late Intake Valve Closing as an Emissions Control Strategy at Tier 2 Bin 5 Engine-Out* NO_x *Level"*, SAE 2008-01-0637

4. Grimaldi, C. N. et al. *"Experimental and Numerical Analysis of Charge Motion Characteristics Depending on Intake Valves Actuation Strategies"*, SAE 2005-01-0242

5. Blechstein, A. et al., "*Effects of Charge Motion Characteristics on Engine Variables Such as Emission Behavior and Efficiency*", SAE 2007-01-0640

6. Shimada, T. et al. "*Variable swirl inlet system and its effect on diesel performance and emissions*", SAE 861185

7. GT-Power V 7.0.0 Release Build 4, Gamma Technologies

8. Concerto V 3.9 Build 212, AVL

9. Lotus EVPG V 4.01, Control Systems Lotus Engineering, UK

10. MatLab V 7.9.0.529 Release 2009b, The MathWorks

11. Dieselnet, http://www.dieselnet.com/standards/cycles/whsc.php, 07.36 2011-02-04

12. Thien, G., "*Description of Measuring Methods for the Investigation of Stationary Flow Properties at Valve Ports and Statements for the Evaluation of the Measurement Results"*, FA-Report No. 128/General/011, Österreichische Ingenieur-Zeitschrift, 1964

13. Thien, G., *"Development work on Valve Ports of Four-Cycle Diesel Engines, (English Translation by L. Miz, Allis-Chalmers Corp.)",* Heft 9, Österreichische Ingenieur-Zeitschrift, 1965

14. Thien, G. et al., "*Derivation of the Formulas for the Evaluation of Stationary Flow Measurements of Intake and Exhaust Ports"*, FA-Report No. 463/Gen./072, Österreichische Ingenieur-Zeitschrift, 1978

15. GT-power, GT-Suite, *Engine Performance Application Manual*, Version 7.0, Gamma Technologies

16. Morel, T., Keribar, R., "*A Model for Predicting Spatially and Time Resolved Convective Heat Transfer in Bowl-in-Piston Combustion Chambers"*, SAE 850204

17. GT-Power, GT-Suite, *Flow Theory Manual*, Version 7.0, Gamma Technologies

Appendix 1 – Comparison of different pressure differentials

A comparison of the swirl results for tests performed with the standard 25 mBar pressure drop in respect to a higher pressure drop, 50 mBar, is seen in Figure 71. The figure shows that there are small differences between the measured swirl numbers and the differences can be said to be within the accuracy of the measurements.

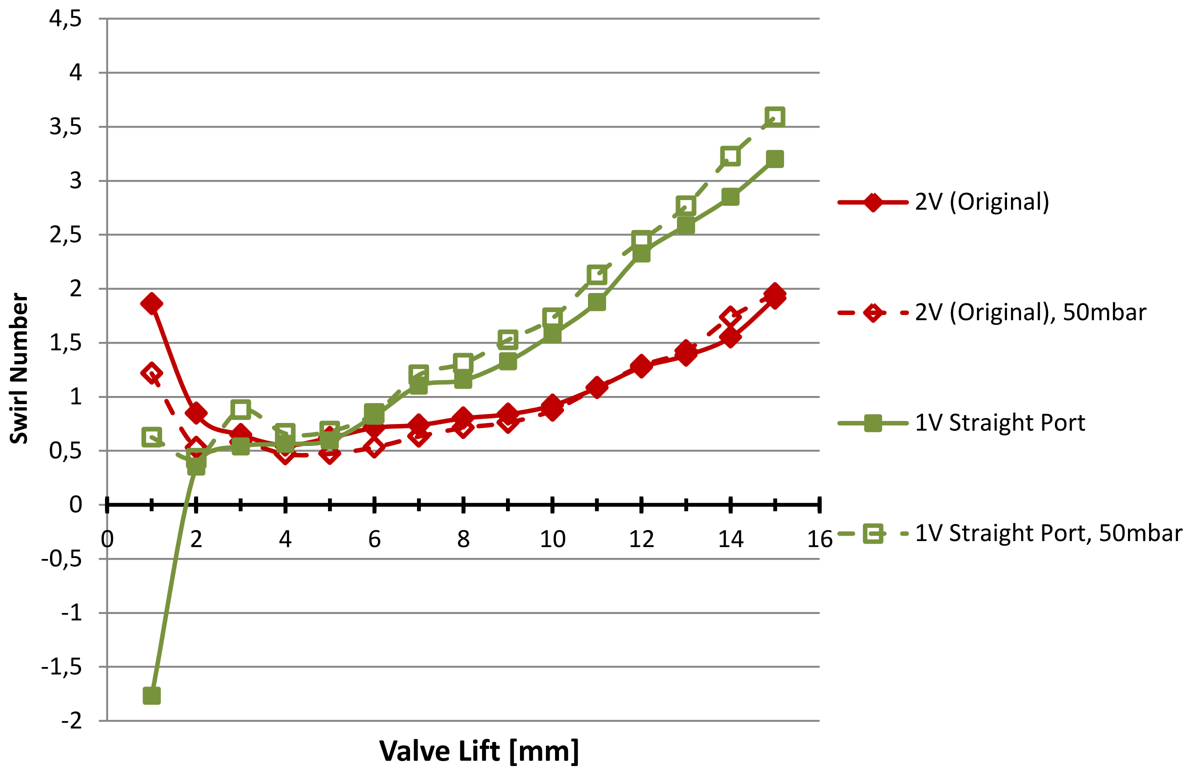

Figure 71. *Measurements for the 2 valve strategy and with only the valve to the straight port activated with different pressure drop.*

Appendix 2 – Intake Manifold Effect High-Swirl Head

The effect of the intake manifold from KTH on the measured swirl numbers for the high-swirl cylinder head is seen in Figure 72. The same trends as for the low-swirl cylinder head can be seen, the swirl numbers are decreased with the intake manifold and the trends are equally no matter which case is studied.

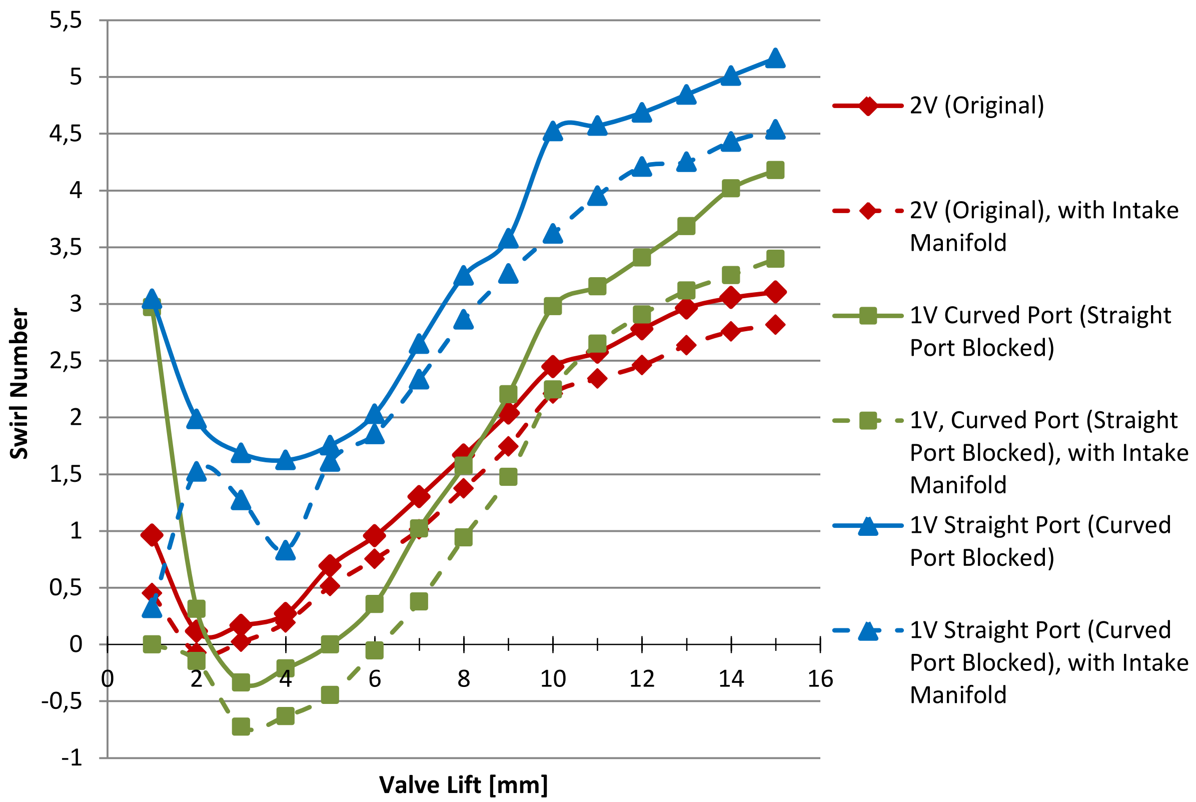

Figure 72. *The effects from the intake manifold on the measured swirl numbers for the high-swirl head.*

Appendix 3 – Intake Manifold Effect on Tumble High-Swirl Head

The effect of the intake manifold from KTH on the measured tumble numbers for the high-swirl cylinder head is seen in Figure 73, showing on almost no effect from the intake.

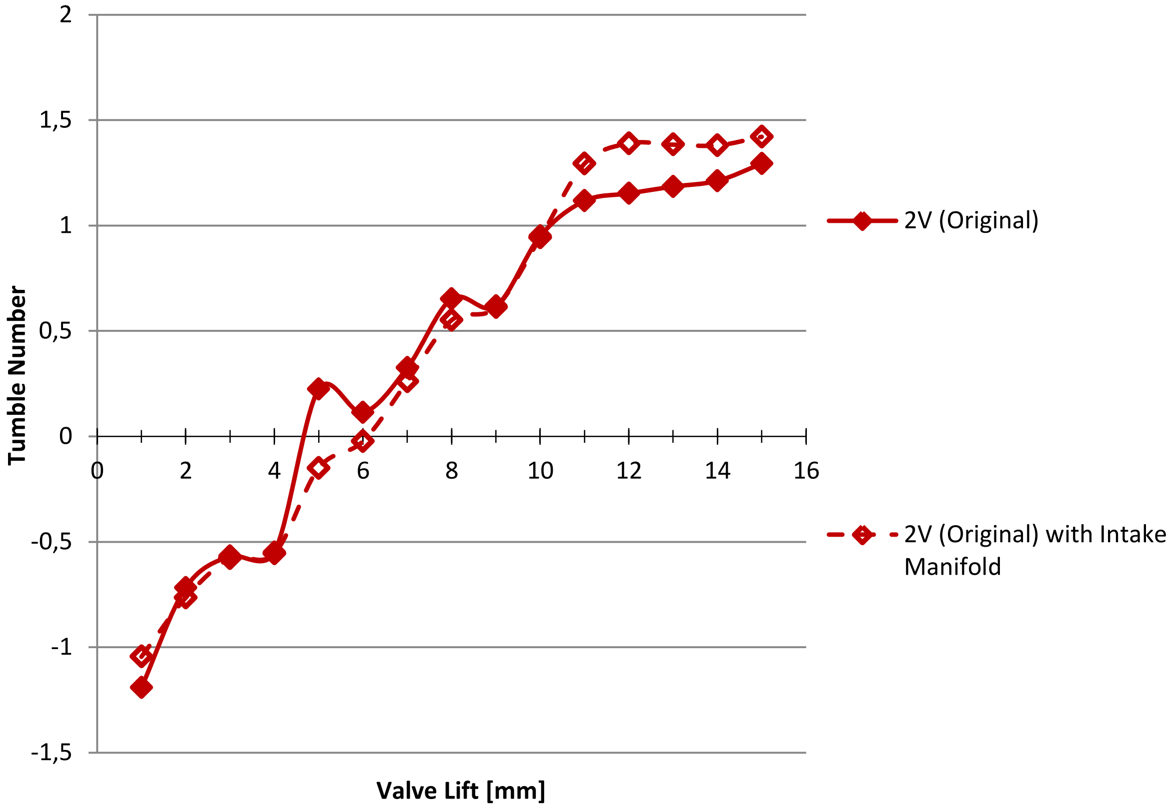

Figure 73. *The effects from the intake manifold on the measured tumble numbers for the high-swirl head.*

Appendix 4 – Comparison Swirl before and after Engine Test

In Figure 74 the swirl measurement for the 2V (Original) case before and after the engine test can be seen, showing on a very good compliance.

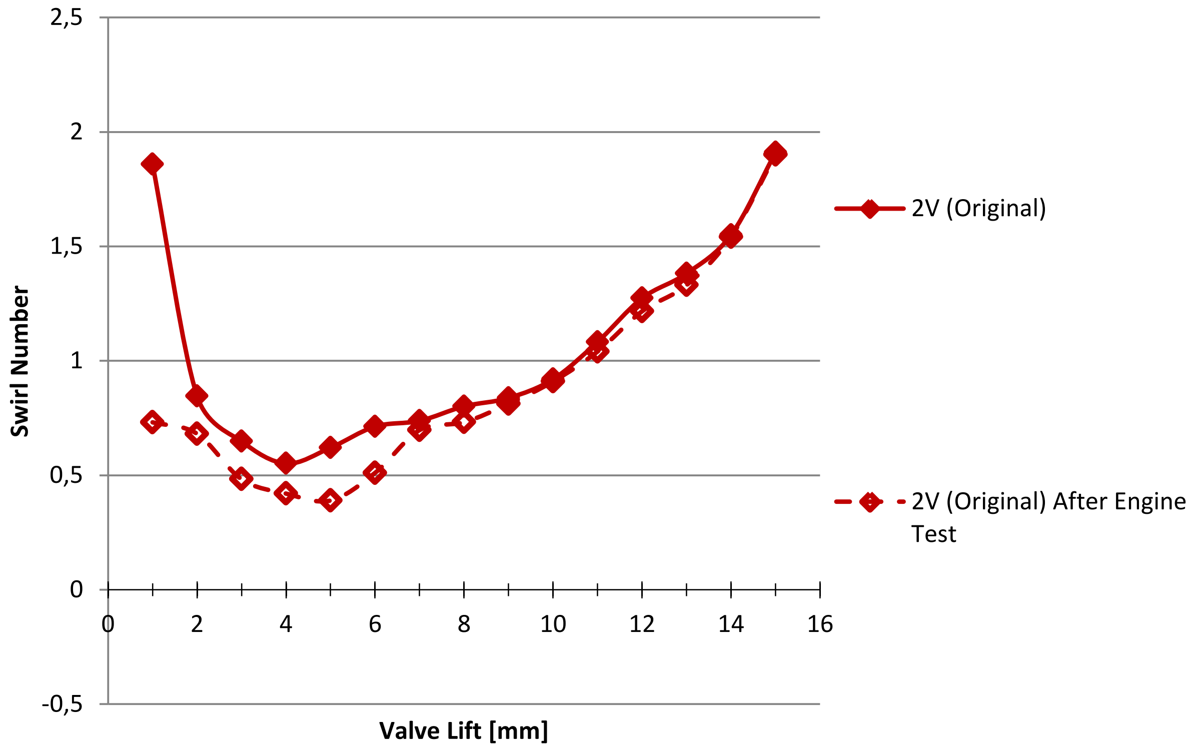

Figure 74. *The swirl measurement before and after the engine tests for the 2V (Original) case.*

Appendix 5 – MatLab script calculating Mean Swirl and Tumble

The script needs the valve profiles from the Lotus EVPG program saved as *ValveProfiles.csv* and the swirl data for asymmetrical valve lifts saved in matrix as *SwirlData.xls*.

```
close all, clear all, clc
%Program for calculating meanswirl

%% Defining different fix parameters
R=80E-3; %[m] Radius from crankshaft to connecting rod
L=255E-3; %[m] Connecting Rod length
r=127E-3/2; %[m] Cylinder Radius
h=R/L;

%% Loading data from files
load 'ValveProfiles.csv' %[mm] The different valve profiles
swirldata=xlsread('SwirlData'); %Swirl Ratio for different valve lifts

%% Making the valve profile data consist of only "di" diggits
di=100;
valveprofiles=round(ValveProfiles*di)/di; %[mm]

%% Making a Swirl Ration map with bether resolution
lift=0:15; %[mm]
liftny=0:1/di:15; %[mm]
[X Y]=meshgrid(lift,lift); %[mm] A meshgrid of the messured valve lift in
the flow rigg
[XI,YI]=meshgrid(liftny,liftny); %[mm] A meshgrid for valve lifts with
bether resolution
ZI=interp2(X,Y,swirldata,XI,YI); %Swirl Ratio with a bether resolution for
different valve lifts

%Preallocating
Nmean=zeros(16,16);
calc=0;

for k=1:16; %The profiles to be used on valve 1
    lift_v1=valveprofiles(:,k); %[mm]
    for l=1:16 %The profiles to be used on valve 3
        if k~=1 || l~=1 %Taking away the case with no lift on each valve
            lift_v3=valveprofiles(:,l); %[mm]
            %Preallocating
            alphav=[];
            Intv=[];
            test=[];
            index1=[];
            index3=[];
            dzv=[];
            for m=1:720;
                if lift_v1(m)~=0 || lift_v3(m)~=0 %Checking if anyone of
the valves is lifted
                    [value,index_v1]=min(abs(liftny-lift_v1(m))); %Finding
index for the lift on valve 1 to be used to get the swirl ratio
                    [value,index_v3]=min(abs(liftny-lift_v3(m))); %Finding
index for the lift on valve 3 to be used to get the swirl ratio
                    index1=[index1 index_v1];
                    index3=[index3 index_v3];
                    Nuse=ZI(index_v1,index_v3); %Finding the swirl ratio
for the lift condition
                    alphause=(m-1)*pi/180; %[rad] Crank shaft angle
```

```
                    alphav=[alphav alphause];

dz=1/2*sin(alphause)+h/2*sin(alphause)*cos(alphause)/(sqrt(1-
h^2*sin(alphause)^2));
%R*sin(alphause)+L*h^2*sin(alphause)*cos(alphause)/(sqrt(1-
h^2*(sin(alphause))^2))/(2*R);
                    if dz<0
                        dz=0;
                    end
                    Int=pi*Nuse*dz^2;
                    Intv=[Intv Int];
                    dzv=[dzv dz];
                    test=[test length(Intv)-length(alphav)];
                end
            end
            Nmeanuse=trapz(alphav,Intv);
            Nmean(k,l)=Nmeanuse;
            calc=calc+1;
        end
    end
end
```

Appendix 6 – Speed and geometrical effects on Mean Swirl GT-Power

Simulation with different engine speed in GT-Power, both at 1316 rpm according to WHSC-mode 9 and at 1000 rpm is shown in Figure 75. This shows on almost no affect on the mean swirl if the engine speed is changed.

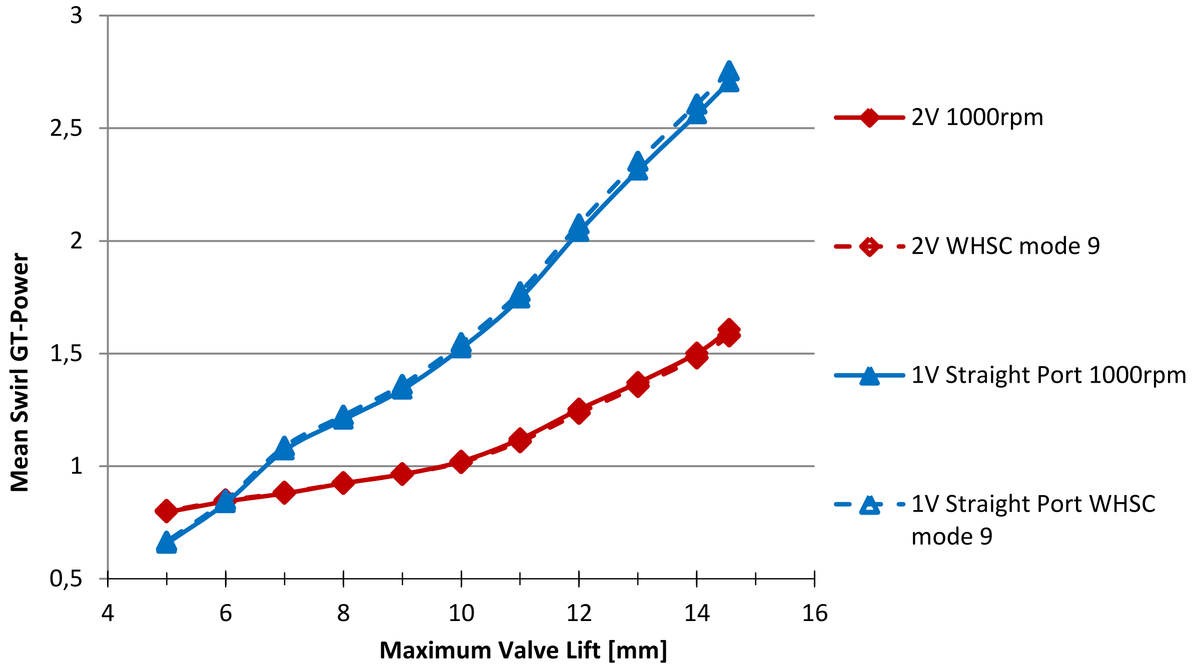

Figure 75. *Simulation with different engine speed in GT-Power and its effect on mean swirl.*

Figure 76 illustrates how the inlet system influence the mean swirl calculation in GT-Power. It can be seen that there are really small differences.

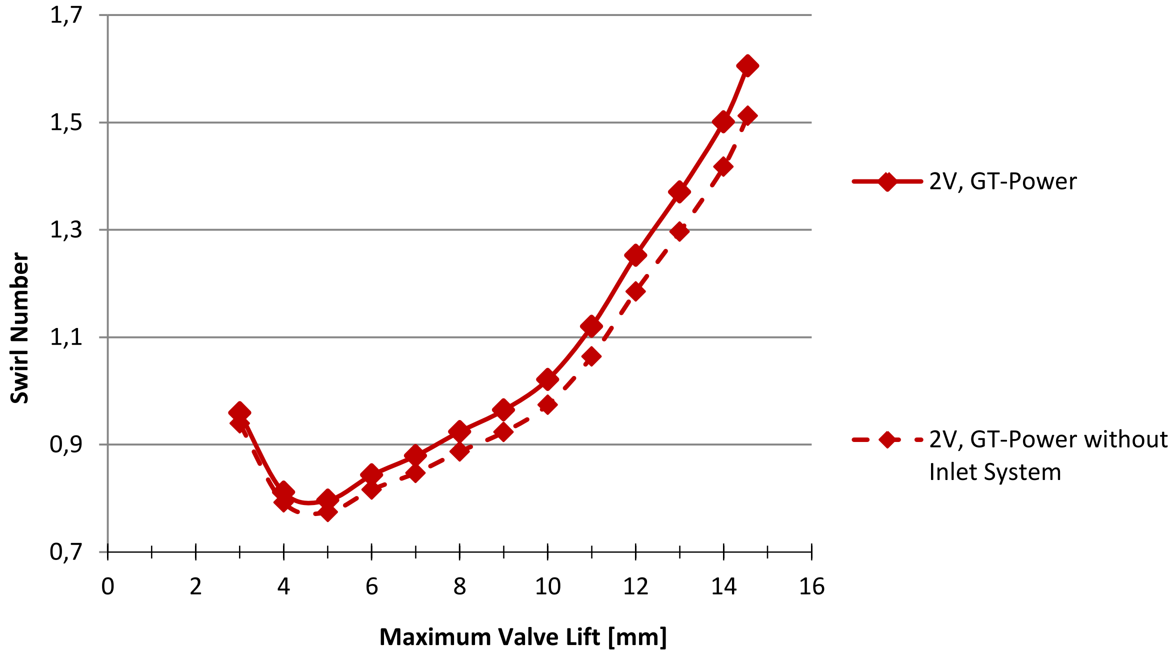

Figure 76. *The effects on mean swirl from the inlet system in GT-Power.*

Appendix 7 – The complete set of flow bench data for the valve strategies

In this appendix mean swirl and tumble are presented in Table 14 to Table 21 for different valve strategies. The description of the valve strategies are according to the index in the matrix used in the Lotus AVT software during the engine tests. Number 1 to 15 is used for the valve profiles with standard appearance. Profile 1 has a maximum valve lift of 1 mm, and in the same way the other valve profiles are directly related to the lift, except for valve profile 15 that has a maximum valve lift of 14.55 mm. The trapezoidal valve profiles has index 101 to 115 and are related to the maximum valve lift in the same way as the ones with standard appearance. The first index of the valve strategy gives the valve profile used for valve 1, i.e. for the curved port, while the second index corresponds to valve 3, the straight port.

Table 14. *The 2V (Original) cases.*

Valve Strategy		Mean Swirl				Mean Tumble	
		Thien	GT-Power	Thien Intake E1		Thien	GT-Power
15,15		1.59	1.61	1.51		1.25	0.92
14,14		1.47	1.50	1.42		1.21	0.88
13,13		1.32	1.37	1.29		1.22	0.89
12,12		1.19	1.25	1.17		1.21	0.89
11,11		1.05	1.12	1.07		1.15	0.86
10,10		0.93	1.02	0.99		1.01	0.77
9,9		0.86	0.96	0.90		0.80	0.63
8,8		0.80	0.92	0.80		0.50	0.44
7,7		0.74	0.88	0.73		0.11	0.16
6,6		0.69	0.84	0.64		-0.38	-0.14
5,5		0.63	0.80	0.55		-1.02	-0.63
4,4		0.66	0.81	0.51		-1.37	-0.88
3,3		0.84	0.96	0.55		-1.67	-1.10

Table 15. *The 1V Straight Port cases.*

Valve Strategy		Mean Swirl				Mean Tumble	
		Thien	GT-Power	Thien Intake E1		Thien	GT-Power
0,15		2.79	2.71	2.98		2.68	1.78
0,14		2.63	2.56	2.86		2.68	1.77
0,13		2.35	2.31	2.68		2.78	1.84
0,12		2.05	2.04	2.52		3.15	2.11
0,11		1.74	1.75	2.36		3.56	2.42
0,10		1.50	1.52	2.10		4.03	2.79
0,9		1.30	1.34	1.67		4.55	3.19
0,8		1.14	1.21	1.41		5.08	3.60
0,7		0.98	1.07	1.24		5.44	3.90
0,6		0.75	0.84	1.15		5.70	4.12
0,5		0.58	0.66	1.15		5.90	4.26
0,4		0.47	0.55	1.19		5.95	4.19
0,3		0.25	0.36	1.07		5.64	3.80

Table 16. *The 1V Curved Port cases.*

Valve Strategy	Mean Swirl			Mean Tumble	
	Thien	GT-Power	Thien Intake E1	Thien	GT-Power
15,0	3.31	3.17	1.57	2.99	-
14,0	3.08	2.97	1.35	3.03	-
13,0	2.66	2.60	0.97	3.12	-
12,0	2.25	2.24	0.73	3.32	-
11,0	1.80	1.83	0.51	3.74	-
10,0	1.41	1.45	0.20	4.14	-
9,0	1.11	1.15	0.06	4.60	-
8,0	0.71	0.76	-0.08	5.27	-
7,0	0.45	0.50	-0.29	5.69	-
6,0	0.21	0.22	-0.50	6.06	-
5,0	0.03	0.02	-0.73	6.29	-
4,0	0.00	-0.04	-1.09	6.23	-
3,0	0.09	0.04	-1.67	5.77	-

Table 17. *The 2V Straight Port (Curved Port Blocked) cases.*

Valve Strategy	Mean Swirl			Mean Tumble	
	Thien	GT-Power	Thien Intake E1	Thien	GT-Power
15,15	3.14	2.98	-	2.77	1.86
14,14	3.01	2.86	-	2.88	1.95
13,13	2.76	2.64	-	3.17	2.17
12,12	2.58	2.47	-	3.43	2.36
11,11	2.42	2.34	-	3.77	2.64
10,10	2.30	2.23	-	4.13	2.92
9,9	2.22	2.17	-	4.58	3.27
8,8	2.17	2.14	-	5.04	3.65
7,7	2.01	1.97	-	5.25	3.83
6,6	1.89	1.82	-	5.38	3.95
5,5	1.87	1.76	-	5.25	3.82
4,4	1.82	1.66	-	4.52	3.21
3,3	1.45	1.26	-	3.11	2.13

Table 18. *The 2V Trapeze case.*

Valve Strategy	Mean Swirl			Mean Tumble	
	Thien	GT-Power	Thien Intake E1	Thien	GT-Power
115,115	2.09	1.99	1.91	1.45	1.03
114,114	1.89	1.80	1.76	1.31	0.94
113,113	1.65	1.63	1.58	1.38	0.98
112,112	1.52	1.51	1.43	1.49	1.06
111,111	1.30	1.30	1.27	1.58	1.12
110,110	1.10	1.12	1.19	1.57	1.11
109,109	0.95	1.03	1.09	1.48	1.04
108,108	0.90	0.98	0.94	1.28	0.91
107,107	0.80	0.91	0.86	0.89	0.63
106,106	0.76	0.87	0.76	0.57	0.41
105,105	0.60	0.76	0.62	-0.59	-0.39
104,104	0.50	0.67	0.48	-1.00	-0.67
103,103	0.62	0.77	0.57	-1.55	-1.02

Table 19. *The 1V Straight Port Trapeze cases.*

Valve Strategy		Mean Swirl				Mean Tumble	
		Thien	GT-Power	Thien Intake E1		Thien	GT-Power
0,115		3.60	3.31	3.58		2.34	1.56
0,114		3.40	3.14	3.39		2.18	1.45
0,113		3.10	2.88	3.17		1.74	1.15
0,112		2.80	2.62	3.02		2.06	1.39
0,111		2.29	2.16	2.94		2.44	1.65
0,110		1.95	1.84	2.98		2.93	2.01
0,109		1.65	1.56	2.16		3.53	2.44
0,108		1.44	1.37	1.71		4.44	3.03
0,107		1.37	1.31	1.38		5.05	3.45
0,106		1.03	0.98	1.17		5.44	3.71
0,105		0.75	0.70	1.11		5.86	3.95
0,104		0.71	0.64	1.30		6.18	4.00
0,103		0.68	0.57	1.35		6.15	3.74

Table 20. *The 1V Curved Port Trapeze cases.*

Valve Strategy		Mean Swirl				Mean Tumble	
		Thien	GT-Power	Thien Intake E1		Thien	GT-Power
115,0		4.48	4.03	2.55		2.57	-
114,0		4.25	3.84	2.30		2.54	-
113,0		3.73	3.41	1.64		2.43	-
112,0		3.33	3.06	1.24		2.22	-
111,0		2.74	2.56	1.25		2.71	-
110,0		2.07	1.95	0.53		3.17	-
109,0		1.91	1.80	0.40		3.30	-
108,0		1.16	1.12	0.34		4.53	-
107,0		0.83	0.80	0.10		5.15	-
106,0		0.43	0.42	-0.12		5.76	-
105,0		0.06	0.06	-0.29		6.31	-
104,0		-0.10	-0.09	-0.49		6.66	-
103,0		-0.08	-0.07	-1.26		5.90	-

Table 21. *The 2V Straight Port (Curved Port Blocked) Trapeze cases.*

Valve Strategy		Mean Swirl				Mean Tumble	
		Thien	GT-Power	Thien Intake E1		Thien	GT-Power
115,115		3.74	3.41	-		2.08	1.40
114,114		3.61	3.30	-		2.02	1.36
113,113		3.22	2.96	-		2.42	1.66
112,112		2.93	2.71	-		2.53	1.72
111,111		2.71	2.50	-		2.92	2.01
110,110		2.51	2.32	-		3.26	2.24
109,109		2.34	2.16	-		3.77	2.57
108,108		2.47	2.27	-		4.79	3.26
107,107		2.23	2.05	-		5.20	3.48
106,106		1.96	1.78	-		5.70	3.81
105,105		2.00	1.76	-		6.19	4.01
104,104		2.07	1.75	-		6.06	3.73
103,103		2.38	1.88	-		4.47	2.58